İSTANBUL TECHNICAL UNIVERSITY ★ INSTITUTE OF SCIENCE AND TECHNOLOGY

GROWTH PHYSIOLOGY AND METABOLIC REMODELLING OF *SACCHAROMYCES CEREVISIAE* UNDER OXIDATIVE STRESS CONDITIONS

M.Sc. Thesis by
Ali ALTINTAŞ

Department : Advanced Technologies

Programme : Molecular Biology-Genetics and Biotechnology

JANUARY 2011

İSTANBUL TECHNICAL UNIVERSITY ★ INSTITUTE OF SCIENCE AND TECHNOLOGY

GROWTH PHYSIOLOGY AND METABOLIC REMODELLING OF *SACCHAROMYCES CEREVISIAE* UNDER OXIDATIVE STRESS CONDITIONS

M.Sc. Thesis by
Ali ALTINTAŞ
(521081051)

Date of submission : 20 December 2010
Date of defence examination: 27 January 2011

Supervisor (Chairman) : Assoc. Prof. Dr. Zeynep Petek ÇAKAR (ITU)
Co-Supervisor : Assoc. Prof. Dr. Christopher WORKMAN (DTU)
Members of the Examining Committee : Prof. Dr. Tülay TULUN (ITU)
Assoc. Prof. Dr. Eda TAHİR TURANLI (ITU)

JANUARY 2011

İSTANBUL TEKNİK ÜNİVERSİTESİ ★ FEN BİLİMLERİ ENSTİTÜSÜ

SACCHAROMYCES CEREVISIAE'NİN OKSİDATİF STRES KOŞULLARI ALTINDA BÜYÜME FİZYOLOJİSİ VE METABOLİZMASININ YENİDEN MODELLENMESİ

YÜKSEK LİSANS TEZİ

Ali ALTINTAŞ
(521081051)

Tezin Enstitüye Verildiği Tarih : 20 Aralık 2010
Tezin Savunulduğu Tarih : 27 Ocak 2011

Tez Danışmanı : Doç. Dr. Zeynep Petek ÇAKAR (İTÜ)
Tez Eş Danışmanı : Doç. Dr. Christopher WORKMAN (DTU)
Diğer Jüri Üyeleri : Prof. Dr. Tülay TULUN (İTÜ)
Doç. Dr. Eda TAHİR TURANLI (İTÜ)

OCAK 2011

This M.Sc. thesis project was completed in Technical University of Denmark (DTU) via support of Erasmus Exchange Programme between Istanbul Technical University (ITU) and Technical University of Denmark (DTU).

“As for me, all I know is that I know nothing.”

Socrates

(469 BC-399 BC)

FOREWORD

I am thankful to my supervisor Assoc. Prof. Dr. Zeynep Petek Çakar. I have been working with Dr. Çakar since 2006 and I really learned a lot from her. Moreover, I always got inspired by her scientific point of view. During my period in Denmark, I also felt her kind support with me.

I would like to express my deep appreciation and thanks for my co-supervisor Assoc. Prof. Dr. Christopher Workman. This project would not exist without his excellent ideas. I am grateful to his support during the project and my education period in Denmark. Also, his passion of science was my driving force all the time. I cannot remember how many times late in the night we talked about data analysis and biological interpretation of experiments. Throughout the experiments and writing thesis, every little idea of mine was considered and contributed kindly by Dr. Christopher Workman.

I also would like to thank Emmanouil Papadakis, Alessandro Fazio and Jacopo Martini. They made our office and laboratory an enjoyable place to work. There is not such a word or sentence that I can describe the joy of working with them and their friendship. For instance, Emmanouil always discussed my experimental results even in his little breaks, Alessandro was bombarding me with articles and Jacopo helped me in the laboratory many times and so on.

Most of spelling and grammar check of thesis was done by Dr. Christopher Workman. Also my friends, Bahtiyar Yılmaz and Tammi Camilla Vesth, kindly proofread my thesis. The thesis you are holding now would not shape properly without the efforts of Bahtiyar, Tammi and mostly Dr. Christopher Workman. I am thankful to them.

I always felt the support of my family nearby even though they were kilometres far away from me. I am so grateful to their everlasting love, support and patience. I believe that I can do everything as long as their love is with me.

Many thanks also go to my friends in Denmark. Although my stay in Denmark was just one year, I had many friends that I cannot allude all their names. I could not survive in Denmark without their kind support and help.

My apologies to whom I may have forgotten. I can feel the neurons that are firing for my thesis; hence my temporary amnesia is not intentional to you.

September 2010

Ali Altıntaş

Molecular Biologist & Geneticist

TABLE OF CONTENTS

Page

FOREWORD ..... **ix**
TABLE OF CONTENTS ..... **xi**
ABBREVIATIONS ..... **xiii**
LIST OF TABLES ..... **xv**
LIST OF FIGURES ..... **xvii**
SUMMARY ..... **xix**
ÖZET ..... **xxi**
1. INTRODUCTION **1**
1.1 *Saccharomyces cerevisiae* as a Model Organism 2
1.1.1 The model organism features of *Saccharomyces cerevisiae* 4
1.1.2 Life cycle of *Saccharomyces cerevisiae* 5
1.2 Carbon Source Dependent Growth Physiology of *Saccharomyces cerevisiae* 7
1.2.1 Metabolic remodelling in diauxic shift 8
1.2.2 BioLector: monitoring batch cell growth by light scattering 9
1.3 Stress Responses of *Saccharomyces cerevisiae* 11
1.3.1 Key concepts of stress response studies 12
1.3.2 Mitogen activated protein kinase (MAPK) pathways and stress response 13
1.3.3 Oxidative stress response 14
1.3.4 Heat shock response 21
1.3.5 Osmotic & salt stress response 24
1.3.6 Freeze-thaw stress response 26
1.3.7 Ethanol stress response 26
1.3.8 Metal stress response 26
1.3.9 Cross stress resistance 27
1.4 DNA Damage Checkpoints, Oxidative DNA Damage and Repair Mechanisms of *Saccharomyces cerevisiae* 28
1.5 Aim of the Study 31
2. MATERIALS AND METHODS **33**
2.1 Materials 33
2.1.1 Yeast strains 33
2.1.2 Yeast culture media: 34
2.1.3 H_2O_2 dilutions for treatment of strains in flower plates 36
2.1.4 HPLC stock solutions and HPLC standards 37
2.1.5 Laboratory equipment 38
2.2 Methods 39
2.2.1 Selection of yeast deletion strains 39
2.2.2 Cell incubation conditions 39
2.2.3 Preparing BioLector plates 41
2.2.4 Determination of metabolite contents by HPLC 42

2.2.5 Data analysis 42
3. RESULTS 45
3.1 Growth Physiology of KO and Wild Types 45
3.2 Analysis of Growth Curves 48
3.3 HPLC Results and Data Analysis 50
4. DISCUSSION 59
4.1 Growth Physiology of Strains and Gene Deletion Effects on Oxidative Stress and DNA Repair Responses 59
4.2 Regulation of Carbon Metabolism under Oxidative Stress and Importance of Diauxic Shift 61
4.3 Conclusion and Future Aspects 65
REFERENCES 67
APPENDICES 75
APPENDIX A: Background genotype of the wild types 77
APPENDIX B: Genotype of the mutant strains. 79
APPENDIX C: Information about knock-out genes: names, functions and descriptions 81
APPENDIX D: The Whole Growth Curves and LSU to OD Conversions of 38 KO Mutants and Wild Types 85
CURRICULUM VITAE 113

ABBREVIATIONS

CDW	**:** Cell Dry Weight
GSH	**:** Glutathione
H_2O_2	**:** Hydrogen Peroxide
H_2SO_4	**:** Sulphuric Acid
KO	**:** Knock Out
LSU	**:** Light Scattering Unit
MAT	**:** Mating Type
MAPK	**:** Mitogen Activated Kinase
MAPKK	**:** Mitogen Activated Kinase Kinase
MAPKKK	**:** Mitogen Activated Kinase Kinase Kinase
NaCl	**:** Sodium Chloride
OD	**:** Optical Density
ROS	**:** Reactive Oxygen Species
rpm	**:** Revolutions per minute (1/60 Hertz)
SD-Media	**:** Synthetic Defined Media
TCA Cycle	**:** Tricarboxylic Acid Cycle – Citric Acid Cycle – Krebs Cycle
TF	**:** Transcription Factor

LIST OF TABLES

Page

Table 1.1: Taxonomy of *Saccharomyces cerevisiae* 3
Table 1.2: Oxidative Stress Response Mechanisms of *S. cerevisiae* [35] 17
Table 2.1: The KO genes and functions of 38 mutant strains..... 33
Table 2.2: YPD Media Composition 34
Table 2.3: Composition of Synthetic Defined (SD) Media 35
Table 2.4: Stock Solutions of SD Media 35
Table 2.5: YNB w/o Amino Acids + $(NH_4)_2SO_4$ Solution..... 35
Table 2.6: 20% Glucose Stock Solution 36
Table 2.7: 10X Amino Acid Solution..... 36
Table 2.8: H_2O_2 dilution table for well treatments 37
Table 2.9: Stock Solutions of HPLC Standards..... 37
Table 2.10: HPLC Standard Solution Dilutions 38
Table 2.11: Metabolite Concentrations of HPLC Standards 38
Table 2.12: Functions of KO genes and the biological processes they are involved in 40
Table 2.13: Physical Conditions of BioLector Fermentations..... 41
Table 2.14: HPLC Sampling Times for Metabolite Detection 42

LIST OF FIGURES

Page

Figure 1.1: Reactions of Alcoholic Fermentation 2
Figure 1.2: A. Scanning electron microscopy picture of *S. cerevisiae* B.Transmission electron micrograph of *S. cerevisiae* 4
Figure 1.3: Reproduction of *Saccharomyces cerevisiae* 5
Figure 1.4: Transitions in life cycle of *S. cerevisiae* 6
Figure 1.5: Cell Density Profile and Growth Phases of *S. cerevisiae* in a Batch Culture 7
Figure 1.6: Gene expression profile of carbon flux before (left) and after (right) diauxic shift. Red refers increase in gene expression while green refers decrease in gene expression. Only key genes/gene groups for carbon flux branches are shown 8
Figure 1.7: Metabolic Adjustments During Diauxic Shift 9
Figure 1.8: BioLector Microfermentation System 10
Figure 1.9: LSU vs. OD Correlation with CDW 11
Figure 1.10: Generation of reactive oxygen species in the cell 14
Figure 1.11: Enzymatic & Non-Enzymatic Oxidative Defence Mechanisms of *S. cerevisiae* and Their Relationship 16
Figure 1.12: Stress responsive MAPK (SAPK) Pathway in *S. cerevisiae* 18
Figure 1.13: Sln1 Phosphorelay System of *S. cerevisiae* 19
Figure 1.14: The role of Yap1 on ROS Sensing and Transcriptional Regulation.... 20
Figure 1.15: Chemical formula of trehalose 22
Figure 1.16: Biosynthesis of trehalose 22
Figure 1.17: Early and late heat shock responses of *S. cerevisiae* 23
Figure 1.18: Hyper/Hypo-osmotic stress response of *S. cerevisiae* 24
Figure 1.19: HOG pathway and summary of response mechanisms to osmotic stress in *S. cerevisiae* 25
Figure 1.20: Cross-adaptation Hierarchy of Adaptive to Lethal Doses of Oxidants 27
Figure 1.21: Genes Involved in DNA Damage & Replication Checkpoints During Cell Cycle 28
Figure 1.22: Signalling cascades due to DNA damage in *Saccharomyces cerevisiae* 29
Figure 1.23: Chemical Structure of 8-oxo-G 30
Figure 1.24: Repair of 8-oxo-G Lesion by OGG1 DNA Glycosylase 31
Figure 3.1: Growth curve of wild type BY4741 under different H_2O_2 conditions 45
Figure 3.2: Linear fits of LSU and OD for *S. cerevisiae* strains 46
Figure 3.3: OD equivalent of BY4741 growth curve 47
Figure 3.4: Slow growing KO strains: *vps15*Δ, *oca1*Δ, *bud32*Δ and *ptc1*Δ 48
Figure 3.5: Clustering of all KO and wild type strains due to their relative growth area, relative growth rate and relative diauxic response times 49

Figure 3.6: Growth curve of wild type BY4741 50
Figure 3.7: Spline Interpolation for HPLC Standards 51
Figure 3.8: Diauxic Shift Response Times for each H_2O_2 Treatment 52
Figure 3.9: Diauxic Shift Response Times According to H_2O_2 Concentrations 53
Figure 3.10: Glucose concentration change at different H_2O_2 concentrations by time 54
Figure 3.11: Ethanol concentration change at different H_2O_2 concentrations by time 55
Figure 3.12: Glycerol concentration change at different H_2O_2 concentrations by time 56
Figure 3.13: Acetate concentration change at different H_2O_2 concentrations by time 57
Figure 3.14: Pyruvate concentration change at different H_2O_2 concentrations by time 58
Figure 4.1: Diauxic Remodelling of Carbon Metabolism 64

GROWTH PHYSIOLOGY AND METABOLIC REMODELLING OF *SACCHAROMYCES CEREVISIAE* UNDER OXIDATIVE STRESS CONDITIONS

SUMMARY

Saccharomyces cerevisiae is the major eukaryotic model organism used to study molecular biology, genetics, cellular functions and processes. In recent years, there have been many molecular studies on *S. cerevisiae* to identify the oxidative stress response mechanism to which all aerobically growing organisms suffer exposure, partially reduced forms of molecular oxygen, known as reactive oxygen species (ROS) and these ROS are extremely and inevitably capable of damaging cellular constituents such as DNA, lipids and proteins.

The objective of the project was to reveal the growth effects of oxidizing environment on protein kinase/phosphatase knock-out (KO) mutants of *Saccharomyces cerevisiae*. Hence, this study would enhance to investigate the contrast of effects of oxidizing agents as kinase/phosphatase pathways in the cells that have a big impact on signal transduction and various expression pathways.

Two wild type strains of *S. cerevisiae* and 38 different protein kinase/phosphatase KO mutants are investigated for oxidative stress responses. These 38 protein kinase/phosphatase mutants are selected to their known activities on both general/oxidative stress response and DNA damage response as these mutants are the possible candidates for the specific aim of this project.

Hydrogen peroxide (H_2O_2) was used to create an oxidizing environment in different concentrations as 0.25, 0.50, 1.0 and 2.0 mM. All growth data of strains is created by BioLector microfermentation platform.

Principally, this study is composed of oxidative stress effects on growth physiology of *S. cerevisiae* strains and metabolic remodelling of *S. cerevisiae* strains due to oxidative stress.

There are many important findings on growth physiology, but the most important ones can be said that the compensatory mechanism of protein kinase/phosphatase, the central activity of *OCA1* gene among responses of oxidative stress, DNA damage and cell cycle arrest, and also the investigation of slow grower KO mutants: *bud32*Δ, *vps15*Δ, *ptc1*Δ and *oca1*Δ.

BioLector microfermentation platform allowed us to detect the exact time interval of diauxic phases of *S. cerevisiae* upon different H_2O_2 stress conditions. The important metabolites of carbon metabolism which were sampled before, during and after diauxic phase of *S. cerevisiae* were detected by HPLC. The metabolic delay of carbon utilization proved that the cells decrease the metabolic activity with increasing H_2O_2 stress conditions in the environment. Moreover, the harsh stress concentrations make the cells undergo a metabolic turn-down.

SACCHAROMYCES CEREVISIAE'NİN OKSİDATİF STRES KOŞULLARI ALTINDA BÜYÜME FİZYOLOJİSİ VE METABOLİZMASININ YENİDEN MODELLENMESİ

ÖZET

Saccharomyces cerevisiae; moleküler biyoloji, genetik ve hücre fonksiyonlarını çalışmada kullanılan önemli bir ökaryotik model organizmadır. Bütün aerobik büyüyen organizmalar moleküler oksijenin indirgenmiş formu olan reaktif oksijen türlerine (ROT) maruz kalırlar. ROTlar; DNA, lipitler, proteinler gibi hücre bileşenlerine önemli ölçüde hasar verirler. Son yıllarda, *S. cerevisiae*'nin oksidatif strese tepkisi hakkında birçok moleküler çalışma yapılmaktadır.

Bu projede, *Saccharomyces cerevisiae*'nin protein kinaz/fosfataz geni silinmiş (knock-out) mutantlarında yükseltgen ortamın hücre büyümesine etkisini açıklamak amaçlanmış, ayrıca hücre içi sinyal aktarımında ve çeşitli gen ekspresyon yolizlerinde büyük etkisi olan protein kinaz/fosfataz yolizleri hakkında yükseltgen ajanların etkileri araştırılmıştır. Bunun için *S. cerevisiae*'nin 2 yaban tipi ve 38 farklı protein kinaz/fosfataz geni silinmiş (knock-out) mutanları incelenmiştir. Bu 38 protein kinaz/fosfataz mutantları, oksidatif stres tepkisinin iletilmesinde en muhtemel adaylar olup hem genel/oksidatif stres tepkileri hem de DNA hasar tepkileri üzerine bilinen aktiviteleri üzerinden seçilmiştir.

Yükseltgen ortam koşulları yaratmak için 0.25, 0.50, 1.0 ve 2.0 mM olmak üzere değişik derişimlerde hidrojen peroksit (H_2O_2) kullanılmıştır ve *S. cerevisiae* ırklarının bütün büyüme verileri BioLector mikrofermentasyon platformunda oluşturulmuştur.

Bu çalışma özellikle oksidatif stresin *S. cerevisiae* ırklarının gözlemlenen büyüme fizyolojisi üzerindeki etkilerinden ve metabolizmasının yeniden modellenmesinden oluşmaktadır.

Büyüme fizyolojisi üzerine elde edilen sonuçların en önemlileri: protein kinaz/fosfatazların dengeleyici mekanizması, *OCA1* geninin oksidatif stres tepkilerindeki merkezi etkinliği, DNA hasarı ve hücre döngüsü durması, ayrıca yavaş büyüyen ve geni silinmiş *bud32*Δ, *vps15*Δ, *ptc1*Δ ve *oca1*Δ (knock-out) mutantlarının gözlemlenmesi olarak sıralanabilir.

BioLector mikrofermentasyon platformu, farklı H_2O_2 koşullarında *S. cerevisiae*'nin diauksik fazının kesin zaman aralığını tespit etmeye olanak vermiştir. *S. cerevisiae*'nin diauksik faz öncesi, süreci ve sonrasında örneklenen önemli karbon metabolizması metabolitleri HPLC ile saptanmıştır. Karbon tüketiminin metabolik gecikmesi, hücrelerin ortamda artan H_2O_2 stres koşulu ile metabolik aktivitesini düşürdüğünü göstermekle birlikte, ağır stres derişimleri hücrelerin metabolik kısılmaya girmesine neden olmuştur.

1. INTRODUCTION

Saccharomyces cerevisiae is a unicellular eukaryotic organism which is one of the first domesticated organisms, thus well-known from the ancient times. *Saccharomyces cerevisiae* has been used for thousands of years to make bread, beer and wine, thus it is also called as “baker’s yeast” or “brewer’s yeast”. It is proposed that the domesticated strains of *Saccharomyces cerevisiae* are derived from at least two independent strains isolated from grape wine and saké wine [1].

Throughout recorded history, there can be seen many milestones for the use of *Saccharomyces cerevisiae* by mankind. The first fermented beverage was made in China at 7000 BC while the first wine production took place in Iran at 6000 BC and Egypt at 3000 BC. It seems that Mesopotamian cultures initiated the wine production that would later spread throughout all Mediterranean Sea e.g. Greece in 2000 BC, Italy in 1000 BC and further to Northern Europe in 100 AD and also America 1500 AD. Moreover, beer fermentation is also as old as wine fermentation. The first information about beer history originates in the Middle East and may have been introduced by the Germanic and Celtic tribes in the 1st century AD [2].

The ability of alcoholic fermentation of *Saccharomyces cerevisiae* is used for producing alcoholic beverages and bread. The usage of fermented beverages depends on the ability of the fermented products to have a longer shelf life than non-fermented beverages [3]. Another biotechnological important point is that *Saccharomyces cerevisiae* can tolerate high concentrations of ethanol which gives it competitive advantage in a mixed fermentation [4]. In bread making process, the yeast is added into the dough, hence during the fermentation of *S. cerevisiae*, ethanol is produced along with carbon dioxide gas which makes the bread rise and softer to eat. Also, the ethanol which is produced during the fermentation process evaporates during baking [5].

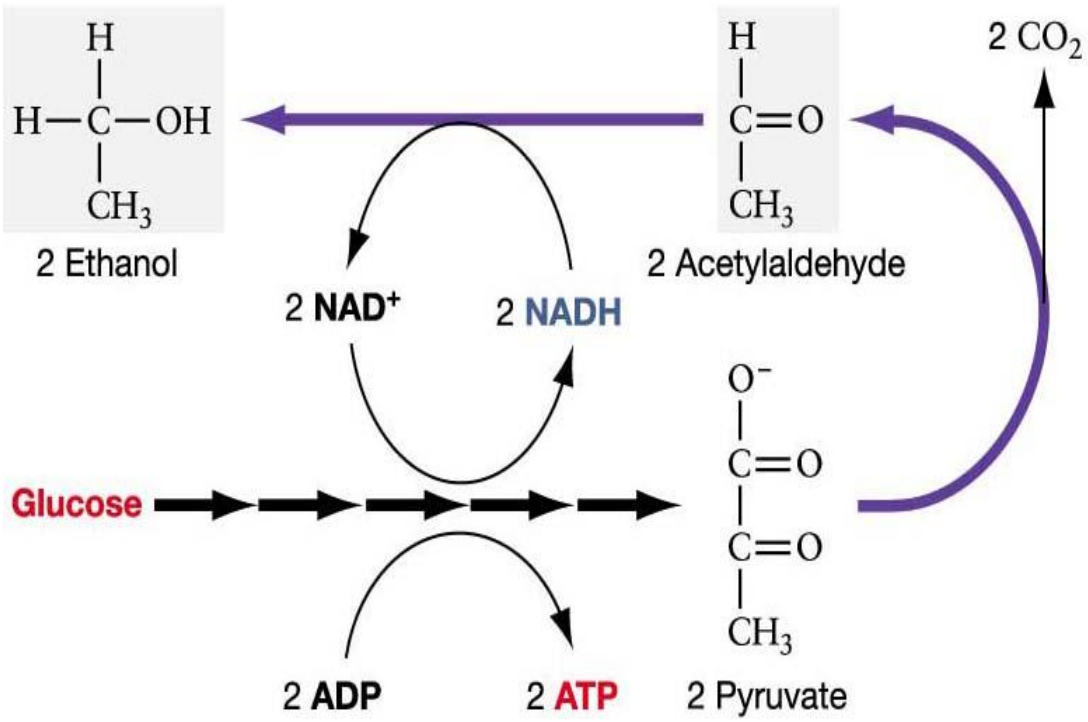

Figure 1.1: Reactions of Alcoholic Fermentation [6]

1.1 *Saccharomyces cerevisiae* as a Model Organism

Saccharomyces cerevisiae is the major eukaryotic model organism used to study molecular biology, genetics, cellular functions and processes. On the other hand, *Saccharomyces cerevisiae* is also important for the industrial productions of bread, beer, wine, enzymes, vitamins, polysaccharides, polyhydric alcohols, pigments, lipids, glycolipids and pharmaceuticals [7].

The word "*Saccharomyces*" is a Greek word means "sugar mold" or "fungus". Besides, the origins of the word "*cerevisiae*" come from Gaelic word "kerevigia" and old French word "cervoise" which both means "beer" [8]. In 1838 *Saccharomyces cerevisiae* was first named and in 1870 the first morphological descriptions of *Saccharomyces cerevisiae* were defined by Reess. The taxonomy of *Saccharomyces cerevisiae* was defined by Hensen in 1883 via physiological characteristics of pure *Saccharomyces cerevisiae* cultures [9].

Table 1.1: Taxonomy of *Saccharomyces cerevisiae*

Superkingdom	Eukaryota
Kingdom	Fungi
Phylum	Ascomycota
Subphylum	Saccharomycotina
Class	Saccharomycetes
Order	Saccharomycetales
Family	Saccharomycetaceae
Genus	Saccharomyces
Species	*Saccharomyces cerevisiae*

The *S. cerevisiae* cells are ellipsoidal and their dimensions of the yeast cells are roughly 4.76 µm (long axis) by 4.19 µm (short axis) for haploids and 6.01 µm by 5.06 µm for diploids. Thus, diploid cells have a twice bigger (83% bigger) volume of haploid yeast cells [10]. *Saccharomyces cerevisiae* has 5-10 µm round shape which has a thick cell wall (see Figure 1.2), mitochondria but has no chloroplast. Because of this, it is evolutionary more related to animals than plants in modern aspects. The evolutionary linkage between animals and fungi is also approved via protein cluster analysis [11]. *Saccharomyces cerevisiae* can grow in a simple nutrient medium which contains only water, carbon and nitrogen source such as yeast minimal medium. In optimal conditions, *Escherichia coli* can divide every 20 minutes [12] whereas *Saccharomyces cerevisiae* can divide every 1-2 hours [13]. However, *Saccharomyces cerevisiae* can also grow and divide nearly as fast as a bacterium [14] if nutrients in the media are plentiful.

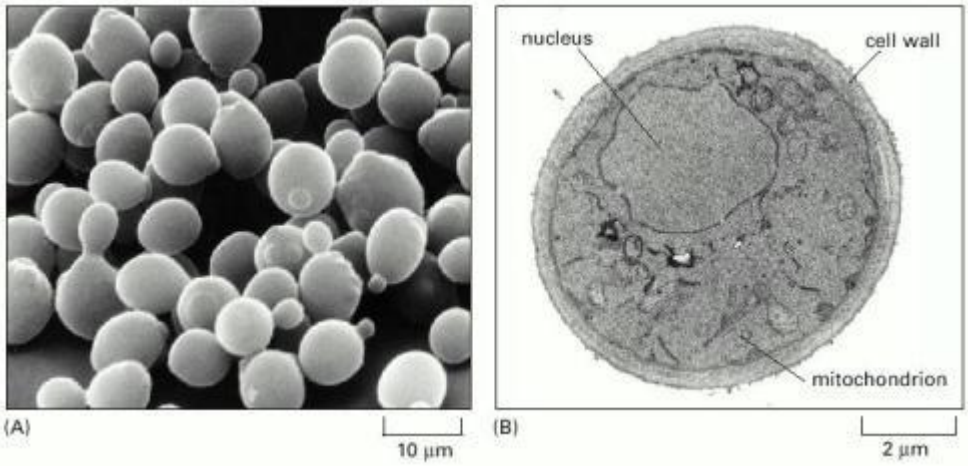

Figure 1.2: A. Scanning electron microscopy picture of *S. cerevisiae*
B.Transmission electron micrograph of *S. cerevisiae* [14]

1.1.1 The model organism features of *Saccharomyces cerevisiae*

Saccharomyces cerevisiae shares notable similarities with other higher eukaryotes by means of molecular and cellular architecture. The common features that favour *Saccharomyces cerevisiae* as a model organism are listed below:

i. It is a unicellular eukaryotic organism and relatively uncomplicated compared to other higher eukaryotes like *Homo sapiens* [15; 16].

ii. It has a short doubling time (1.5-2 hours at 30ºC) which enables fast processing. Large quantities of cells can grow on simple medium which makes the process cheaper. It can be inoculated in both liquid and solid (agar) medium easily [15; 16].

iii. *Saccharomyces cerevisiae* has a relatively small genome that has been completely sequenced and is composed of ~6000 genes [17].

iv. *Saccharomyces cerevisiae* can be genetically manipulated easily. It uses homologous recombination which favours simple knock-out of genes. In addition, *Saccharomyces cerevisiae* can be maintained in a haploid state, such that the phenotypic effects of knock-outs can be easily detected [15; 16].

v. There are many orthologs of yeast genes in the human genome. Thus, many human genes can be substituted with yeast genes and those genes function properly after transfection to the yeast. There are many constructed plasmids and mutant yeast strains for this purpose [15; 16].

vi. Major cellular processes can be understood via several developed molecular genetic tools for *Saccharomyces cerevisiae* such as response to stress, protein degradation, intracellular trafficking, genetic recombination, signal transduction, cell cycle control, and switch mechanisms from mitosis to meiosis etc [16].

1.1.2 Life cycle of *Saccharomyces cerevisiae*

Saccharomyces cerevisiae reproduce via a process called "budding" and it is therefore often called "budding yeast". *Saccharomyces cerevisiae* can exist either in haploid or diploid state. A new diploid yeast cell forms when the two haploid cells fuse. This process is called as mating. As a unicellular organism, *Saccharomyces cerevisiae* can also have different mating types like male and female gametes (sperm and egg) as higher eukaryotes do. The two mating types for *Saccharomyces cerevisiae* are α and a. These mating types can fuse each other forming a new *Saccharomyces cerevisiae* cell with genetic material of these two mating type cells. Thus, *Saccharomyces cerevisiae* can reproduce both sexually and asexually. Mating only occurs if the two haploid cells have different mating types that could be said to be their sex (see Figure 1.3). These mating types are located in a single locus on chromosome III and called mating-type (*MAT*) locus [10; 14; 18].

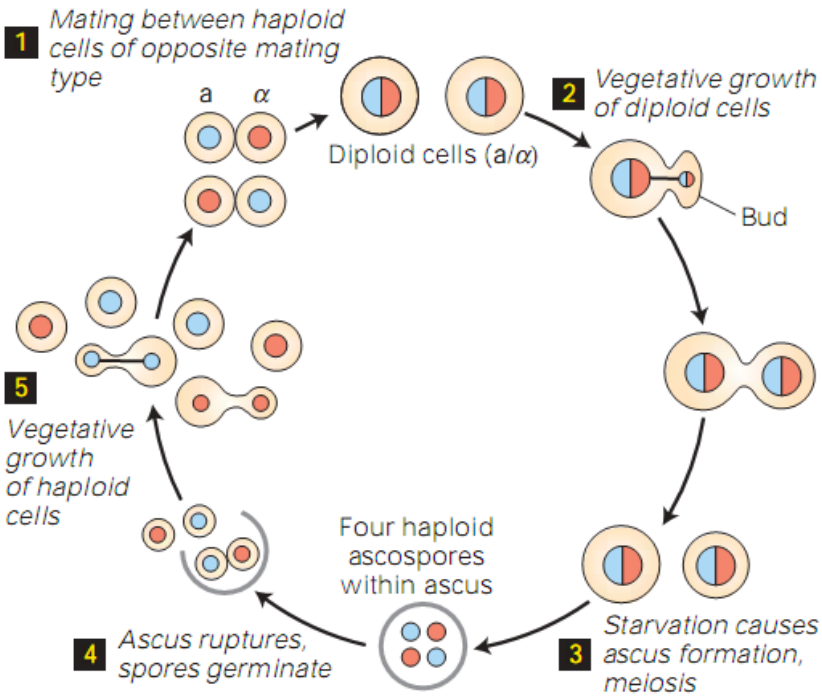

Figure 1.3: Reproduction of *Saccharomyces cerevisiae* [18]

A diffusible signalling molecule (the mating factor) and a specific cell-surface receptor protein is encoded by both mating type a (*MAT* a) and mating type α (*MAT α*). Yeast cells differ in mating types via these *MAT* a*/a* products, recognize themselves and fuse each other forming a diploid yeast cell called a/α which cannot further mate but can sporulate under starvation conditions by meiosis. Ascospores which are formed by sporulation can grow into haploid cells once conditions are favourable [10]. Having a stable haploid state for *S. cerevisiae* allows it to be manipulated genetically and to have stable knock-outs due to having one set of chromosomes [16]. In addition to this, the entire cell types as **a**, α, **a**/α are able to induce mitosis [10].

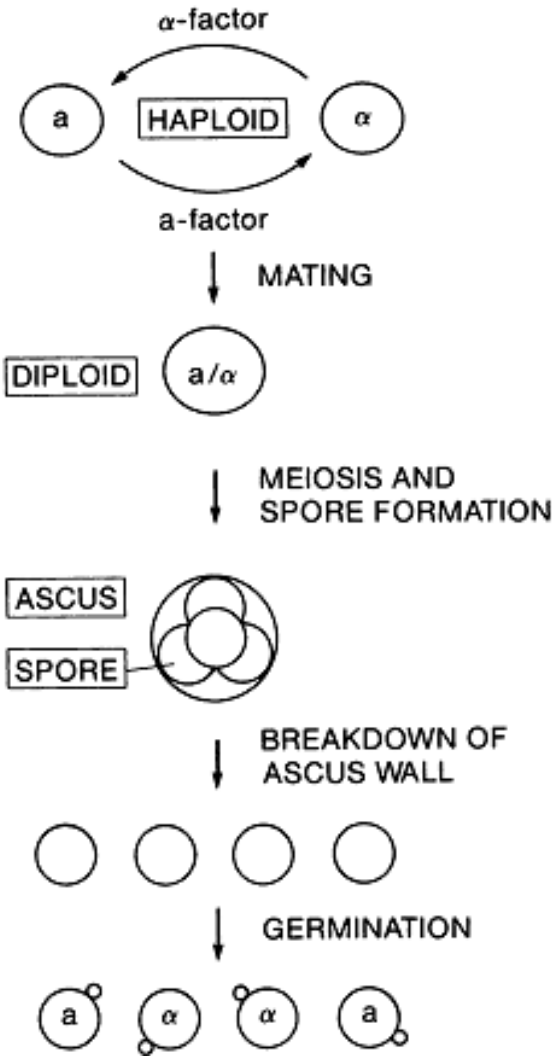

Figure 1.4: Transitions in life cycle of *S. cerevisiae* [10]

1.2 Carbon Source Dependent Growth Physiology of *Saccharomyces cerevisiae*

S. cerevisiae is able to adapt to various different chemical and nutritional conditions. It has evolved to adapt its metabolism to changing environment. *S. cerevisiae* is a "Crabtree" positive microorganism which means that it prefers to produce ethanol rather than tricarboxylic acid cycle products in excess glucose media. Basically, *S. cerevisiae* tends to ferment even though there is enough O_2 in the environment for aerobic respiration [19].

If there are enough nutrients in the media, the cells in a batch culture start to grow exponentially (2-fold increase in biomass per cell division time) after a lag phase. Exponential growth of the cell population continues up to the exhaustion of glucose in the media. In a typical fermentative batch culture of *S. cerevisiae*, the metabolism and the biosynthetic tendency are reprogrammed during a phase called the "diauxic shift". The diauxic shift occurs when glucose is exhausted and cells begin to consume ethanol and acetate, which are produced in the exponential growth. This phase is generally called as post-diauxic phase. When there is no more carbon source in the surrounding media, cells undergo stationary phase (see

Figure **1.5**) [20].

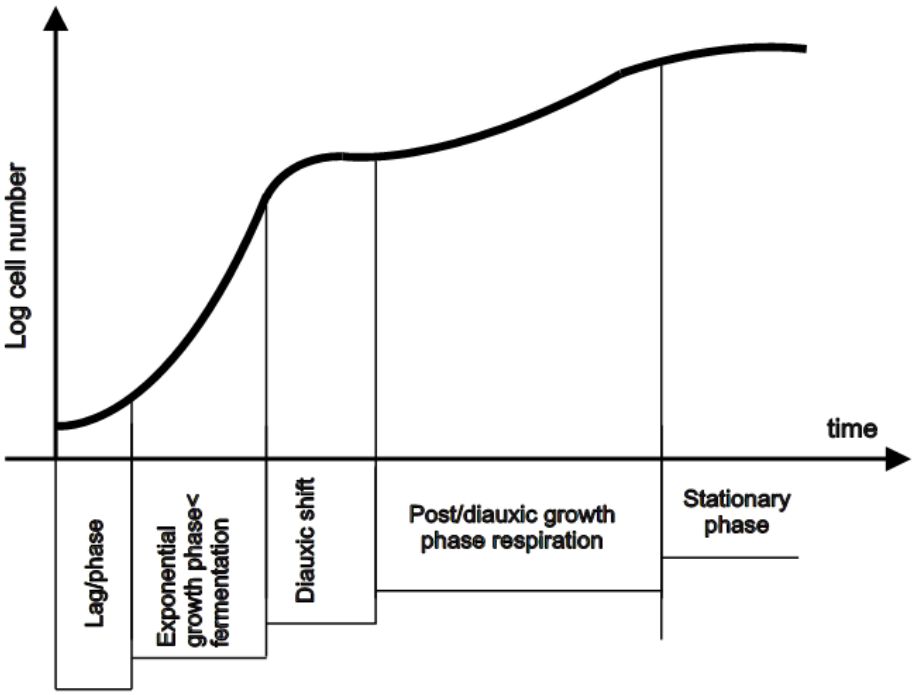

Figure 1.5: Cell Density Profile and Growth Phases of *S. cerevisiae* in a Batch Culture [20]

1.2.1 Metabolic remodelling in diauxic shift

Before the diauxic shift, cells tend to use fermentative pathways rather than the TCA cycle and oxidative phosphorylation. After the diauxic shift, the fermentative products are utilized in respiration and oxidative phosphorylation in mitochondria [19; 21].

In exponential phase, aerobic respiration of glucose, somehow, has a lower flux as compared to fermentative metabolic flux. In diauxic shift, all metabolic events related to energy metabolism are directly affected by redirection of carbon flux from fermentative pathway to respiratory pathway (see Figure 1.6). Apart from energy metabolism change, switching to aerobic respiratory pathways increases the ROS production, which may elicit an oxidative stress response [22].

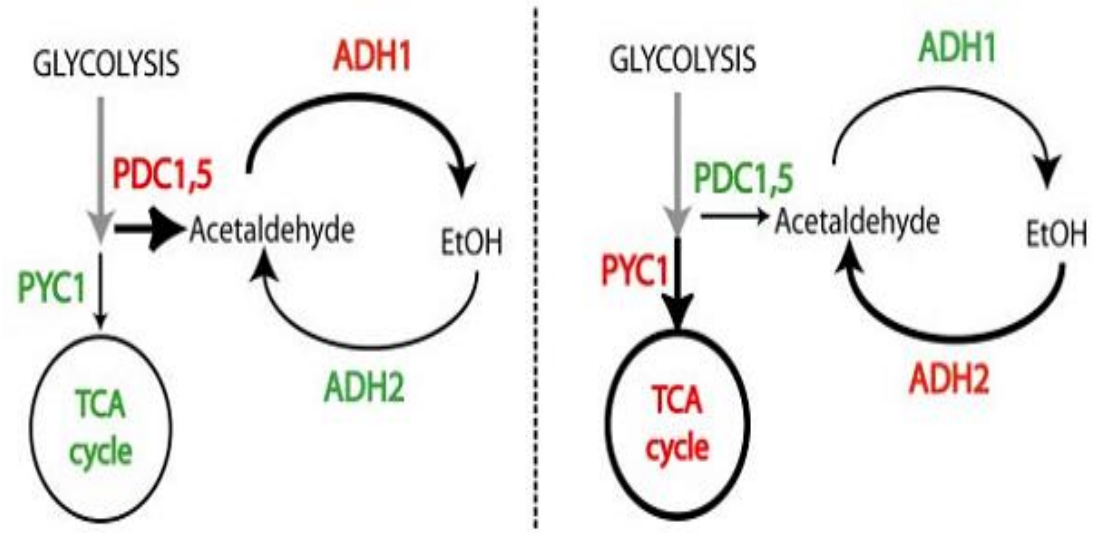

Figure 1.6: Gene expression profile of carbon flux before (left) and after (right) diauxic shift. Red refers increase in gene expression while green refers decrease in gene expression. Only key genes/gene groups for carbon flux branches are shown [21].

The genes involved in protein synthesis are up-regulated before diauxic shift. After diauxic shift, protein synthesis genes are down-regulated to recover the energetic state of the cell. Although there is some oxidative phosphorylation activity during the exponential growth, the genes related to oxidative phosphorylation are strongly induced in the post-diauxic shift phase, which favours aerobic respiration [21].

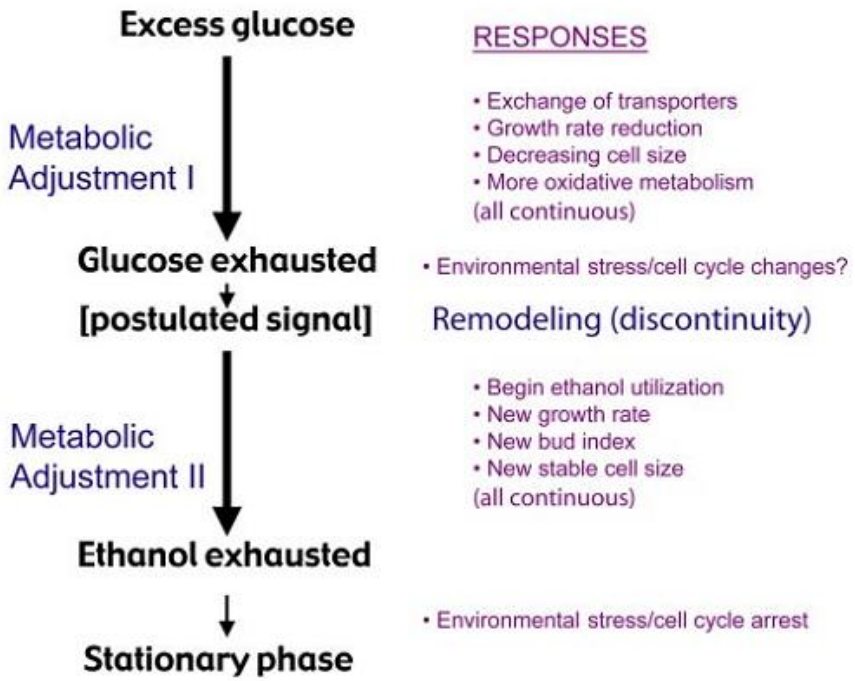

Figure 1.7: Metabolic Adjustments During Diauxic Shift [21]

As indicated in Figure 1.7, during the diauxic shift (just after glucose is exhausted) there is a discontinuous period of carbon metabolism while metabolism is remodelled. In the time period while glucose is being exhausted, cells continuously exchange their transporters from low affinity to high affinity, decrease cell growth and cell size and increase the oxidative respiration metabolism. When glucose is completely exhausted, there is a metabolic adjustment which triggers this discontinuous remodelling. After remodelling, cells begin to utilize ethanol and acetate (also other TCA products), create a new bud index and stabilize their cell size [21].

1.2.2 BioLector: monitoring batch cell growth by light scattering

The BioLector (from DASGIP AG) is a bench top, microfermentation system based on light scattering technology (see Figure 1.8). It enables automated, rapid and simultaneous screening of biomass, green fluorescence protein (GFP) signal detection, pH and pO_2 all together while performing up to 96 reactions at 100-1500 µl scale. It can be used for cellular screening, growth activity, media optimization, gene & protein expression, enzyme activity and toxicity tests. Specially designed 48 well growth plates, so called “flower plates”, provide improved mixing compared to

round or square well plates and allow cell cultures up to 1500 µl. The LSU measurements can be taken as frequently as once every 3 minutes for each well in the 48-well flower plates. In addition to this, flower plates are sealed with gas permeable membranes, which allow O_2 exchange but do not allow infiltration by microorganisms that could cause contamination of the cultures inside the plate wells.

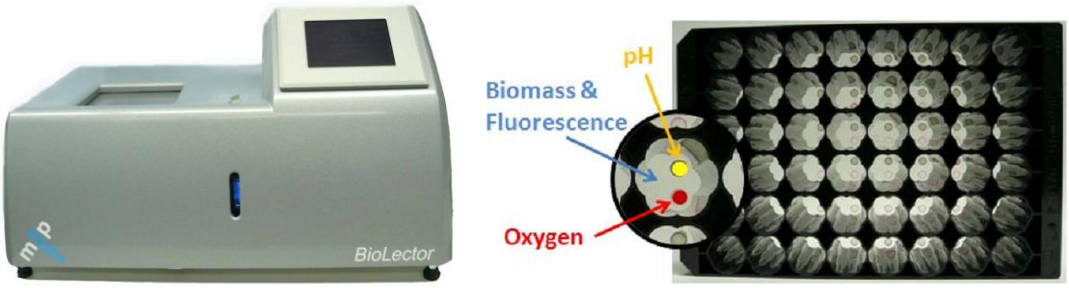

Figure 1.8: BioLector Microfermentation System (Left) and 48 Well Flower Plate (Right)

There are three common methods to measure the cell density in a particular batch fermentation progress: cell dry weight (CDW), optical density (OD) and cells per volume (C/v using a Coulter counter). The use of light scattering properties, measured in light scattering units (LSU), is a fourth method and has been shown to compare well to OD methods [23]. Cell dry weight has to be determined by washing the cells with physiological water (9 g/L NaCl solution) and drying the cells at a high temperature (like 105ºC) until the dry weight of the cells remain constant. On the other hand, OD measurements take place in spectrophotometers which are generally set to 600 nm wavelength and the absorption of light at 600 nm is related to the biomass/cell density. BioLector microfermentation platform uses light scattering at 620 nm for cell density measurements [23]. The advantages of the BioLector system are discussed below.

Biomass calibrations for the BioLector have been done with both CDW and OD. Nevertheless, OD and CDW correlation is linear only between the 0.1-0.3 OD range. Thus, it is vital to dilute the samples and re-measure their ODs if the measured value is outside this range, likely introducing error in the dilution process. Scattered light measurements have an advantage over OD measurements because biomass concentrations have been shown to have a more linear correlation to LSU up to high

LSU ranges [23]. Since OD measurements are not linear correlated with high biomass, LSU can alleviate this problem for on-line measurements (see Figure 1.9).

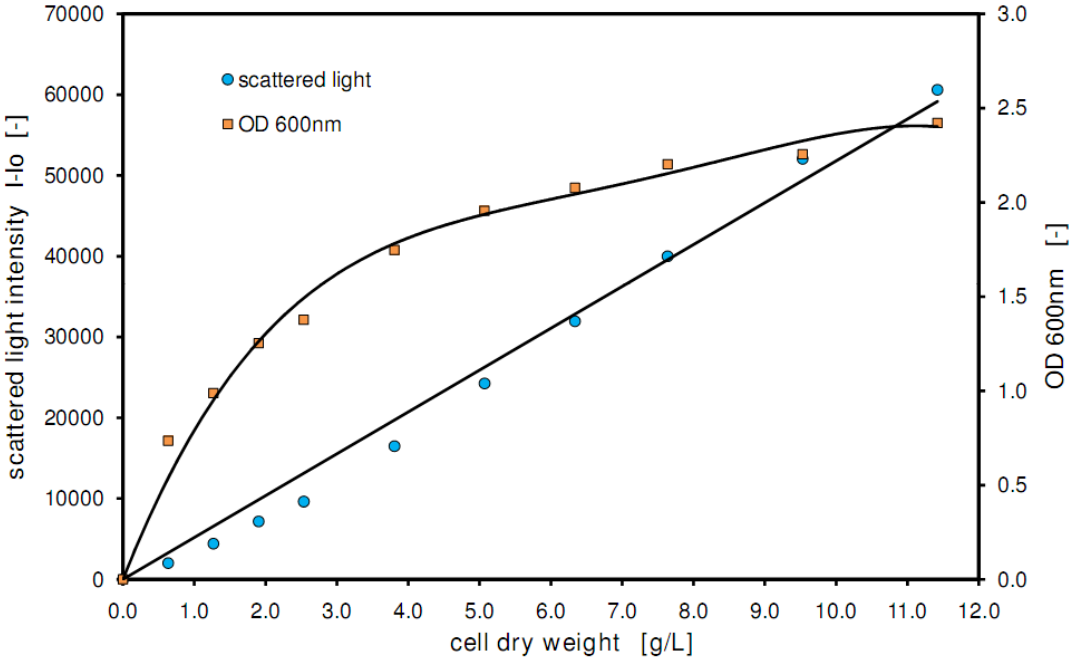

Figure 1.9: LSU vs. OD Correlation with CDW [23]

For standard microtiter plates, OD measurements have two common disadvantages. Firstly, wells of the microtiter plates are sealed with gas permeable membranes due to protection against contamination; therefore it is not possible to make transmission measurements. Secondly, the shaking of the microtiter plate has to be stopped to take samples for OD measurements which could cause the sedimentation of cells and the dissolved O_2 distribution in the wells of microtiter plate, thus all fermentative metabolism can be effected by the sampling process [23].

1.3 Stress Responses of *Saccharomyces cerevisiae*

All cell types share common features such as growth, cell division, responding to the environmental changes and also adapting to these environmental changes. Unicellular organisms like *S. cerevisiae* are faced with many diverse environmental conditions that may vary in the physical or chemical nature such as temperature, pressure, pH, concentration of chemicals and ions, availability of water, radiation, toxic chemicals etc. Behind such responses to the environmental changes, there is a complex network of sensors that detect changes and stimulate various signal transduction pathways which lead to the adaptation of cell to these environmental

changes by changing the gene expression profile, metabolic activities etc. In this project, "stress" refers to environmental conditions that negatively affect the survival, repress the optimal growth or other functions of the cell. To overcome various stress conditions, *S. cerevisiae* evolved many different stress response mechanisms [24-38]. Responses to various stress types of *S. cerevisiae* are complex. Developing molecular tools like transcription analysis using DNA microarrays [22] and screening the entire sets of yeast deletion mutants [24; 25] increased the understanding of which genes are involved for a particular type of stress or common response pathways.

1.3.1 Key concepts of stress response studies

Studies about stress responses are generally carried out by shifting one particular condition to another like medium without H_2O_2 and then 5 mM H_2O_2 containing medium [26] or shifting temperature from 25ºC to 36ºC [27]. Dramatic shifts of conditions, however, can be tricky to understand the real mechanisms behind the stress responses, because these dramatic shifts may not always be always related to the environmental conditions which cells face in nature, for example changes in nature can be slow and gradual. On the other hand, rapid shifts in conditions can provide convenient means to study these conditional changes. Indeed, there are many studies in literature whose findings are based on conditions that severely injure or kill cells.

Initially, a cell has to sense the stress, create a signal transduction for that and finally a gene expression against the stress occurs. In this particular flow of processes, time points are important to study the response. A closer inspection of early time points is also important in order to study any delay in the stress response.

Global gene/protein expression is another way to identify the stress response pathways. In global expression analysis of genes and/or proteins, genetic alteration may not generate a clear interpretable stress phenotype due to:

i. Minor effects may not be detected by present methods,

ii. Functional redundancy,

iii. Compensating pathways,

iv. Indirect gene expression which may not be effective on that particular stress response [28].

As another consideration, unicellular organisms are typically studied in populations and dramatic shifts of environmental conditions, even though they are considered to be sub-lethal, can cause death to some fraction of the population. At this point, it is important to understand how individual cells behave. Thus, it is good to support the stress response analysis with individual cell data of e.g. flow cytometry [20].

When *S. cerevisiae* is treated with a stress that leads to tolerance for this type of stress, cells can somehow induce a tolerance for other similar kinds of stress. This mechanism is known as "cross-resistance". For instance, pre-treatment of *S. cerevisiae* cells with menadione is protective against a later treatment of menadione or H_2O_2. However, pre-treatment with H_2O_2 is only protective against a later treatment of H_2O_2, not menadione [26]. Thus, it is important to keep in mind that, one type of stress may not always create a bilateral cross-resistance to another type of stress.

1.3.2 Mitogen activated protein kinase (MAPK) pathways and stress response

To create a stress response, a cell has to be stimulated by a stress factor which triggers a signalling cascade of molecules as discussed in section 1.3. One of the most important set of cellular signalling cascades is the mitogen activated protein kinase (MAPK) pathways. MAPK are vital cell signalling molecules which are found in all eukaryotic organisms [29].

MAPK pathways are composed of three binders of protein kinases as a MAP kinase (MAPK), a MAP kinase kinase (MAPKK) and a MAP kinase kinase kinase (MAPKKK). The MAPKKK phosphorylates and activates MAPKK. Afterwards MAPKK immediately phosphorylates MAPK. MAPK is phosphorylated at its threonine and tyrosine residues which are located in the catalytic domain of MAPK [29-31].

One of the most well-studied MAPK pathways is the high osmolarity glycerol (HOG) pathway of *Saccharomyces cerevisiae* and it is discussed in section 1.3.5.

1.3.3 Oxidative stress response

Oxidative metabolism is considered to be both essential and dangerous for aerobic respiration. The evolution of aerobic metabolism from anaerobic metabolism provided efficient and high energy for the aerobic organisms. The dangerous part of aerobic metabolism is that it can induce reactive oxygen species (ROS) formation. ROS is able to react with and damage sub-cellular components especially DNA and proteins and result in vital damage. Indeed, oxidative stress is related to a variety of diseases like neurodegenerative, cardiovascular diseases, cancer and also aging [32; 33]. The response to oxidative stress differs according to the level of the stress. Cells can adapt to the low levels of oxidants and thus can more resistant whereas high levels of oxidants can cause a delay on cell cycle while inducing antioxidant synthesis and repair systems. On the other hand, very high concentrations of ROS can induce apoptosis [34].

The major ROS are composed of singlet oxygen ($^1O_2$), superoxide anion ($O_2^{-}\cdot$), hydrogen peroxide (H_2O_2), hydroxyl radical (·OH) and reactive nitrogen species nitrogen and oxygen containing molecules such as nitric oxide radical (NO·) and nitrogen oxide radical ($NO_2\cdot$). In particular, mitochondria produces most of the ROS because aerobic reaction is generated in mitochondria [35]. Figure 1.10 summarizes how ROS is generated in the cell.

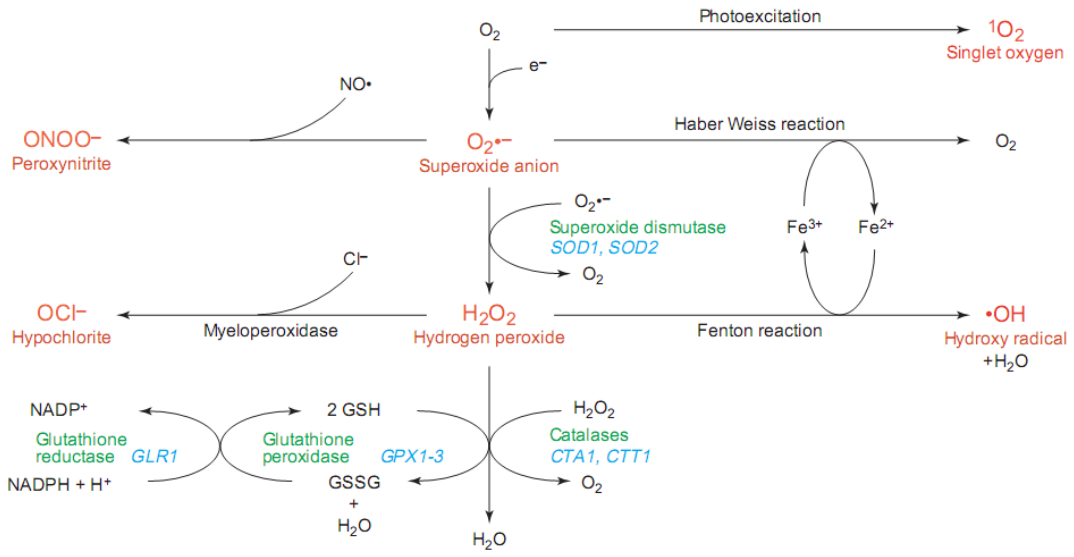

Figure 1.10: Generation of reactive oxygen species in the cell [34]

S. cerevisiae has two common defence mechanisms for oxidative stress response as non-enzymatic and enzymatic defence systems. Non-enzymatic defence systems are composed of small molecules which act as radical scavengers to remove the oxidant form the environment whereas enzymatic defence systems are required to remove the oxygen radicals and repair the oxidative damage [36].

1.3.3.1 Non-enzymatic oxidative defence systems

Non-enzymatic defence system includes glutathione (GSH), ascorbic acid, trehalose (see section 1.3.4), metallothioneins, thioredoxin, and glutaredoxin.

Glutathione: Glutathione is a tripeptide called γ-l-glutamyl-L-cystinylglycine (glutamate-cysteine-glycine) which protects cells from the harmful effects of ROS. GSH is mediated by *GSH1* (γ-glutamylcysteine synthase) and *GSH2* (glutathione synthase) in *S. cerevisiae*. A cysteine residue of GSH has low redox potential (-240 mV) which means that it tends to donate its electrons to other cysteines. Thus, when a GSH is oxidized, it dimerizes to GSSG. To reduce GSSG to GSH form, a glutathione reductase (*GLR1*) is involved. Normally, the cytoplasmic GSH:GSSG ratio in a yeast cell is in a range of 30:1 to 100:1 [37]..

Glutaredoxins: Glutaredoxins are also small proteins that contain two active redox-sensitive cysteines and two dithiol glutaredoxins that are encoded by *GRX1* and *GRX2* and three monothiol glutaredoxins that are encoded by *GRX3*, *GRX4*, *GRX5* [36; 38]. In recent years, redox sensitive green fluorescent proteins (roGFP) are used to detect cellular redox potential by coupling with glutaredoxins [39; 40].

Metallothioneins: These are small cysteine rich proteins (encoded by *CUP1* and *CRS5*), which have antioxidant properties, and they can bind to some metal ions such as Cu^{+} or Fe^{++} to reduce oxidative stress. For example, Cup1 is able to compensate for oxidative stress when they are over-expressed in Δ*sod1* mutants [41].

Thioredoxins: Thioredoxins are the other small proteins which contains two redox active cysteines in the conserved active site, Trp-Cys-Gly-Pro-Cys [20]. It has a low redox potential (-270 mV in *E. coli*) and it does not directly reduce ROS unlike GSH. Its duty is to activate the ROS scavenging enzymes Trx1, Trx2, Trx3 and Trr1, Trr2 [42; 43].

Ascorbic Acid: Ascorbic acid is a general antioxidant in eukaryotic organisms including higher eukaryotes, some plants and also *Saccharomyces cerevisiae* although the amounts found are low for *S. cerevisiae* [36; 44].

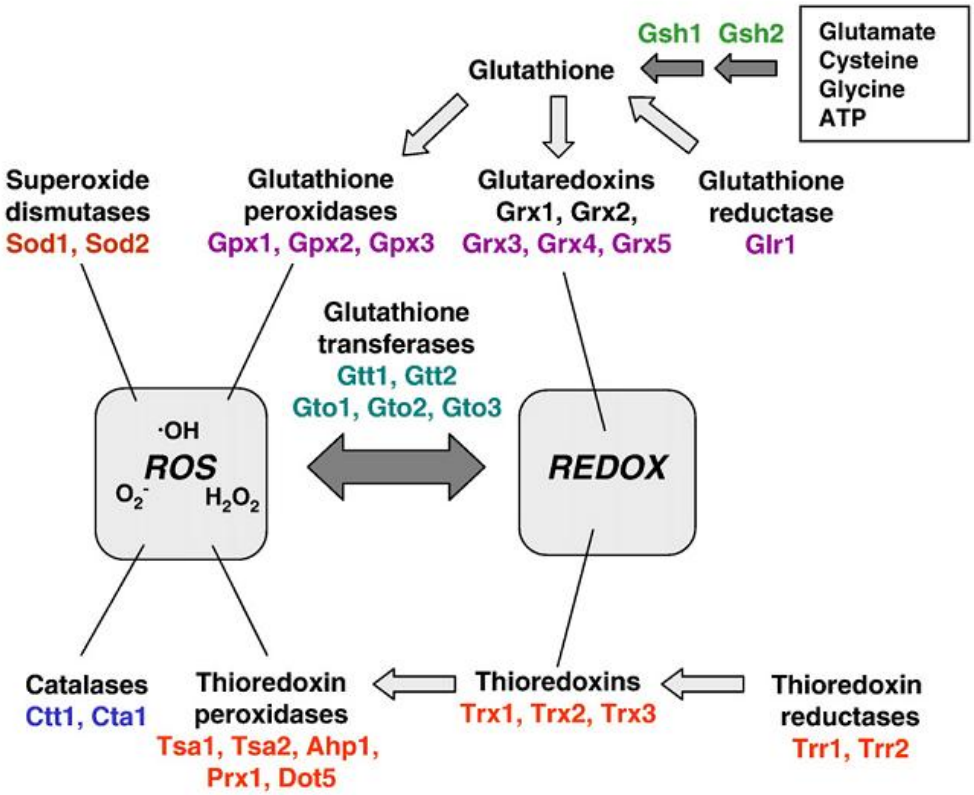

Figure 1.11: Enzymatic & Non-Enzymatic Oxidative Defence Mechanisms of *S. cerevisiae* and Their Relationship [44]

1.3.3.2 Enzymatic oxidative defence systems

Catalase is the most well-known enzyme in the oxidative stress response. Two types of catalase are expressed in *S. cerevisiae* as catalase A and catalase T encoded by *CTA1* and *CTT1*, respectively. Catalase mediates the breakdown of H_2O_2 to O_2 and H_2O and thus prevents the damages caused by H_2O_2. On the other hand, glutathione reductase, encoded by *GLR1*, reduces the oxidized GSH and glutathione peroxidase catalyses hydroperoxides (e.g. H_2O_2) with GSH. Thioredoxin peroxidase and thioredoxin reductase reduce H_2O_2 and alkyl-hydroperoxides by the formation of thioredoxin reductase-thioredoxin-NADPH complex. Lastly, Apn1 endonuclease (encoded by *APN1*) is an apurinic/apyrimidinic endonuclease which is highly sensitive to the oxidants that can damage DNA [36; 44].

Table 1.2: Oxidative Stress Response Mechanisms of *S. cerevisiae* [35]

Function	Gene(s)	Location*	Role
Antioxidant metabolites			
glutathione		General	Aqueous redox buffer, excretion of xenobiotics
ubiquinone		Mit, ER and Mem	Lipid soluble antioxidant, respiratory chain component
D-erythroascorbate		Cyt?	Water-soluble antioxidant
Enzymes			
catalases	*CTT1*	Cyt	Dismutation of H_2O_2 to H_2O+O_2
	CTA1	Per	
superoxide dismutases	*SOD1*	Cyt, Mit, Nuc?	Dismutation of O_2^- to $H_2O_2+O_2$
	SOD2	Mit	
SOD chaperone	*CCS1*	Cyt	Required for loading copper into Sod1p
thioredoxins	*TRX1*, *TRX2*	Cyt	Deoxyribonucleotide synthesis, sulphate assimilation, cofactor for some peroxidases, redox control
dithiol glutaredoxins	*GRX1*, *GRX2*,	Cyt, Nuc	Overlap with thioredoxins in many enzymatic functions, have glutathione peroxidase activity
monothiol glutaredoxins	*GRX3*, *GRX4*, *GRX5*	Nuc Mit matrix	Protect cells from redox damage Fe/S cluster assembly
peroxiredoxins	*AHP1*, PRX1	Cyt Mit	Reduction of alkyl peroxides, ROOH+R'SH=R'SSR'+ROH
thioredoxin peroxidase	*TSA1*	Cyt	Peroxiredoxin activity, thioredoxin peroxidase activity H_2O_2+ RSH=H_2O+RSSR. Also mediates nuclear localisation of Yap1p
sulfiredoxin	*SRX1*	Cyt, Nuc	Reduces cystein-sulfinic acid residues in Tsa1p, Ahp1p
glutathione peroxidases	*GPX1*, *GPX2*	Cyt/Mem	Reduction of oxidised lipid hydroperoxides
phospholipid hydroperoxide GSH peroxidase	*GPX3/ORP1*	Cyt	Has thioredoxin peroxidase activity. hydroperoxide receptor transducing signal to Yap1p
cytochrome *c* peroxidase	*CCP1*	Mit inner membrane space	Reduction of hydrogen peroxide in mitochondrion
glutathione synthesis	*GSH1*, *GSH2*	Cyt	Stepwise synthesis of GSH
glutathione reductase	*GLR1*	Cyt	Reduction of GSSG to GSH
pentose phosphate pathway enzymes	*ZWF1*, *GND1*, *TAL1*, *TKL1,2*, *RPE1*,	Cyt	Generation of NADPH for recycling of oxidised glutathione, glutaredoxins and thioredoxins
	ALO1, *ARA2*	Mit Outer Mem ?	D-erythroascorbate synthesis
Metal-binding proteins			
metallothioneins	*CUP1*, *CRS5*	Cyt	Copper binding protein, multiple genes at locus, also binds Cd^{2+}
Transcription factors, regulators			
Yap1p	*YAP1*	Cyt/Nuc	Oxidative stress, resistance to xenobiotics, cadmium
Skn7p	*SKN7*	Nuc	Auxiliary transcription factor, functions with Yap1p for some oxidative stress, also acts in osmoregulatin
Msn2/4	*MSN2*, *MSN4*	Cyt/Nuc	General stress responsive transcription factor responding to PKA pathway, responsive to heat, starvation, osmotic and oxidative stress
Yap1-binding protein	*YBP1*	Cyt	Protein involved in one mechanism for nuclear localisation of Yap1p
Haem activated protein	*HAP1*	Nuc	
	HAP2,3,4,5	Nuc	Regulation of respiratory functions
Metal-binding activator	*MAC1*	Nuc	Regulator of genes involved in copper ion homeostasis and H_2O_2-induction of *CTT1*
Cup2p	*ACE1/CUP2*	Nuc	Cu-binding transcription factor activates *CUP1* at high copper

*Cyt: cytoplasm; Mit: mitochondrion; ER: endoplasmic reticulum; Per: peroxisome; Nuc: nucleus; Mem: membrane; ? indicates not known or not certain.

Common oxidative stress response mechanisms are summarized in Table 1.2. In many cases, there are more than one gene encoding listed functions but within different compartments of the cell. Deletion knock-out strains of *S. cerevisiae* have shown that there are at least 450 genes are essential to maintain the redox balance and oxidative stress responses [25; 45].

1.3.3.3 Sensing oxidative stress

Under normal metabolic conditions, all the cells in a human body metabolize ~10^{12} O_2 molecules. ROS is produced from ~1% of these metabolized oxygen molecules. Moreover, heavy metals, UV radiation and alkylating agents stimulate the formation of ROS, too [46].

There are three common oxidative stress sensing mechanisms that trigger transcriptional regulation for oxidative response: stress responsive MAPK (SAPK) cascade, the multistep phosphorelay system and AP-1-like transcription factors [47].

A. SAPK cascade for oxidative response

Since eukaryotic organisms respond to various environmental factors, MAPK cascades are evolutionary well-conserved pathways. MAPK signalling cascades are involved in many cellular processes like proliferation, differentiation, apoptosis and homeostasis [47]. First discovered stress responsive MAPK (SAPK) pathway is HOG pathway of *S. cerevisiae* (see section 1.3.5).

Earlier studies stated that HOG MAPK pathway is only stimulated under high osmolarity. In contrast to this, recent studies refer that Hog1 is also involved in oxidative stress response whereas *hog1* mutants are sensitive to H_2O_2 and diamide [48].

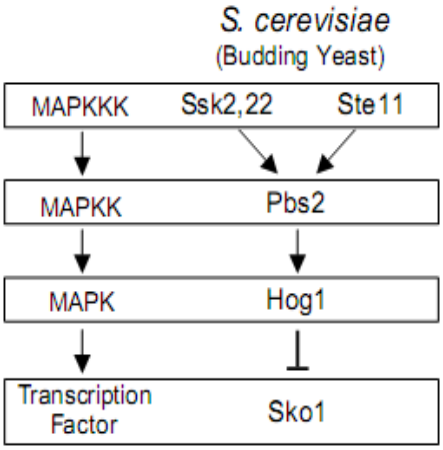

Figure 1.12: Stress responsive MAPK (SAPK) Pathway in *S. cerevisiae* (adapted from [47])

B. Multistep phosphorelay system for oxidative response

In multistep phosphorelay system, there are two regulatory kinases. One of them is a histidine kinase known as "sensor kinase". Sensor kinase phosphorylates its own kinase domain and this phosphate group is then transferred to the aspartate residue of the "response regulator protein". Response regulator protein acts as a transcription factor (TF) and activates the transcriptional oxidative stress response.

Sln1 phosphorelay system in *S. cerevisiae* is the regulator of HOG pathway (see details in section 1.3.5). Sln1 sensor kinase is a transmembrane protein. In its

cytoplasmic region, there is a histidine kinase domain. Sln1 is only active to autophosphorylate its histidine residue when there is low osmolarity conditions in the surrounding environment. A histidine containing phosphotransfer protein (HPt), Ypd1, transfers the phosphate group of Sln1 to Ssk1. The phosphorylated form of Ssk1 is inactive. When cells are exposed to high osmolarity conditions, Ssk1 is dephosphorylated and gets activated. As soon as Ssk1 gets active, it binds and activates Ssk2 and Ssk22 MAPKKKs and triggers the activation of HOG pathway starts [47]. The *sln1*Δ *ssk1*Δ double mutant is sensitive to H_2O_2 stress, thus Sln1 phosphorelay system also regulates oxidative stress responses [48].

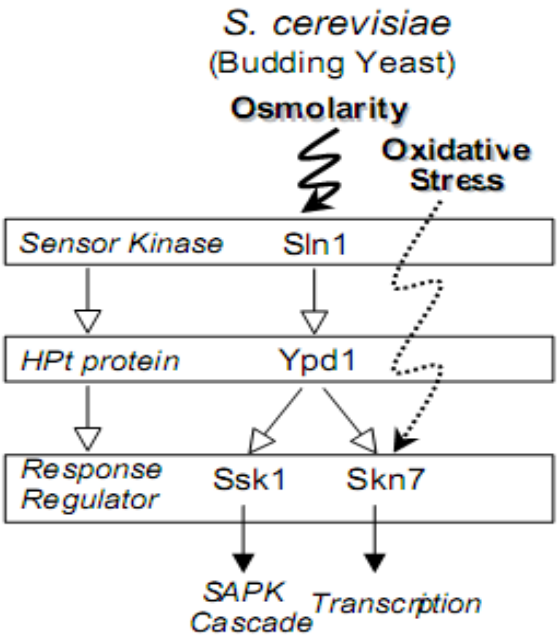

Figure 1.13: Sln1 Phosphorelay System of *S. cerevisiae* (adapted from [47])

C. AP-1-like transcription factors for oxidative response

Activating Protein-1 (AP-1) is a family of transcription factors. Jun, Fos and ATF are examples of this AP family in mammalians. Yeast homolog of this protein is Yap1 (Yeast Activating Protein-1). *yap1*Δ mutants of *S. cerevisiae* are H_2O_2 sensitive although they do not have obvious growth defects. In addition to this, Yap1 regulates many antioxidant genes like *TRX2*, *TRR1*, *GLR1*, *GSH1* [47].

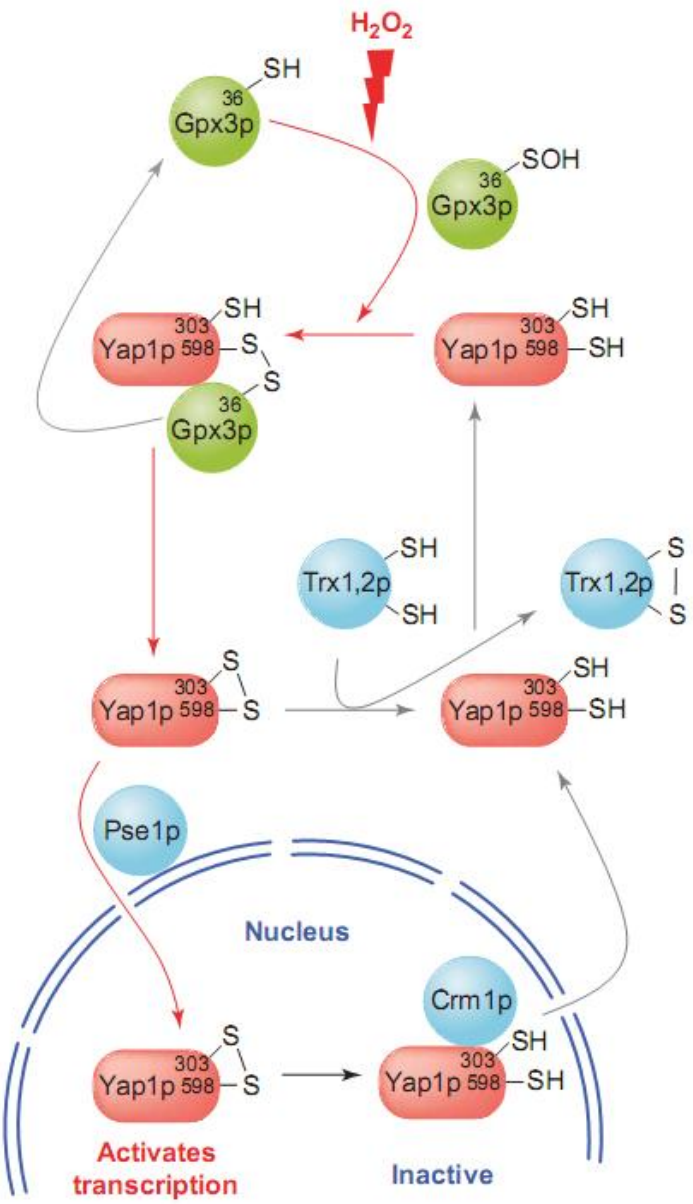

Figure 1.14: The role of Yap1 on ROS Sensing and Transcriptional Regulation [34] Red arrows: H_2O_2 induced nuclear localization of Yap1, Grey Arrows: Restoring the inactive state of Yap1; Grx3: H_2O_2 sensor, Trx1/2: Thioredoxins; Pse1: import activator of Yap1; Crm1: export activator of Yap1

Yap1 can be found in both cytosol and nucleus. This localization is encoded to the signal sequences of Yap1. Yap1 has a DNA binding nuclear localization signal (NLS) at N-term and nuclear export signal (NES) at its C-term. In resting conditions, NES is dominant to NLS which triggers the export of Yap1 form the nucleus. When the cell is exposed to H_2O_2; Gpx3 acts as a H_2O_2 sensor and triggers the two cysteines of Yap1, C598 (in NES) and C303 to form a disulfide bridge and thus

inhibits the activity of NES and as a result, nuclear accumulation of Yap1 starts [34; 47].

In addition to this, Yap1 regulates the synthesis of thioredoxin 2 and thioredoxin reductase by forming a regulatory loop which stimulates reduced thioredoxin formation. Once redox potential is recovered and maintained, the Yap1 is deactivated [34].

1.3.4 Heat shock response

All living organisms have a range of temperature they live and grow. Higher temperatures than the optimal living temperature lead to some heat-induced damages such as DNA strand breakdown, protein denaturation or aggregation, ribosome breakdown and some other metabolic damages. An important effect of heat shock on the cell membranes is increase of the membrane fluidity [49] and therefore permeability of the membrane to ions.

There are two different stages of response to the heat shock as early response and late response. Trehalose synthesis and then the heat shock protein synthesis are activated at early and late stages of heat shock response, respectively.

At early heat shock response, *S. cerevisiae* increases the synthesis of trehalose (see Figure 1.15) which is a disaccharide and produced by a variety of organisms. Trehalose is an important disaccharide for *S. cerevisiae*, because it is used both as energy-carbon source in vegetative cells and a stress response metabolite. It also acts like a chaperon against protein denaturation. The intracellular accumulation of trehalose leads adaptive protection to various kinds of stress like heat shock, nutrient starvation, dehydration and oxidative stress. Since trehalose is a non-reducing chemical, it can substitute with water molecules nearby the polar head groups of phospholipids [50; 51].

In 1858, M. Berthelot found this disaccharide in the cocoons of the beetle *Larinus* which is used for medical purposes in Persia and Ottoman Empire. The *Larinus* cocoons were called “trehala” thus Berthelot used this term for naming this sugar as “trehalose” [52].

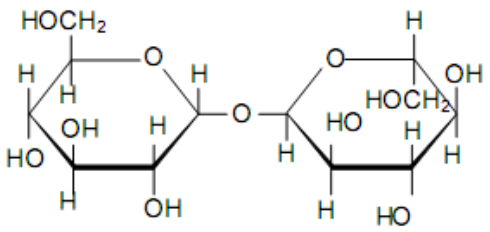

Figure 1.15: Chemical formula of trehalose [52]

The enzymes Tps1 and Tps2 catalyze synthesis of trehalose in *Saccharomyces cerevisiae*, respectively. Production of trehalose occurs in two steps in the cytosol. First, the glucose part of uridine-diphosphate-glucose molecule joined to glucose-6-phosphate, which then makes the formation of trehalose-6-phosphate while uridine-diphosphate is released. Finally, the phosphate group in trehalose-6-phosphate is released to be inorganic phosphate and so regenerated while forming just trehalose. Tps1 and Tps2 associates a "trehalose-synthase complex" with either Tsl1 or Tps3 to regulate the synthesis of trehalose [52].

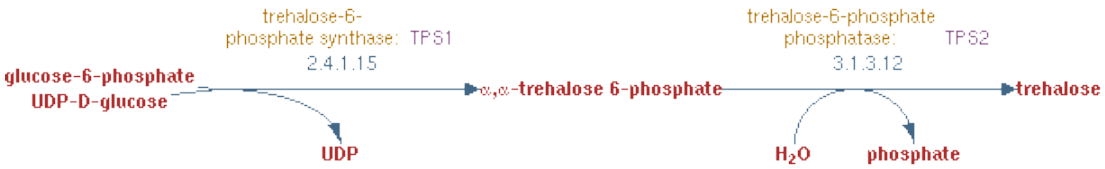

Figure 1.16: Biosynthesis of trehalose [53]

Trehalose accumulation is a marker event of heat-shock response, because a transient cell cycle arrest of G1 phase occurs when exposed to heat-shock. On the other hand, a sudden shutdown of protein synthesis occurs in the cell that defends newly synthesized proteins from denaturing. Following this event is the activation of the heat shock proteins. Trehalose accumulated in the cell prevents native proteins from denaturing and denatured proteins from aggregation, because *in vitro* as heat causes proteins to denature [52].

At late heat-shock response, the induced heat shock proteins (Hsp's) work on refolding the denatured proteins. Two-dimensional SDS-gel electrophoresis has shown that 52 proteins are induced after heat shock whereas the remaining proteins are expressed less than the control condition. This expression profile means that these 52 proteins are involved in heat shock response, while the remaining proteins

are not expressed more due to sudden shut-down of protein synthesis. When there is a heat shock of temperature shift from 25°C to 38°C, heat shock transcription factor (Hsf1) and the stress-responsive transcription factors Msn2 and Msn4 are expressed in late phase of heat-shock response. Half of the induced proteins are dependent on Hsf1 and the other half of the induced proteins are dependent on Msn2 and Msn4 [54]. Figure 1.17 below states an overall flow of heat-shock response as a summary of the heat shock response of *Saccharomyces cerevisiae*.

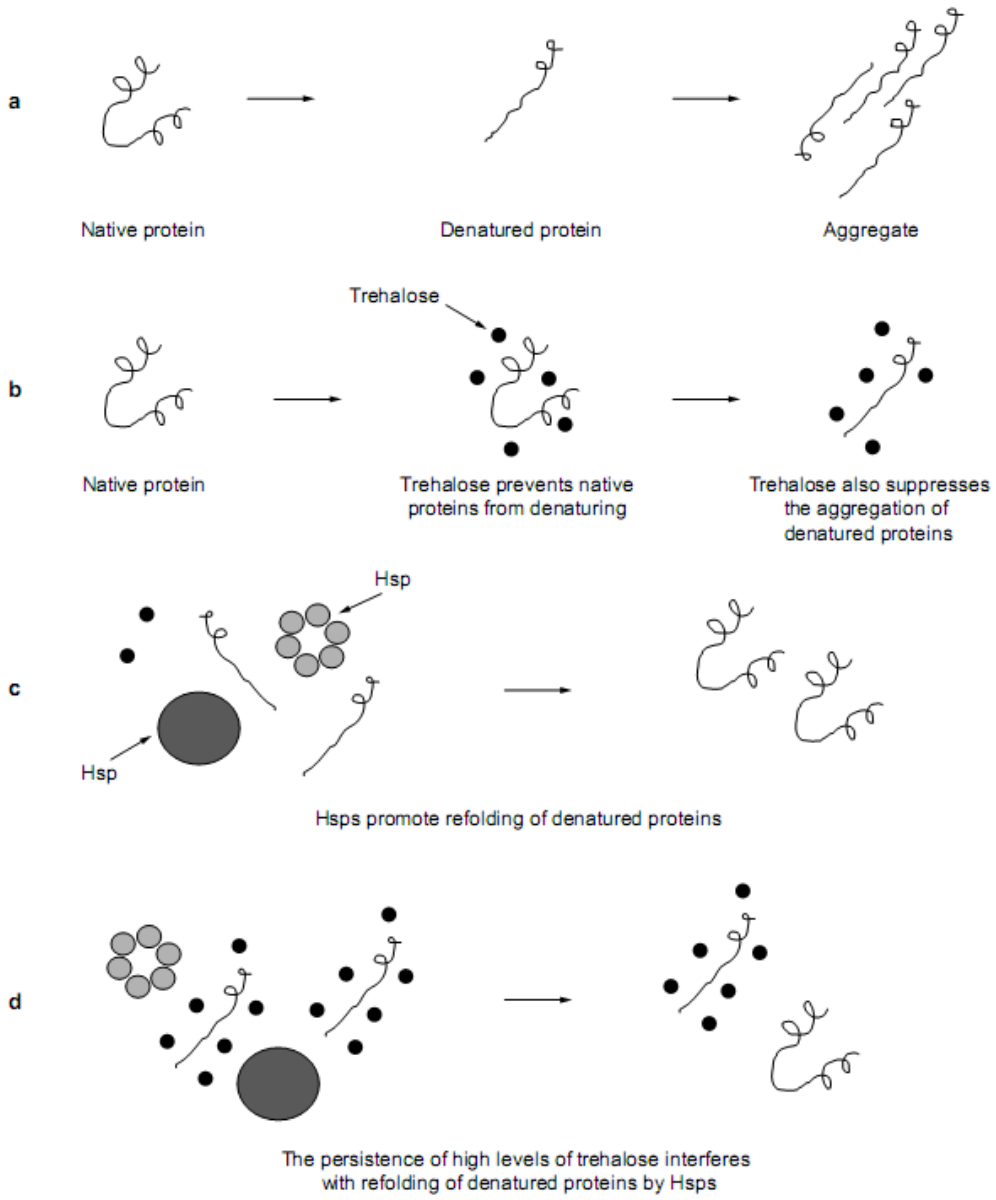

Figure 1.17: Early and late heat shock responses of *S. cerevisiae* **A.** The effect of heat shock to the proteins **B.** Early heat shock response - Protective effect of trehalose against heat shock **C.** Late heat shock response - Response of heat shock proteins to heat shock stress **D.** Reactivation of denatured proteins trigger trehalose degradation during heat shock recovery [52]

1.3.5 Osmotic & salt stress response

Dissolved molecules in the media that cells live in can cause osmotic stress due to altering the availability of water. If the dissolved molecules in the water increase, osmolarity will also increase which results in decreased water activity and water potential. The opposite is also true and reduced concentration of dissolved molecules leads decreased osmolarity. The principle of osmosis is that water always flows through a semi-permeable membrane to the higher osmolyte concentration. Microorganisms tend to stabilize their internal osmotic pressure a bit higher than the surrounding medium (see Figure 1.18). The differences of these internal and external pressures are counteracted by the cell wall and thus it is called as cell turgor pressure. Since water can pass across all biological membranes more than other solutes, all of the living organisms are affected due to solute concentration. Therefore, hypo-osmotic stress (decrease in external osmolarity) causes water inflow to the cell and yeast cells produce and accumulate osmoprotectants (e.g. glycerol) to increase internal osmolarity. Furthermore, hyper-osmotic stress (increase in external osmolarity) causes water outflow from the cell and so yeast cells tend to export the solutes immediately to avoid excessive turgor pressure or later cell burst [20].

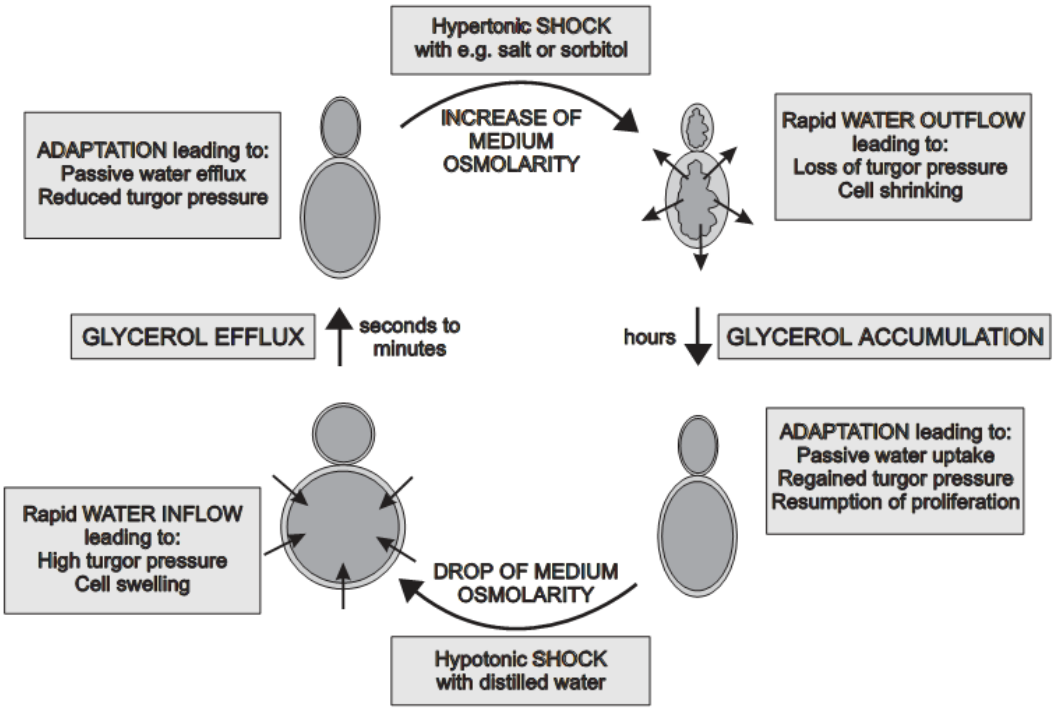

Figure 1.18: Hyper/Hypo-osmotic stress response of *S. cerevisiae* [20]

In hyper-osmolarity conditions, *S. cerevisiae* shrinks in seconds and the glycerol export channel Fps1 is closed in less than 1 minute to prevent glycerol leakage. At the same time, high-osmolarity glycerol (HOG) pathway is activated via a mitogen-activated protein (MAP) kinase pathway (see Figure 1.19) whose homologous osmo-sensing pathways exist. To prepare the cell to lower water amount, the metabolism is adjusted to produce protective molecules and glycerol is accumulated. If the osmolarity changes to hypo-osmotic conditions, rapid export of glycerol occurs unlike hyper-osmolarity conditions [20; 31].

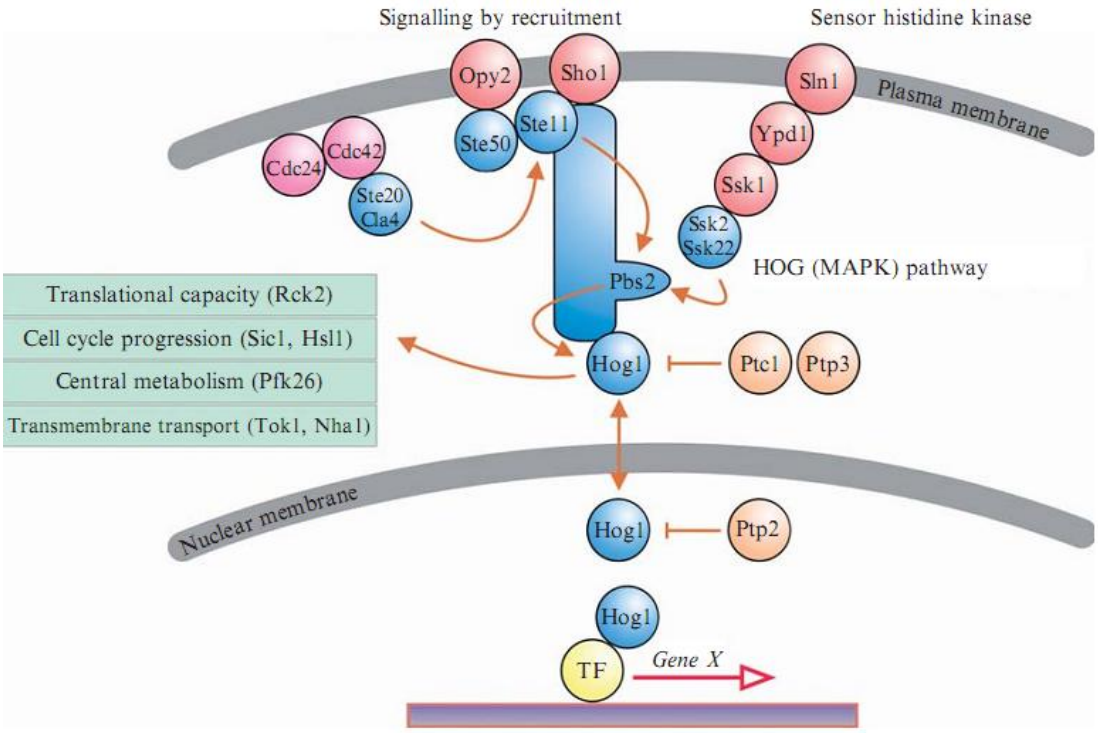

Figure 1.19: HOG pathway and summary of response mechanisms to osmotic stress in *S. cerevisiae* **A. Sho1 Branch:** Cdc42/24:G protein, Ste20: PAK protein kinase, Opy2, Sho1: membrane protein scaffold, Ste11/Ste50: MAPKKK, Pbs2: MAPKK **B. Sln1 Branch:** Sln1-Ypd1-Ssk1: sensing histidine kinase phospho-relay system, Ssk2/22: MAPKKK **C. Shared Branch:** Hog1: MAPK; Ptc1, Ptp2/3: protein phosphatases, TF: transcription factor [31]

As defined in Figure 1.19, there is a complex network of MAPK cell signalling for HOG pathway. There are two main branches of HOG pathway as Sho1 branch and Sln1 branch. These two paths intersect at Hog1 MAPK transduction. In addition to these, Ptc1, Ptp2/3 are the protein phosphatases which down regulates the activity of Hog1 MAPK, thus HOG pathway is compensated with the activity of these phosphatases [31].

1.3.6 Freeze-thaw stress response

Freezing the yeast cells may induce two types of damage in the cell as an effect of dehydration and crystallization. First, cellular dehydration occurs when the cells are frozen and thus, proteins can be denatured due to dehydration. In addition, the ice crystals are formed during freezing process. These ice crystals expand as compared to the liquid water form and therefore, they can damage cellular macromolecules. The survival of the yeast cell after thawing would decrease due to these two injuries [55]. The HOG pathway (section 1.3.5) is activated to tolerate these injuries, which increases intracellular glycerol production [56].

1.3.7 Ethanol stress response

S. cerevisiae is a Crabtree positive yeast, thus it tends to use glucose for ethanol fermentation by Embden-Meyerhof pathway although there is oxygen in the environment [19-21]. During fermentation process, ethanol is produced and it is accumulated in the surrounding medium of *S. cerevisiae* population. Increasing ethanol concentration can affect the components of cell membrane of the yeast by dissolving lipids of the membrane. Therefore the stability of the membrane decreases and membrane fluidity is not maintained. As a response to increasing concentration of ethanol in the surrounding environment of *S. cerevisiae*, it is reported that yeast can adapt to ethanol by increasing intracellular trehalose and proline concentration; and also changing the membrane components to maintain the fluidity of membrane [57].

1.3.8 Metal stress response

Heavy metal stress is generally related to the oxidative stress since the presence or absence of little amounts of heavy metal ions can dramatically change the redox state of the cell. Heavy metal ions are charged positively and they can show both redox as well as non-redox effects [58]. H_2O_2 is moderately degraded to hydroxyl radical (·OH), in the presence of reduced transition metals. Therefore, heavy metal stress is strongly related with oxidative stress [44]. In addition to this, various kinds of heat shock proteins are also involved in heavy metal stress response [59].

Iron molecules have oxidative effects as described in the Fenton Reactions (see Figure 1.10). Moreover, cobalt makes oxidative stress by increasing the ROS in the

cell. Indeed, cobalt can substitute magnesium and calcium, which are involved in essential metabolic reactions [60].

1.3.9 Cross stress resistance

In this section 1.3, the stress responses of *S. cerevisiae* are discussed. There are many stress response mechanisms related to each other. For example, the signalling pathway of oxidative stress response is extremely related to high osmolarity glycerol (HOG) response while heavy metal stress response shows some connections to oxidative response systems. This type of related adaptation mechanisms are referred as “cross-adaptation”.

Even though the mechanism of cross-adaptation is not well understood, one oxidant can increase another kind of oxidant so cellular response could share common response pathways. Figure 1.20 indicates some of the cross adaptation hierarchy upon different oxidants.

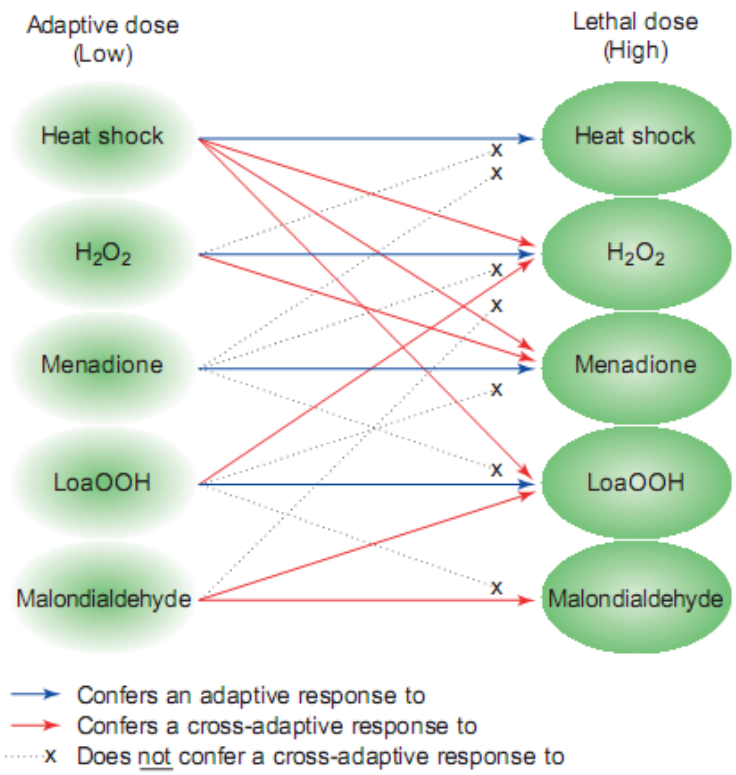

Figure 1.20: Cross-adaptation Hierarchy of Adaptive to Lethal Doses of Oxidants [34]

1.4 DNA Damage Checkpoints, Oxidative DNA Damage and Repair Mechanisms of *Saccharomyces cerevisiae*

DNA damage is a natural process occurred in cells due to radiation, ROS, replication etc. When there is DNA damage in a cell, there are two fates for cell: inducing apoptosis or repairing the damaged DNA. In response to DNA damage, cells undergo cell cycle arrest which is triggered by DNA damage checkpoints, hence enough time is provided for the cells to repair damaged DNA chromosomes before entering mitosis [61].

Naturally, *S. cerevisiae* has DNA damage, replication and mitotic checkpoints as defined in Figure 1.21. As a response to DNA damage, *RAD17*, *RAD24* and *MEC3* are activated in G1, S and G2 phases. These checkpoint genes trigger a downstream transducer and effector functions (via the genes below the line, listed in Figure 1.21) when DNA damage is detected [62]. *S. cerevisiae* lacks a true ortholog for the p53 gene so there is not a long G1 arrest and a robust apoptosis mechanism compared to higher eukaryotes. The cell cycle arrest occurs before anaphase when the mitotic spindle is attached to the centromeres of replicated chromosomes and it is called as G2/M transition arrest [61].

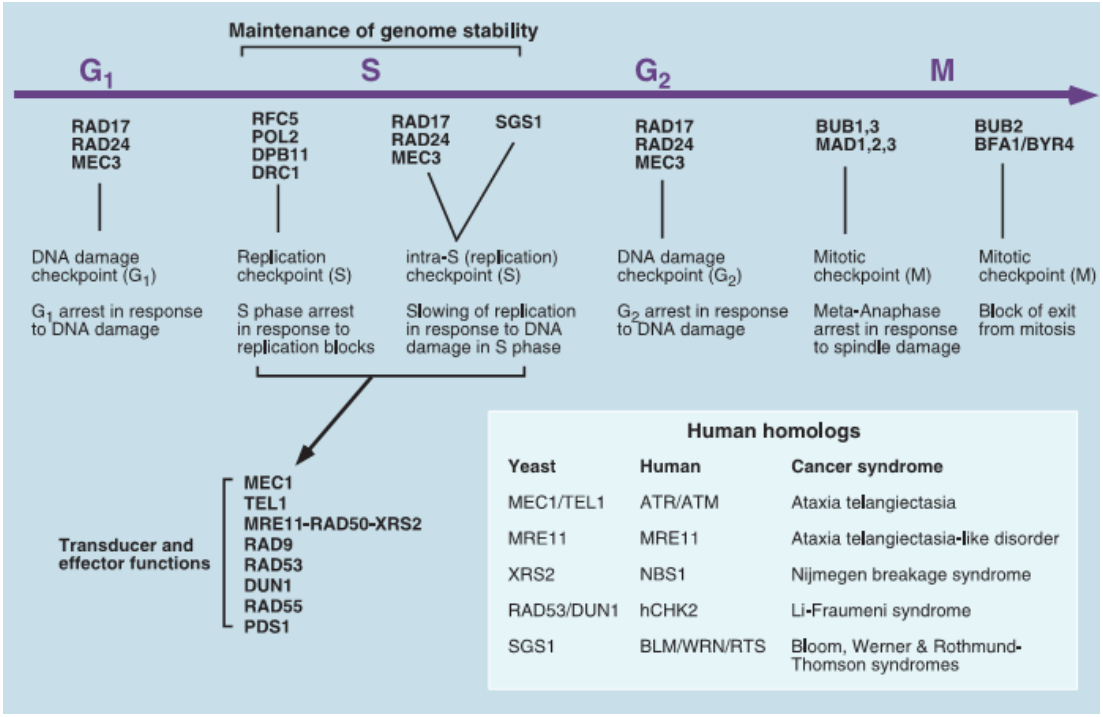

Figure 1.21: Genes Involved in DNA Damage & Replication Checkpoints During Cell Cycle [62]

Single-stranded DNA (ssDNA) damage is detected by Mec1, which is an important sensor kinase (see Figure 1.22). Then Mec1 transmits the DNA damage checkpoint signal to Rad53 and Chk1 and these two kinases amplify the checkpoint signal generated by Mec1. Hence, the checkpoint signal stimulates arrest of cell cycle prior to mitosis. In addition to this, Rad53 and Chk1 also require Rad9 for their activation [61; 63].

As a DNA damage response, nucleotide excision repair (NER) and base excision repair (BER) are activated and thus ssDNA gaps increases in DNA. Mec1 is also activated by the increasing gaps due to BER and NER. Besides, blunt-ended DNA is recognized by Tel1 and MRX complex. In some cases when Mec1 is absent or deleted [61], Tel1 can also activate Rad53 as an S-phase checkpoint inducer (dashed black arrow in Figure 1.22).

DNA damage checkpoints create three different responses [61]:

i. Phosphorylation of histone H2AX (γ-H2AX)
ii. Arrest of cell cycle prior to anaphase (G2/M transition)
iii. Induction of DNA damage genes and posttranslational regulation of ribonucleotide reductase (RNR). The *mec1*Δ or *rad53*Δ cells increase RNR activity to compensate DNA damage response signalling [64].

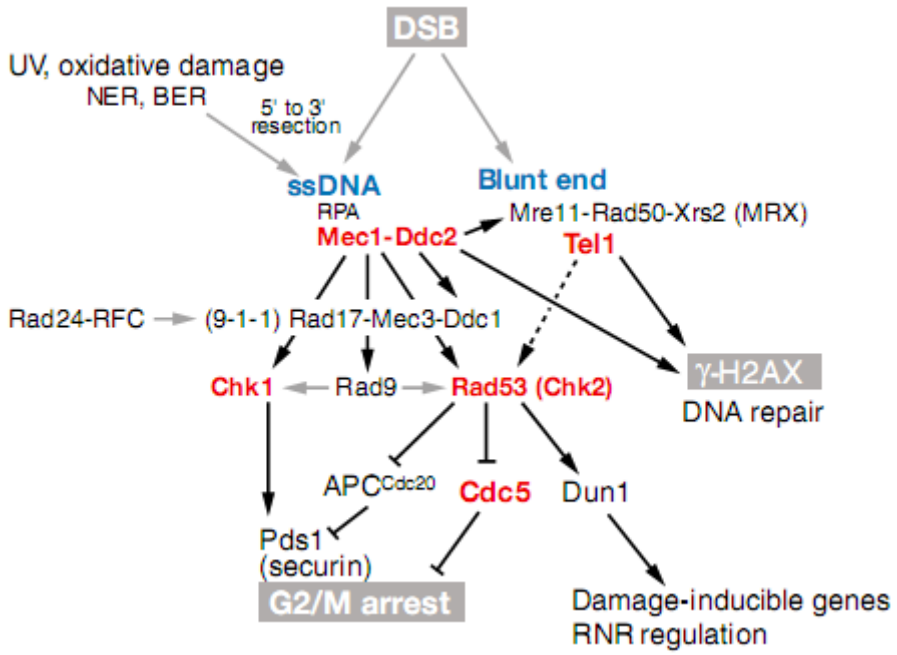

Figure 1.22: Signalling cascades due to DNA damage in *Saccharomyces cerevisiae* [61]

Oxidative DNA damage is an unavoidable consequence of cellular metabolism. ROS is constantly generated due to the aerobic metabolic events and it has damaging effects on many cellular structures. As discussed in section 1.3.3, oxygen paradox of aerobic life has the advantage of high efficiency energy production but it is highly dangerous for the organism, because of this; organisms have many oxidative stress response activities.

There are more than 20 identified base lesions of DNA due to oxidative stress, but only a few of them are well-studied and referred to be a measurement index for oxidative stress in cells [65]. A biologically important lesion is 7,8-dihydro-8-oxoguanine (8-oxo-G) base structure on DNA is generated under ROS activity. 8-oxo-G (see Figure 1.23) is able to make a pairing with adenine (A) which will later cause C:G to A:T transversion mutation at the following replication. There are two common reasons of 8-oxo-G structure has a steady state in the mitochondria. First, there are no histone molecules in mitochondria, which will protect the DNA strands from interaction with any molecule, and second, the oxygen metabolism (e.g. oxidative phosphorylation) in mitochondria is higher than the other compartments of cell [66].

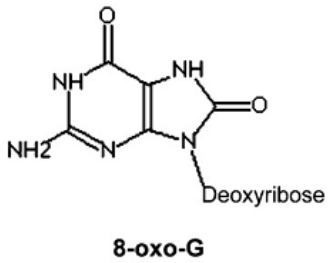

Figure 1.23: Chemical Structure of 8-oxo-G [67]

A human cell can generate 1000-2000 8-oxo-G lesions in a day. The presence of 8-oxo-G is the indicator of oxidative stress and C:G to A:T transversions. In recent studies it is found that C:G to A:T transversions lead cancer. [67]. In addition to this, it is known that oxidative DNA damage causes mitochondrial genomic instability of *S. cerevisiae*. Sod2 neutralizes the ROS to decrease the oxidative DNA damage while Ntg1 removes the oxidative DNA lesions [68].

On the other hand, 8-oxo-G DNA glycosylase (encoded by *OGG1*) is an important enzyme that recognizes the 8-oxo-G:C base pairs and catalyzes the cleavage of 8-

oxo-G. The human OGG1 DNA glycosylase (*hOGG1*) shows a considerable homology with *S. cerevisiae* OGG1 (*yOGG1*) [67].

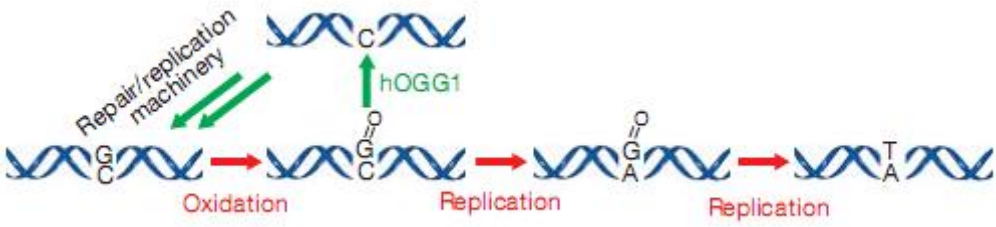

Figure 1.24: Repair of 8-oxo-G Lesion by OGG1 DNA Glycosylase. Green arrows indicate the repair pathway while red arrows indicate the C:G to A:T transversion due to oxidative DNA damage [69]

Once 8-oxo-G lesion is recognized by Ogg1, 8-oxo-G base is excised. The abasic site of the DNA is later repaired by base excision repair machinery. Otherwise, if the replication occurs, the C:G to A:T transversion follows it immediately which causes the mutagenesis [69].

1.5 Aim of the Study

The objective of the project is to reveal the growth effects of oxidizing environment on protein kinase/phosphatase knock-out (KO) mutants of *Saccharomyces cerevisiae*. As a growth effect, oxidizing environment has effects on both DNA damage and protein damage. Hence, studying with protein kinase/phosphatase KOs would enhance to investigate the contrast of effects of oxidizing agents as kinase/phosphatase pathways in the yeast cells would reveal the importance of them on the signal transduction and various expression pathways.

Two wild type strains of *S. cerevisiae* and 38 different protein kinase/phosphatase KO mutants were investigated for their oxidative stress responses. These 38 protein kinase/phosphatase mutants were selected according to their known activities on both general/oxidative stress response and DNA damage response which makes them candidates for the specific aim of this project.

To characterize these strains, hydrogen peroxide (H_2O_2) was used to create an oxidizing environment in different concentrations (as 0.25, 0.50, 1.0 and 2.0 mM) and all growth data for these strains was measured by a BioLector microfermentation platform.

One of the important goals of this project is also to investigate the metabolic remodelling during diauxic shift. At diauxic shift time interval, cells undergo a significant metabolic change. The exact diauxic response delay times were detected using the BioLector fermentation platform. In addition to this, common extracellular carbon sources are examined by using high performance liquid chromatography (HPLC) system at selected time points of diauxic shift, pre-diauxic shift and post-diauxic shift.

2. MATERIALS AND METHODS

2.1 Materials

2.1.1 Yeast strains

In this study, two sets of wild type yeasts and 38 knock-out (KO) mutants have been studied. The genotypes [70; 71] of the wild types are:

BY4741

Mat a, his3Δ1 leu2Δ0 met15Δ0 ura3Δ0

Y7220

Mat α, can1::STE2pr-Sp_his5 ura3::NatR lyp1Δ cyh2 his3Δ leu2Δ met15Δ0

The KO mutants are listed in the table below according to their functions:

Table 2.1: The KO genes and functions of 38 mutant strains

KO Gene	Function	KO Gene	Function
alk1	Protein Kinase	*pph3*	Protein Phosphatase
alk2	Protein Kinase	*prk1*	Protein Kinase
ark1	Protein Kinase	*ptc1*	Protein Phosphatase
bud32	Protein Kinase	*ptc3*	Protein Phosphatase
chk1	Protein Kinase	*ptp2*	Protein Phosphatase
cka2	Protein Kinase	*rad53 sml1*	Protein Kinase
dbf20	Protein Kinase	*rck1*	Protein Kinase
dun1	Protein Kinase	*rck2*	Protein Kinase
hal5	Protein Kinase	*siw14*	Protein Phosphatase
hog1	Protein Kinase	*sps1*	Protein Kinase
kin1	Protein Kinase	*ssk2*	Protein Kinase
mec1 sml1	Protein Kinase	*ssk22*	Protein Kinase
mek1	Protein Kinase	*tel1*	Protein Kinase
mkk1	Protein Kinase	*vhs1*	Protein Kinase
oca1	Protein Phosphatase	*vps15*	Protein Kinase
pbs2	Protein Kinase	*yck1*	Protein Kinase
pkh1	Protein Kinase	*yck3*	Protein Kinase
pkh2	Protein Kinase	*ygk3*	Protein Kinase
pkp1	Protein Kinase	*ykl171w*	Protein Kinase

Table 2.1 summarizes the function of the genes and their descriptions. All of the functional and description information is retrieved from *Saccharomyces* Genome Database (SGD) [70; 71].

2.1.2 Yeast culture media:

2.1.2.1 YPD medium

The cell culture stocks were kept in YPD media with 15% glycerol content at -80ºC. A little amount of dissolved stock cultures were streaked onto the YPD agar plates for growth. The receipt for YPD medium [15] is shown in the table below. YPD is autoclaved at 121ºC for 20 minutes. The YPD agar plates were poured after the liquid form cooled down for easier handling. The antibiotic G 418 was poured into the YPD agar plates after cooling.

Table 2.2: YPD Media Composition

1% Bacto-yeast Extract	10 g
2% Bacto-peptone	20 g
2% Glucose	20 g
2% Bacto-agar (for agar plates)	20 g
G 418 (A1720, Sigma) Disulfate Salt Antibiotic for antibiotic containing plates	200 mg
Add ddH_2O up to / Final Volume	**1000 ml**

G 418 is the selection marker of the mutants for KanR gene [72]. Thus, wild types and *rad53*, *mec1* KO mutants are not able to grow on the G 418 containing agar plates, because they do not have the resistance gene (KanR) against G 418.

2.1.2.2 Synthetic-defined (SD) medium

Synthetic-Defined (SD) Medium is made of the stock solutions listed below. The final solution is filter-sterilized by using 0.22 µm filters. SD media was kept at +4ºC. All of the solutions are completed to their final volume with distilled-deionized water (ddH_2O).

SD media is prepared by using stock solutions for practical reasons. The receipt for SD-media preparation is shown in

Table 2.4. Solution 1 is always prepared immediately before mixing with other two stock solutions.

Table 2.3: Composition of Synthetic Defined (SD) Media

Yeast Nitrogen Base without Amino Acids (YNB w/o Amino Acids)	**1.7 g**
Ammonium Sulfate ($(NH_4)_2SO_4$)	5 g
10X Amino Acid Solution	100 ml
Glucose ($C_6H_{12}O_6$)	20 g (2%)
Add ddH$_2$O up to / Final Volume	**1000 ml**

Table 2.4: Stock Solutions of SD Media

Solution 1	YNB w/o Amino Acids + $(NH_4)_2SO_4$	800 ml
Solution 2 (Stock)	Glucose Stock (20%)	100 ml
Solution 3 (Stock)	10X Amino Acid Stock	100 ml
	Final Volume	**1000 ml**

Stock Solutions for SD Media

There are two stock solutions for SD media: 20% glucose and 10X amino acid stock solutions. In addition to these solutions, YNB w/o Amino Acids + $(NH_4)_2SO_4$ is prepared immediately just before use. All of the stock solutions are filter-sterilized.

Table 2.5: YNB w/o Amino Acids + $(NH_4)_2SO_4$ Solution

YNB w/o Amino Acids	2.125 g
$(NH_4)_2SO_4$	6.25 g
Add ddH$_2$O up to / Final Volume	**1000 ml**

Table 2.6: 20% Glucose Stock Solution

Glucose ($C_6H_{12}O_6$)	200 g
Add ddH$_2$O up to / Final Volume	**1000 ml**

Although 10X amino acid solution seems to be composed of only amino acid, it also contains two nucleotide bases: adenine and uracil (see Table 2.7).

Table 2.7: 10X Amino Acid Solution

Isoleucine (Ile)	300 µg
Valine (Val)	1500 µg
Adenine*	400 µg
Arginine (Arg)	200 µg
Histidine (His)	200 µg
Leucine (Leu)	1000 µg
Lysine (Lys)	300 µg
Methionine (Met)	200 µg
Phenylalanine (Phe)	500 µg
Threonine (Thr)	2000 µg
Tryptophane (Trp)	400 µg
Uracil*	200 µg
Glutamate (Glu)	1000 µg
Aspartate (Asp)	1000 µg
Add ddH$_2$O up to / Final Volume	**1000 µl**

(*) Nucleobase, not amino acid.

2.1.3 H_2O_2 dilutions for treatment of strains in flower plates

For the treatment of cells, stock H_2O_2 (9.8 M, Sigma, H1009) is diluted to the volumes defined in

Table 2.8 to 2000 µl of total volume. At the treatment time, 30 µl of cell medium is removed from each of all flower plate wells which contain 1500 µl cell medium. Then 30 µl H_2O_2 are taken from 2000 µl solutions and then added into each well for the desired concentrations.

Table 2.8: H_2O_2 dilution table for well treatments

Stock H_2O_2 (9.8 M)	ddH_2O (to dilute 9.8 M H_2O_2)	Media Removal Volume/H_2O_2 Addition Volume	**Final H_2O_2 Concentrations in the wells**
0 µl	2000 µl	30 µl	**0 mM**
2.55 µl	1997.45 µl	30 µl	**0.25 mM**
5.10 µl	1994.90 µl	30 µl	**0.50 mM**
10.20 µl	1989.80 µl	30 µl	**1.00 mM**
20.40 µl	1979.60 µl	30 µl	**2.00 mM**
40.80 µl	1959.20 µl	30 µl	**4.00 mM**

2.1.4 HPLC stock solutions and HPLC standards

It is essential to create a standard curve for the HPLC experiments. Stock solutions for the standards and the final metabolite concentrations for each metabolite (see Table 2.11) are listed below. All of the stock solutions are kept at -20ºC. As "eluent" 5 mM sulphuric acid (H_2SO_4) is used.

Table 2.9: Stock Solutions of HPLC Standards

Solution A	
Glucose	120.0 g
Add ddH_2O up to / Final Volume	1 L
Solution B	
Pyruvate	1 g
Succinate	1 g
Acetate	4 g
Glycerol	2 g
Ethanol	30 g
Add ddH_2O up to / Final Volume	1 L

Standard solutions for the HPLC standard curves are prepared with the following dilutions:

Table 2.10: HPLC Standard Solution Dilutions

Standard Solutions	Mixing Volumes		Final Volume
Standard 1	1 ml Solution A 3 ml Solution B	2 ml Eluent	6 ml
Standard 2	0.75 ml Std 1	0.25 ml Eluent	1 ml
Standard 3	0.50 ml Std 1	0.50 ml Eluent	1 ml
Standard 4	0.25 ml Std 1	0.75 ml Eluent	1 ml
Standard 5	0.125 ml Std 1	0.875 ml Eluent	1 ml
Standard 6	0.063 ml Std 1	0.937 ml Eluent	1 ml

Std: Standard Solution

After preparation of all standard solutions, their metabolite concentrations would be the same as shown in Table 2.11.

Table 2.11: Metabolite Concentrations of HPLC Standards

Metabolite (g/L)	Std 1	Std 2	Std 3	Std 4	Std 5	Std 6	RT (min)	Detector
Glucose	20	15	10	5	2.5	1.25	9.28	RI
Pyruvate	0.5	0.375	0.25	0.125	0.0625	0.03125	9.40	UV
Succinate	0.5	0.375	0.25	0.125	0.0625	0.03125	11.53	RI
Glycerol	1	0.75	0.5	0.25	0.125	0.0625	13.53	RI
Acetate	2	1.5	1	0.5	0.25	0.125	14.88 15.13	UV RI
Ethanol	15	11.25	7.5	3.75	1.875	0.9375	22.65	RI

Std: Standard Solution, **RT:** Retention Time, **RI:** Refractive Index, **UV:** Ultraviolet

2.1.5 Laboratory equipment

Microfermentation Platform	BioLector, m2p Labs (Germany)
UV-Visible Spectrophotometer	NanoDrop 1000, Thermo Scientific (USA)
Ultrapure Water System	Milli-Q Plus, Millipore (USA)
Filter Pump & System	Millipore (USA)
HPLC System	Agilent 1100, Agilent (USA)
HPLC Column	Aminex HPX-87H (300 x 7.8 mM)

	Bio-Rad (USA)
Laminar Flow Cabinet	Holten LaminAir, Thermo Scientific (USA)
Balance	Sartorious Basic, Sartorious (Germany)
	Sartorious Analytic, Sartorious (Germany)
Magnetic Stirrer & Hot Plate	Heidolf (UK)
Incubator	Memmert (Germany)
Orbital-Shaker Incubator	Laboshake, Gerhardt (Germany)
Micropipettes	Pipetman 0.2-2 µl, 2-20 µl, 20-200 µl,
	100-1000 µl, 1000-5000 µl; Gilson (USA)
Multi-Pipettes	Research 10-100 µl, Research Pro 50-1200 µl
	Eppendorf (Germany)
Autoclave	Getinge 3200 (Sweden)
Deep Freezers and Refrigerators	-80ºC Sanyo Ultralow MDF-594 (USA)
	-20ºC, +4ºC Gram (UK)

2.2 Methods

2.2.1 Selection of yeast deletion strains

In this study, the protein kinase/phosphatase KO mutants were selected according to their biological functions reported in SGD [71] and the expression profiles shown in the article of Kelley and Ideker in 2009 [73]. The criterion for selection was that the genes be involved in DNA damage response, oxidative stress response or other related stress responses of *S. cerevisiae*. Biological functions related to responses of oxidative stress, DNA damage and other stresses are listed in Table 2.12.

2.2.2 Cell incubation conditions

Cell stocks in 15% glycerol-YPD taken from -80ºC were thawed and streaked on YPD agar plates. After streaking, the cell stocks were immediately put into the -80ºC freezer. YPD agar plates are incubated at 30ºC up to 2-3 days. When the growing colonies were observed and were big enough, agar plates are transferred to +4ºC for later use. It is important not to incubate too long, because colonies get bigger and

later sticks to each other, preventing the selection of single colonies. Before starting BioLector experiments, the single colonies from agar plates were transferred with a sterile loop into 10 ml SD media for preculturing. Precultures were incubated at 30ºC, 160 RPM for ~24 hours.

Table 2.12: Functions of KO genes and the biological processes they are involved in

Gene	*Function*	*Biological Process*	*Gene*	*Function*	*Biological Process*
ALK1	Protein Kinase	Mitosis DNA Damage	**PPH3**	Protein Phosphatase	DNA Damage
ALK2	Protein Kinase	Mitosis Meiosis DNA Damage	**PRK1**	Protein Kinase	Cytokinesis
ARK1	Protein Kinase	Cytokinesis	**PTC1**	Protein Phosphatase	Osmotic Stress
BUD32	Protein Kinase	Cell Cycle	**PTC3**	Protein Phosphatase	Osmotic Stress
CHK1	Protein Kinase	DNA Damage	**PTP2**	Protein Phosphatase	Osmotic Stress
CKA2	Protein Kinase	DNA Damage	**RAD53**	Protein Kinase	DNA Damage Cell Cycle
DBF20	Protein Kinase	Cytokinesis	**RCK1**	Protein Kinase	Oxidative Stress Cell Cycle
DUN1	Protein Kinase	DNA Damage Cell Cycle	**RCK2**	Protein Kinase	Oxidative Stress Osmotic Stress Cell Cycle
HAL5	Protein Kinase	Osmotic Stress	**SIW14**	Protein Phosphatase	Endocytosis
HOG1	Protein Kinase	Osmotic Stress	**SPS1**	Protein Kinase	Meiosis
KIN1	Protein Kinase	Exocytosis	**SSK2**	Protein Kinase	Osmotic Stress
MEC1	Protein Kinase	DNA Damage	**SSK22**	Protein Kinase	Osmotic Stress
MEK1	Protein Kinase	DNA Damage	**TEL1**	Protein Kinase	DNA Damage
MKK1	Protein Kinase	Cell Cycle	**VHS1**	Protein Kinase	Cell Cycle
OCA1	Protein Phosphatase	Oxidative Stress DNA Damage	**VPS15**	Protein Kinase	Vacuolar Transport
PBS2	Protein Kinase	Osmotic Stress	**YCK1**	Protein Kinase	Cytokinesis Endocytosis
PKH1	Protein Kinase	Endocytosis	**YCK3**	Protein Kinase	Endocytosis
PKH2	Protein Kinase	Endocytosis	**YGK3**	Protein Kinase	Oxidative Stress, Osmotic Stress
PKP1	Protein Kinase	Carbon Utilization	**YKL171W**	Protein Kinase	Proteolysis

2.2.3 Preparing BioLector plates

Biomass concentrations were measured at 620 nm scattered light without emission. The gain parameter is a high voltage amplification on the BioLector photomultiplier. It is recommended to be between 1 and 100 by manufacturer. The gain parameter, which was 30 for experiments of this study, sets sensitivity of LSU signal. It has to be set to low values in cases of high signal expectations. Vice versa, it has to be set to high values in cases of low signal expectations. Optimal LSU to achieve from BioLector must be < 500 LSU. The LSU of each well is measured every 3 minutes when using a single filter (minimum 3 additional minutes per cycle for each additional filter). The process parameters and physicals conditions of the BioLector runs are listed in the table below.

Table 2.13: Physical Conditions of BioLector Fermentations

Biomass Filter [Ex/Em]	620 nm/-
Gain	30
Temperature [°C]	30.00
Humidity [rH]	95.00
Shaker Frequency [rpm]	1000.00
Cycle Time [min]	3

After 24 hours incubation of the precultures, the OD_{600} are measured by NanoDrop 1000. The initial OD_{600} of each sample is set to 0.2 ODU, so that the required dilutions with SD media are done upon this criterion. The samples are then transferred into the 48-well BioLector flower plates (MTP-48-B). The plates are sealed with gas permeable adhesive seals (Thermo) after transfer into the wells. All of the strains, except *vps15* (initial OD for *vps15* is set to 0.4 ODU due to slow growth), reached the mid-log phase at ~5.5 hours where the cells are treated with H_2O_2 with desired concentrations as mentioned in section 2.1.3. The BioLector cultivations continued at least up to 36 hours and all microfermentation experiments were done in duplicate. At the end of plate runs, the flower plates are seated onto external shakers and the final OD of each well are measured.

2.2.4 Determination of metabolite contents by HPLC

The aim of HPLC analysis for extracellular organic acids and glucose is to determine the relationship between the growth and metabolite exhaustion/production. Wild type strain BY4741 is inoculated and fermentation in BioLector started at 0.2 absorbance of OD_{600}. There is also a control group in the plate run. During the experiment, the wells of the control group were not sacrificed. At the end of the experiment, the final ODs were measured. The sampling times are determined in the table below.

Table 2.14: HPLC Sampling Times for Metabolite Detection

Time Points (h)	Growth Phase Description
t0	Initial (OD_{600} = 0.2)
t1	Pre-treatment (~5.5 hours)
t2	Pre-Diauxic Shift
t3	Post-Diauxic Shift
t4	Stationary Phase (~36 hours)

Sampling was done by taking 1 ml of medium inside the flower plate wells away with a syringe and filtering it using 0.45 µm filters (MiniStart-plus, Sartorius) to the HPLC vials (Supelco). After filtration, there was ~500-600 µl of sample inside the vials. HPLC vials are kept in -80ºC deep freezers. HPLC analysis was then done with 20 µl injection from these samples. An isocratic method was run at 60ºC with 0.6 ml/minute flow rate of 5 mM sulphuric acid. Metabolite compositions were determined by comparison to known 6 known standards for retention time, UV absorbance and refractive index (RI) signal (see section 2.1.4).

2.2.5 Data analysis

All of the data was analyzed via R scripts (R-2.9.2). A high-throughput microfermentation R package, called “htmf”, was developed by Dr. Christopher Workman for the analysis of BioLector data.

There are three main analyses made for the growth curves: growth area, growth rate and diauxic-shift delay times. Growth area is the integration of growth curves (area under the growth curves) for each different H_2O_2 treatment; growth rate is the biomass (LSU or OD) increase per unit time (dX/dt where X is the biomass indicator) and diauxic delay times are the time points of diauxic shift/phase. All three different data sets were clustered using hierarchical clustering [74].

All three data sets were transformed to "relative" values:

$$\textbf{(Rel Area)}_{\textbf{H2O2=n mM}} = log(Area)_{nontreated} - log(Area)_{H2O2=n\ mM}$$

$$\textbf{(Rel Growth Rate)}_{\textbf{H2O2=n mM}} = log(Growth\ Rate)_{nontreated} - log(Growth\ Rate)_{H2O2=n\ mM}$$

$$\textbf{(Rel Diauxic Response Time)}_{\textbf{H2O2=n mM}} = log(Diauxic\ Response\ Time)_{nontreated} - log(Diauxic\ Response\ Time)_{H2O2=n\ mM}$$

After transforming to relative values, they were hierarchically clustered.

3. RESULTS

3.1 Growth Physiology of KO and Wild Types

Batch growth experiments were done for all of the 38 KO mutants with using 2 wild type strains as BY4741 and Y7220 of *S. cerevisiae*. A typical growth curve of BY4741 is shown in Figure 3.1. The LSU scaled growth curves and their OD transformations are shown in appendix D.

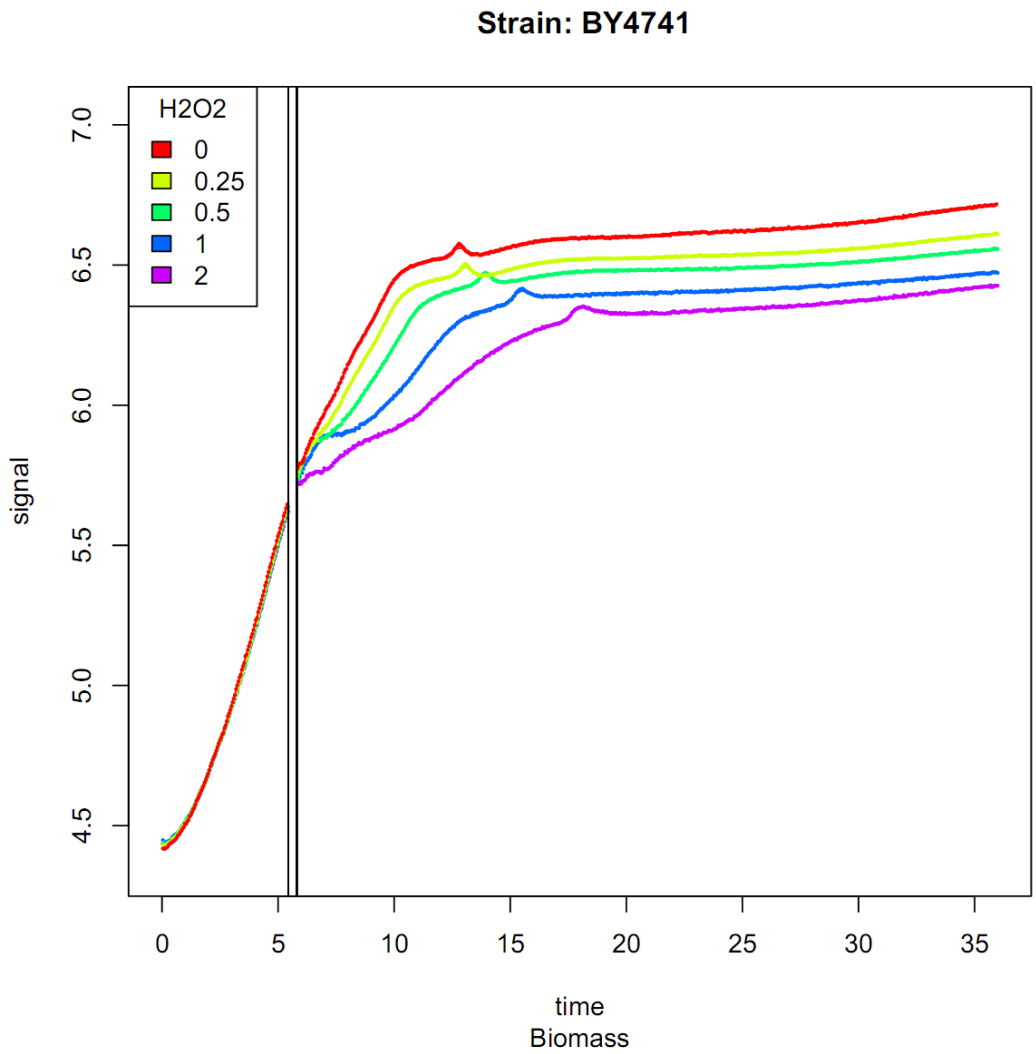

Figure 3.1: Growth curve of wild type BY4741 under different H_2O_2 conditions. y-axis: $\log_2$(LSU), x-axis: time

For growth rate calculations, the LSU scale growth curves were transformed to the OD scale by using linear transformations. The LSU for each well in the flower plates were transformed into OD by using the initial OD and final OD all of the KO mutants and wild types. Some of the linear fits for one plate (plate Ferm48_20100418_H2O2) are shown in Figure 3.2.

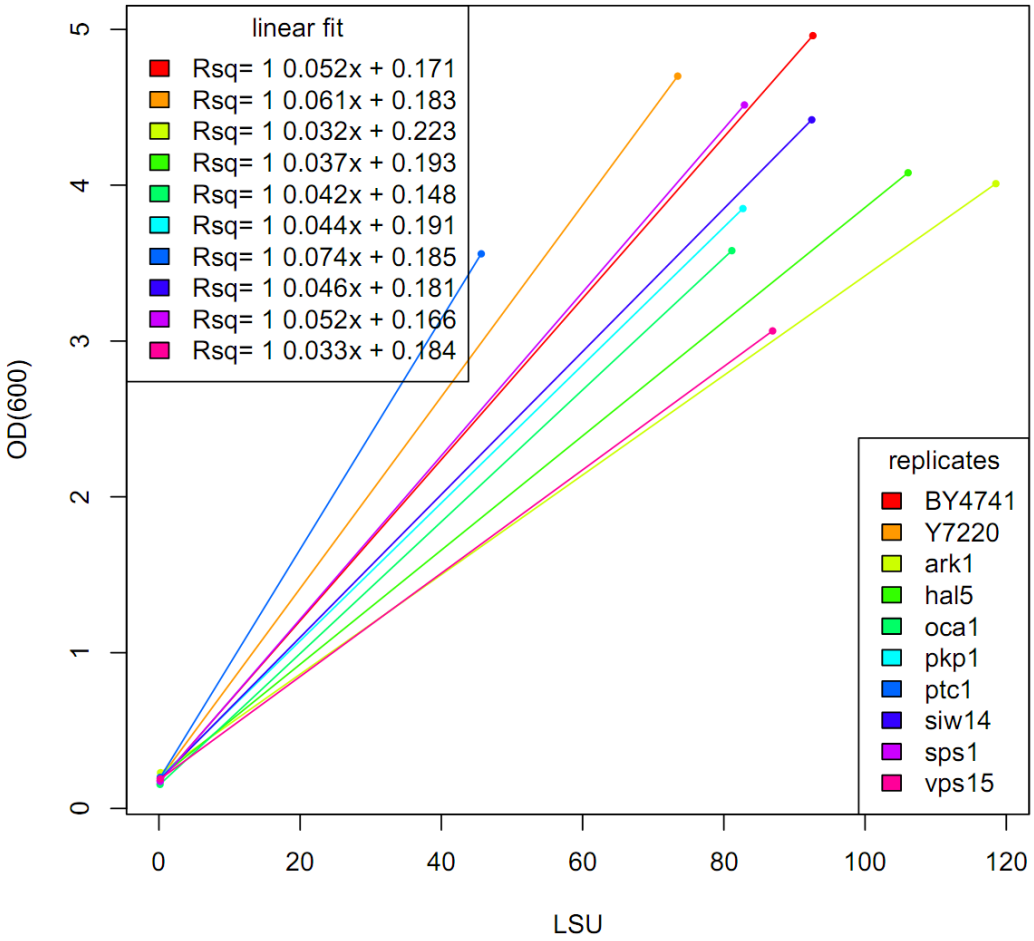

Figure 3.2: Linear fits of LSU and OD for *S. cerevisiae* strains. y-axis: LSU; x-axis: OD; Rsq: R^2; all equations are in form of y = mx + n, where m: slope and n: offset

After transformation from LSU to OD, growth curves look similar. Here is an example of OD transformed growth curve of BY4741 (see Figure 3.3).

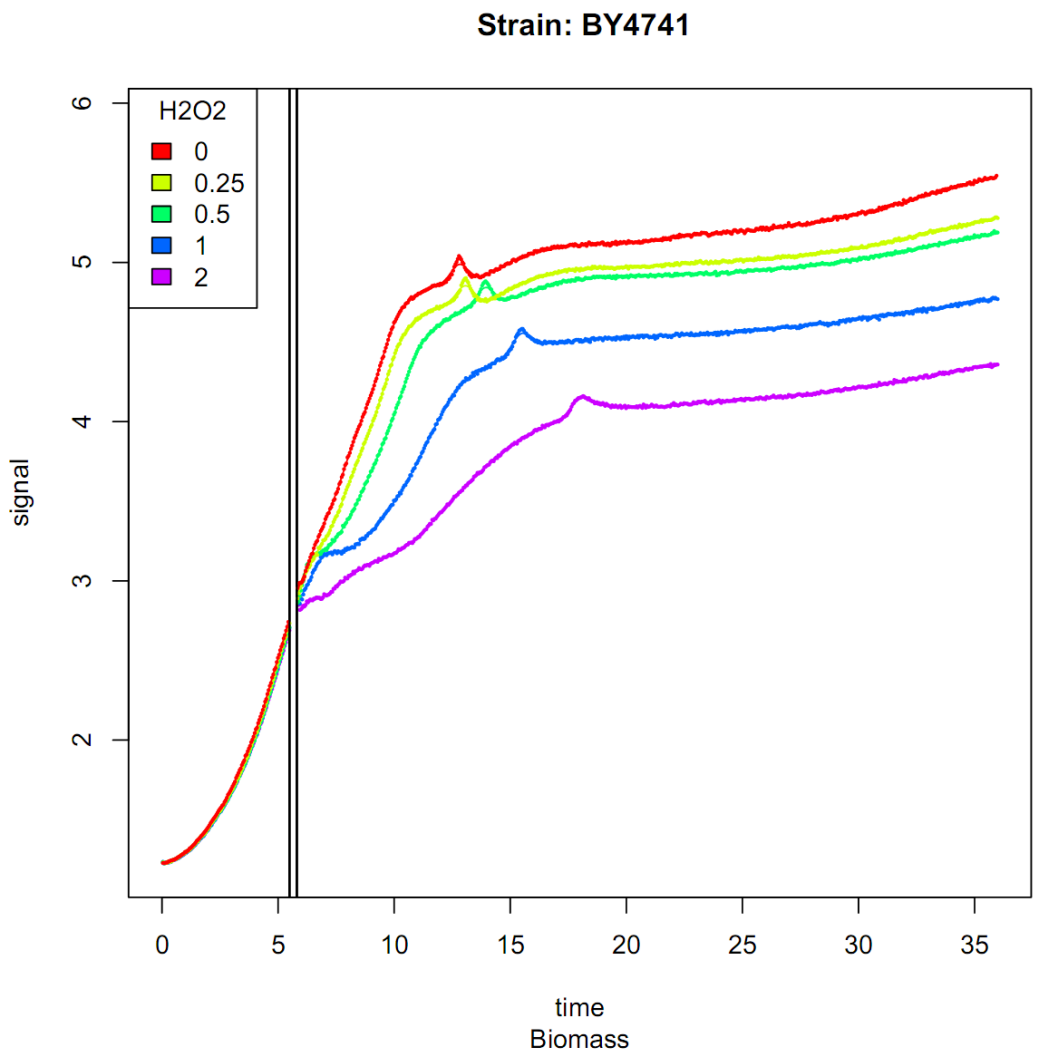

Figure 3.3: OD equivalent of BY4741 growth curve. x-axis: OD, y-axis: time

As an overall result of growth deficiencies, there were four significant strains which grew more slowly compared to the other strains: *vps15*Δ, *oca1*Δ, *bud32*Δ and *ptc1*Δ. Their growth curves are shown in Figure 3.4.

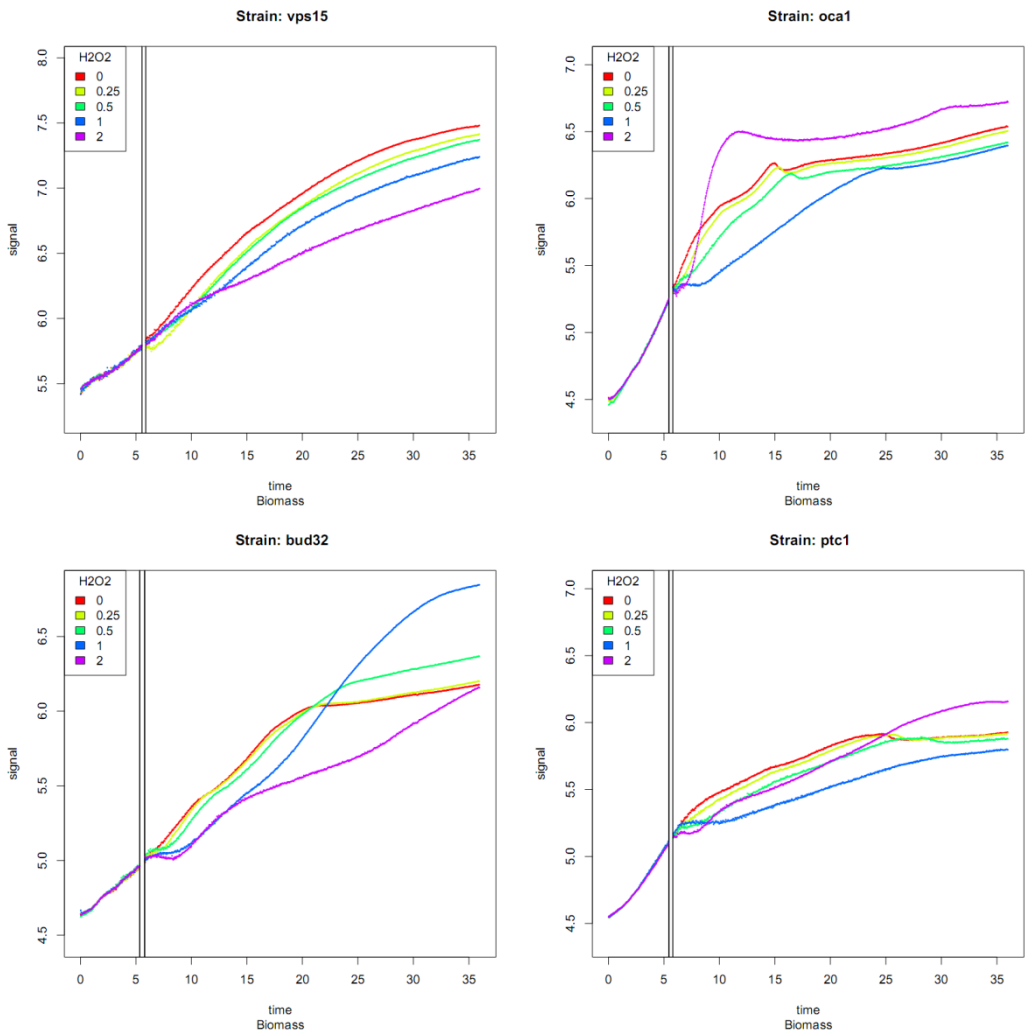

Figure 3.4: Slow growing KO strains: *vps15*Δ, *oca1*Δ, *bud32*Δ and *ptc1*Δ

3.2 Analysis of Growth Curves

Batch fermentation of all of the KO and wild type strains were done at least twice in control and 4 different H_2O_2 treatments: 0 mM (control), 0.25 mM, 0.50 mM, 1 mM and 2 mM.

There are three different growth curve analysis as growth area, growth rate and diauxic delay times. All these data sets are transformed to the relative fitness by using non-treated (0 mM H_2O_2) conditions. To achieve a significant comparison of data, these three sets are based on the time intervals between the treatment time with H_2O_2 (~5.5 h) and 24 hours after treatment (+24 h). Different time windows like +12, +24 and +36 hours after treatment were also examined for better fit but it is concluded that 24 hours data set has the least noisy data set in that time window (data not shown).

In total, there were 15 elements in a vector per strain (5 for each data set). There is no significance of 0 mM relative data for each one, because all values were zero. So the clustering criteria contain 12 significant elements per each strain (see Figure 3.5).

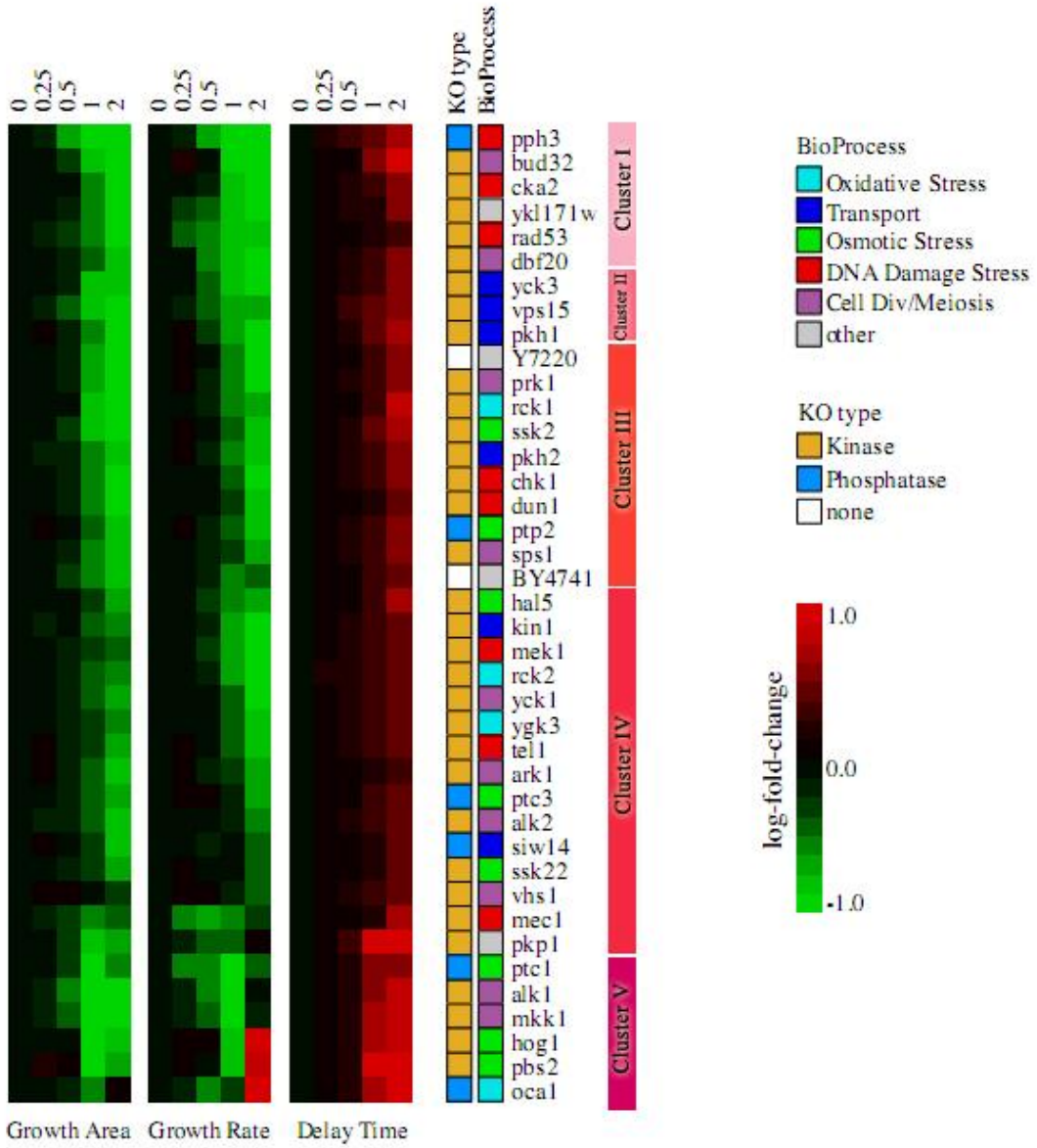

Figure 3.5: Clustering of all KO and wild type strains due to their relative growth area, relative growth rate and relative diauxic response times

There are five different groups of genes which share significant properties. Group I is composed of *pph3*Δ, *bud32*Δ, *cka2*Δ, *ykl171w*Δ, *rad53*Δ, *dbf20*Δ and it is related to cell cycle division and DNA damage response. Group II is the transport related kinases composed of *yck3*Δ, *vps15*Δ and *pkh1*Δ. Group III is the wild type-like group. This cluster is composed of the KOs between wild type Y7220 and BY4741

as: *prk1*Δ, *rck1*Δ, *ssk2*Δ, *pkh2*Δ, *chk1*Δ, *dun1*Δ, *ptp2*Δ and *sps1*Δ. Group IV has a complex set of phenotypes where KOs did not show significant relations among themselves. The last gene cluster, group V, is related to the HOG pathway MAPK (Hog1) and it is consisted of *ptc1*Δ, *alk1*Δ, *mkk1*Δ, *hog1*Δ, *pbs2*Δ and *oca1*Δ.

3.3 HPLC Results and Data Analysis

A 48-well flower plate was used in the HPLC sampling. The growth curves of different H_2O_2 treatments were detected on-line and therefore, the exact sampling times detected for the diauxic shift time points. Figure 3.6 shows the growth curve of BY4741 during sampling.

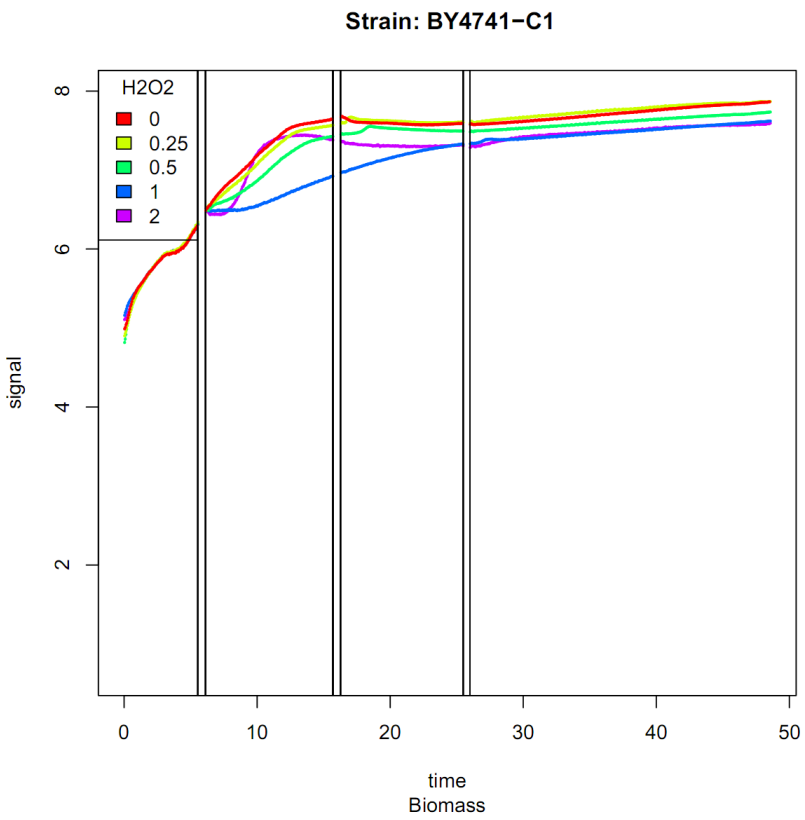

Figure 3.6: Growth curve of wild type BY4741. Double vertical lines indicate sampling times, y-axis: Log2-scale LSU, x-axis: time (hours), C-1: Control group, Legend: H_2O_2 Concentrations (mM)

The concentrations of the metabolites were generally found to have acceptable R^2 values for the linear regression of HPLC standards (R^2 >0.9). Splines were interpolated for more accurate data and the whole metabolite concentrations were calculated according to spline fitting (see Figure 3.7) Note that outliers around 0.5 g/L "Pyruvate" was removed for better fitting.

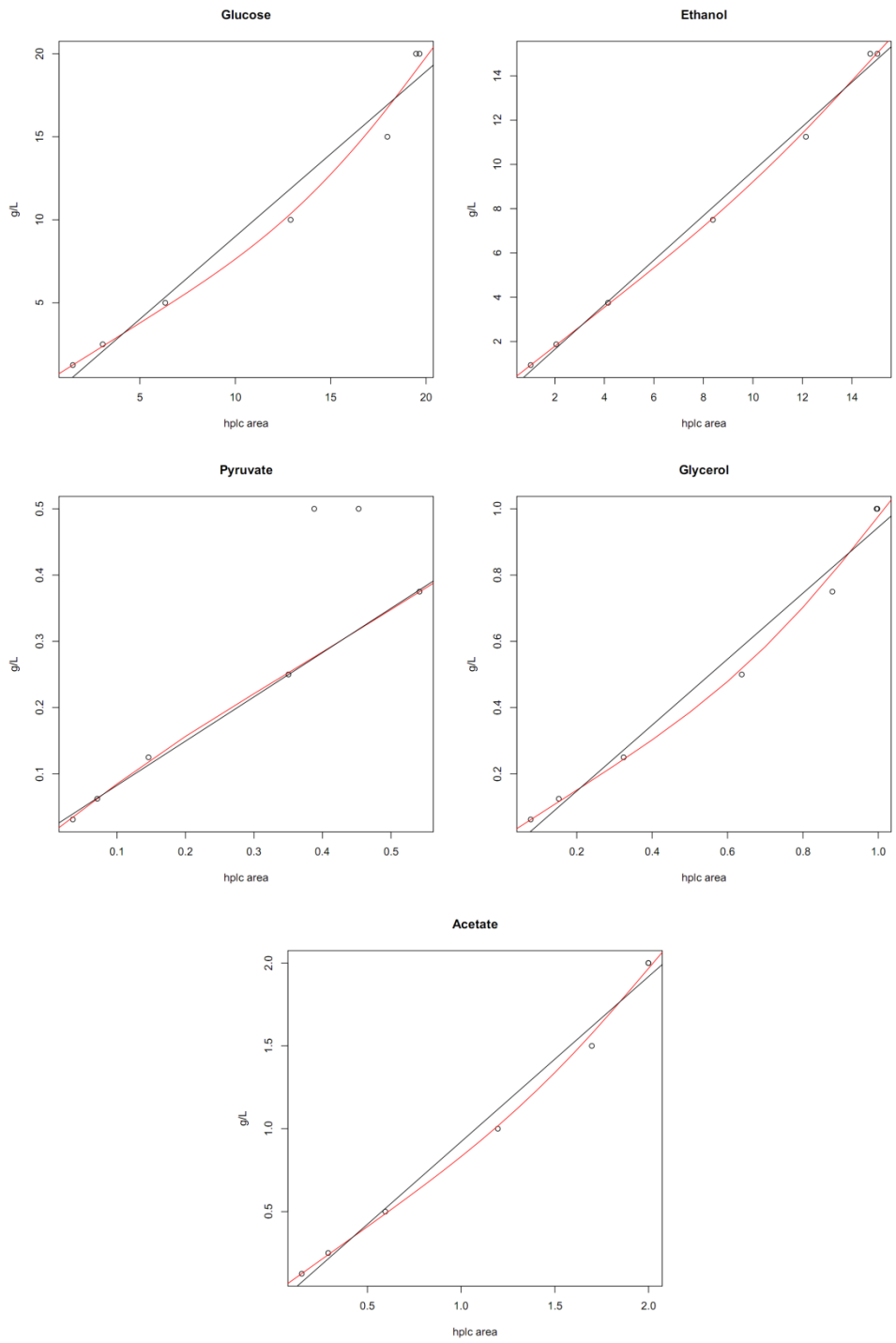

Figure 3.7: Spline Interpolation for HPLC Standards (red: splines, black: linear regressions)

The diauxic shift time intervals are detected by using the first derivatives (*dy/dt*) of the growth plots for each treatment conditions. Dashed vertical lines indicate the maximum *dy/dt* while straight lines indicate the minimum *dy/dt* in the diauxic shift. (see Figure 3.8).

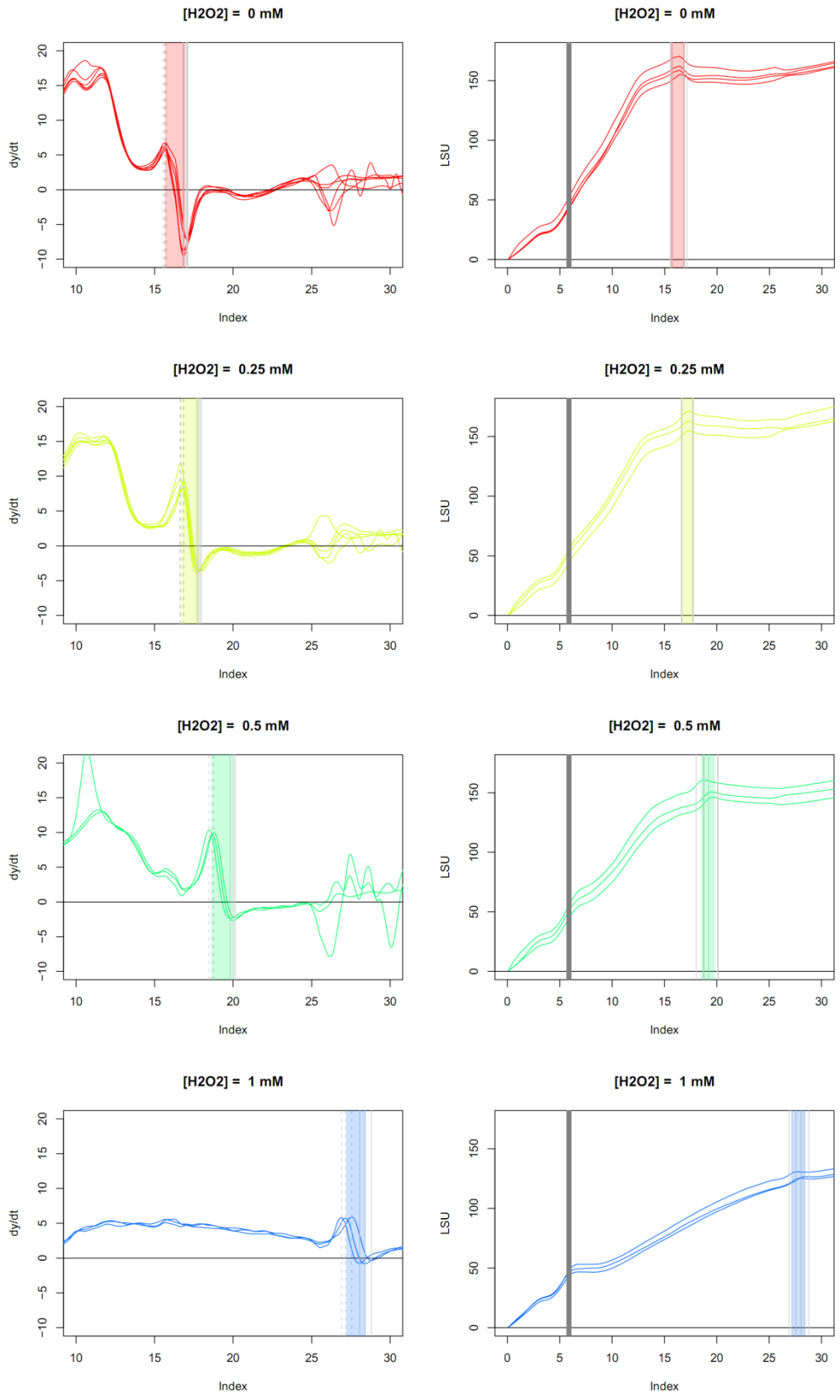

Figure 3.8: Diauxic Shift Response Times for each H_2O_2 Treatment (Left Column: *dy/dt* of growth curves, Right Column: Diauxic Phase on Growth Curves)

In this experiment, there was no diauxic shift detection for 2 mM H_2O_2 stress condition as seen in Figure 3.6. At 2 mM H_2O_2 stress condition, sometimes a fast growth response after 2 mM H_2O_2 treatment is detected for most of the strains. Diauxic shift response times are shown in Figure 3.9 as a function of time and H_2O_2 concentration: red lines show maximum *dy/dt* whereas the green lines show minimum *dy/dt* and the grey lines show *dy/dt = 0* which means that there is no growth at that time.

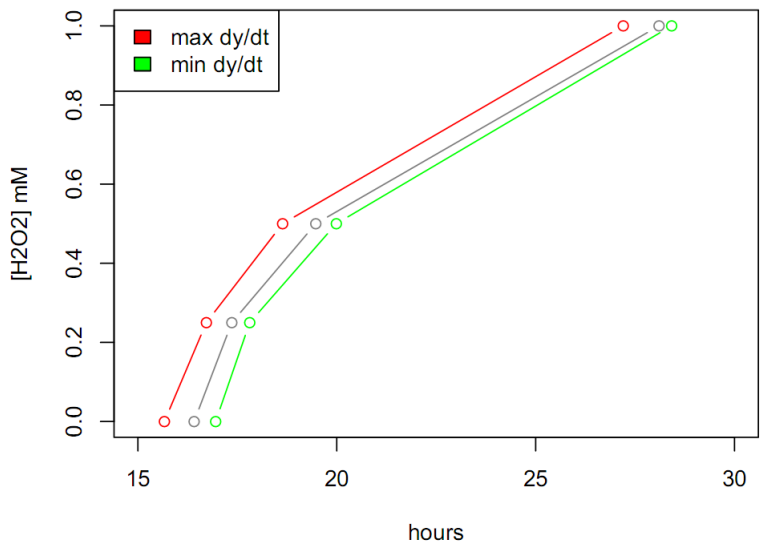

Figure 3.9: Diauxic Shift Response Times According to H_2O_2 Concentrations

There were six extracellular metabolites to be detected by HPLC as glucose, ethanol, succinate, glycerol, acetate and pyruvate. Unfortunately, there were no succinate in the HPLC standards; therefore it could not be quantitated. The remaining metabolites were detected successfully and concentrations of them were recalculated according to spline fits shown at Figure 3.7.

In all metabolite concentration plots, grey transparent vertical lines indicate the time of treatment with H_2O_2. The coloured transparent lines indicate the diauxic shift time interval by the same colour of H_2O_2 treatment. In Figure 3.10, glucose concentration change upon time is shown for different conditions of H_2O_2. Glucose concentrations by time were fit to sigmoidal curves. It is clear that the extracellular glucose is exhausted in the diauxic phase. Treatments with increasing H_2O_2 concentrations

respectively make the diauxic phases delayed. 2 mM H_2O_2 stress is the breakpoint for diauxic response, as there was no diauxic phase observed for 2 mM H_2O_2 treatment. In addition to this, glucose exhaustion takes a much longer time for the 2 mM H_2O_2 treatment.

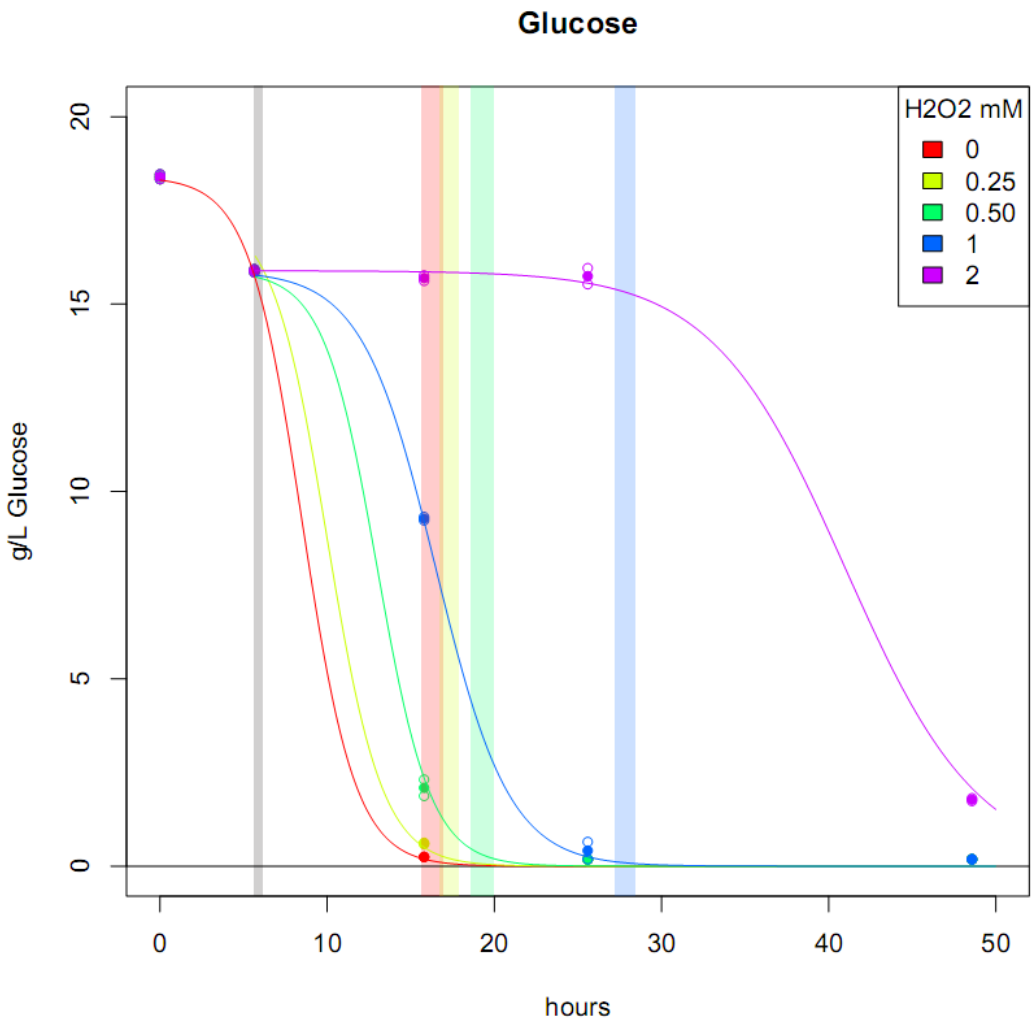

Figure 3.10: Glucose concentration change at different H_2O_2 concentrations by time. Coloured transparent vertical lines indicate diauxic shift time intervals.

Ethanol synthesis increased during exponential growth up to diauxic phase (see Figure 3.11). It can be seen that extracellular ethanol concentration reached its highest concentration at the diauxic phase. Especially, untreated cell population (0 mM) was a good indicator of the increased ethanol level, because the sampling was done exactly at diauxic phase for untreated cell populations. In addition to this, increasing H_2O_2 concentration inhibits the ethanol synthesis for a while causing a

delay for ethanol synthesis. It is obvious that, ethanol synthesis is delayed for a long while at 2 mM H_2O_2 concentration, but after 26th hour, it began to increase again.

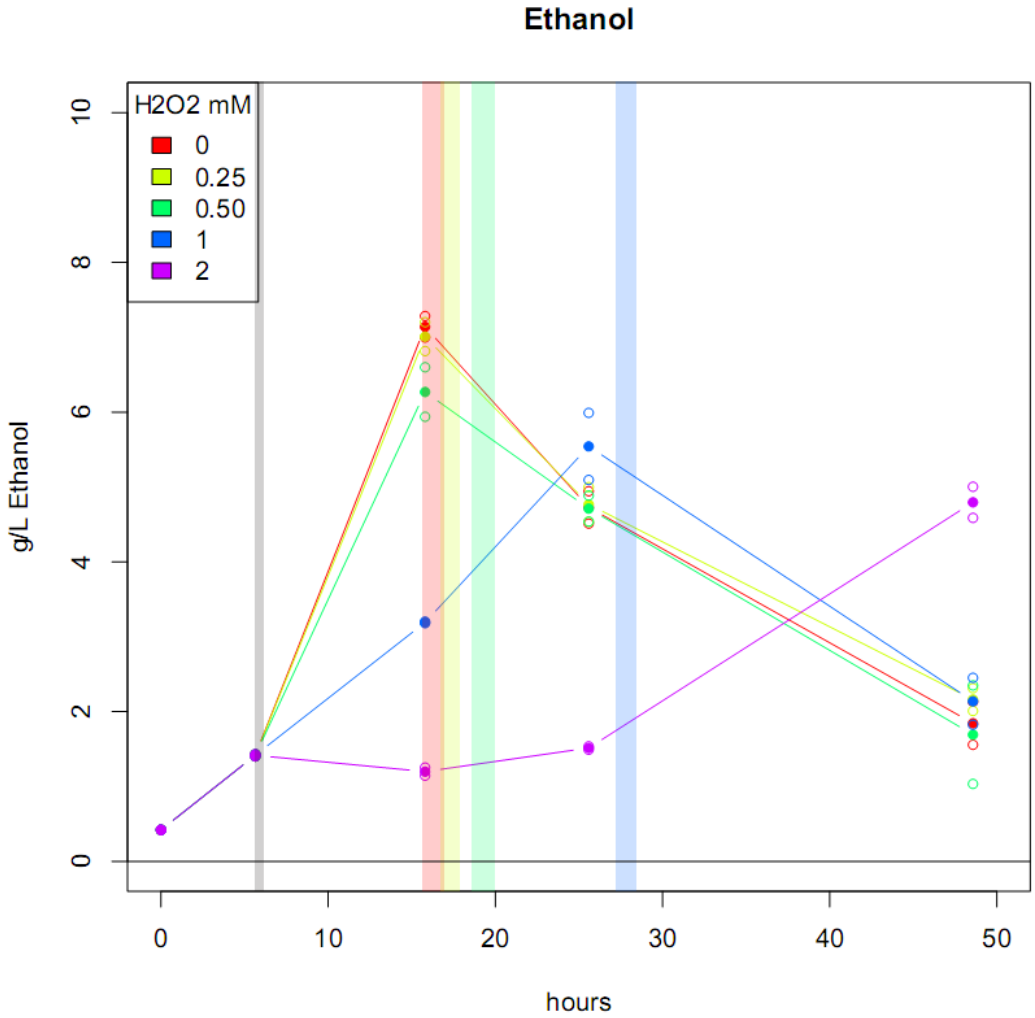

Figure 3.11: Ethanol concentration change at different H_2O_2 concentrations by time. Coloured transparent vertical lines indicate diauxic shift time intervals.

Glycerol synthesis also occurred during growth of *S. cerevisiae* populations (see Figure 3.12). Apparently, there glycerol synthesis is induced as a stress response. At ~26th hour, extracellular glycerol concentrations are correlated to H_2O_2 treatment except at 2 mM H_2O_2; the more H_2O_2 treatment, the more glycerol production observed. There is a time delay of glycerol synthesis for 2 mM H_2O_2 condition; it is getting higher after ~26th hour. Even though the glycerol synthesis is observed, the extracellular scale is at high range, it goes only up to ~1.1 g/L.

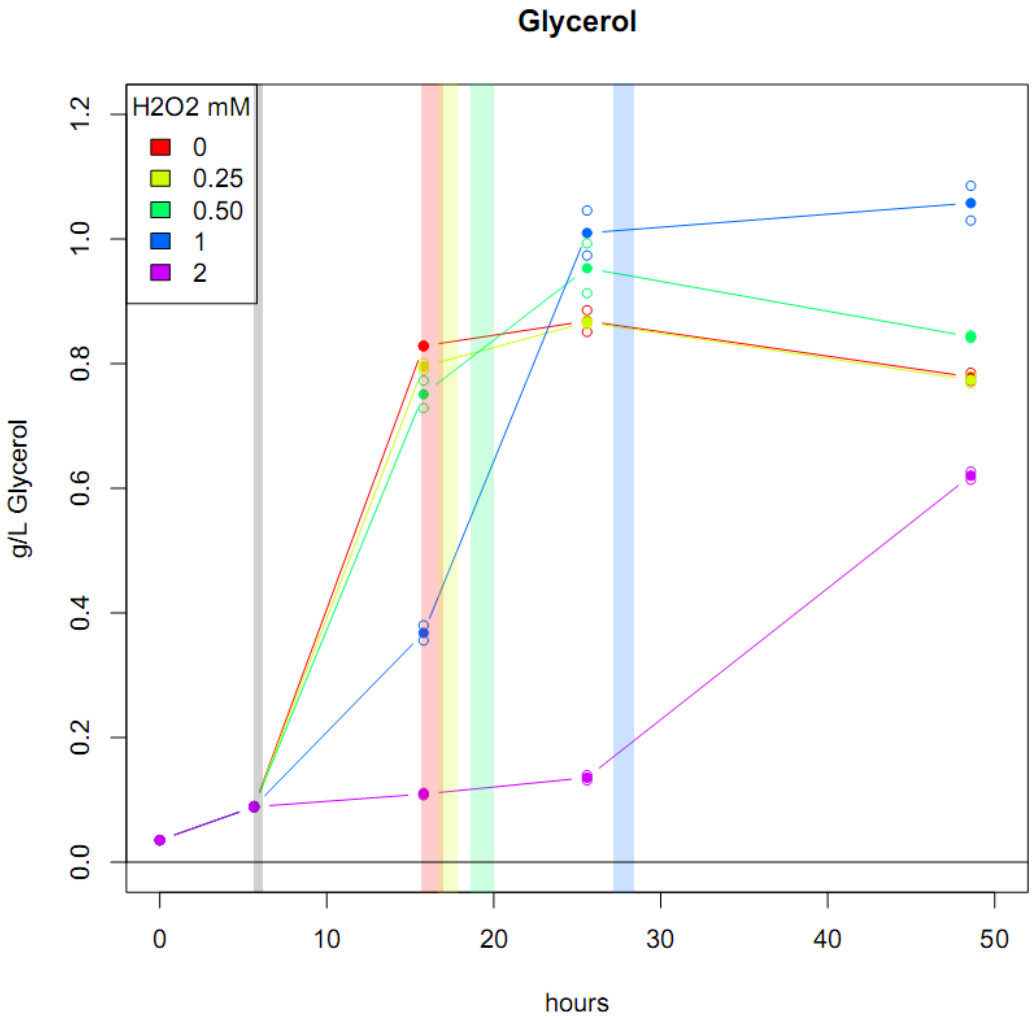

Figure 3.12: Glycerol concentration change at different H_2O_2 concentrations by time. Coloured transparent vertical lines indicate diauxic shift time intervals

Extracellular acetate concentration increased during time as seen in Figure 3.13. The increasing H_2O_2 concentration made the increase of acetate concentration delayed as it happened to the other metabolites. Although there are low extracellular acetate concentrations, the increase in concentration was detected successfully in time series. 2 mM H_2O_2 stress is the most effective condition to make a delay in the synthesis of acetate.

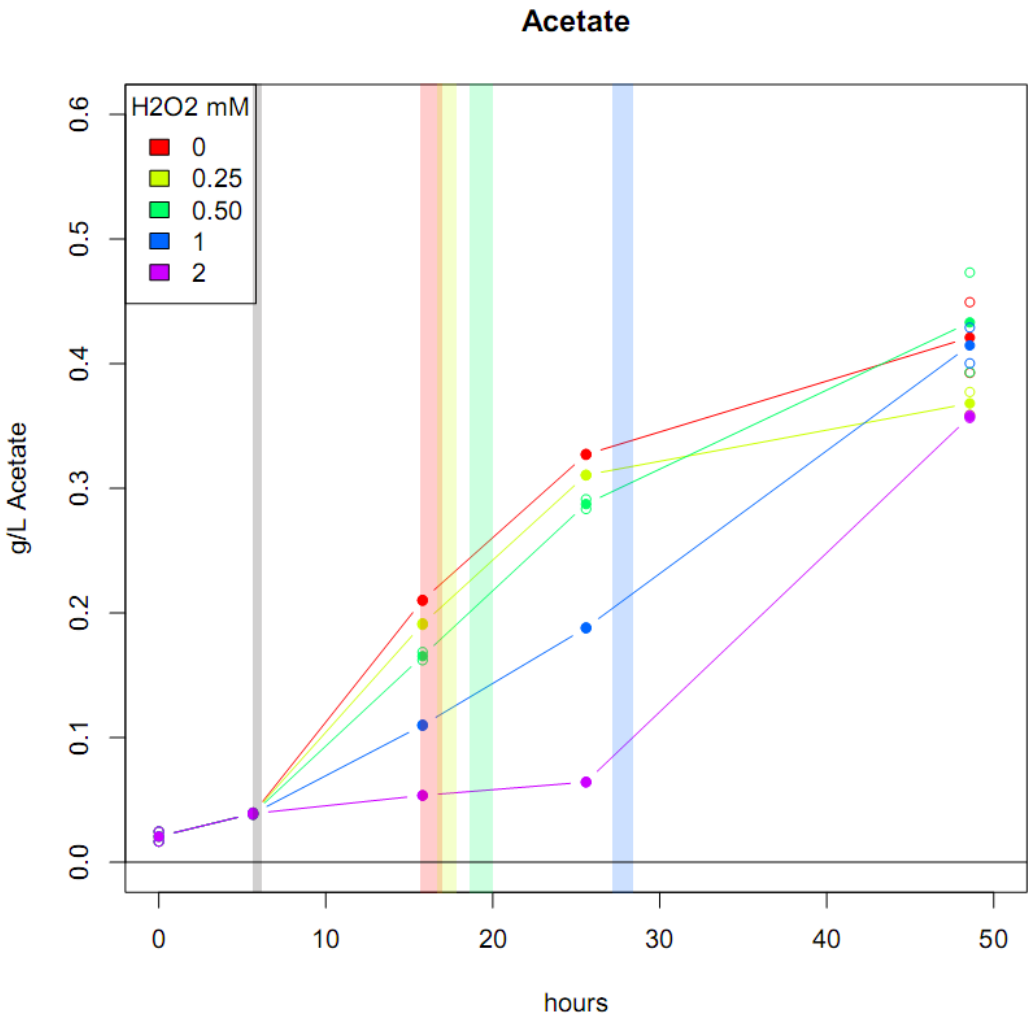

Figure 3.13: Acetate concentration change at different H_2O_2 concentrations by time. Coloured transparent vertical lines indicate diauxic shift time intervals

Extracellular pyruvate concentration increases in the exponential growth up to the diauxic phase (see Figure 3.14). Although the observed concentration of extracellular pyruvate is very few, the increase of pyruvate concentration is detected during exponential growth up to diauxic phase. The important point is that pyruvate concentration dramatically decreases down to the initial concentration after diauxic phase except 2 mM H_2O_2 treatment. The extracellular pyruvate concentration remained stable after treatment with 2 mM H_2O_2 for a while (up to ~26th hour) and then started to increase. Interestingly, extracellular pyruvate concentration went up to 0.09 g/L which was twice as high when compared to the other treatment conditions.

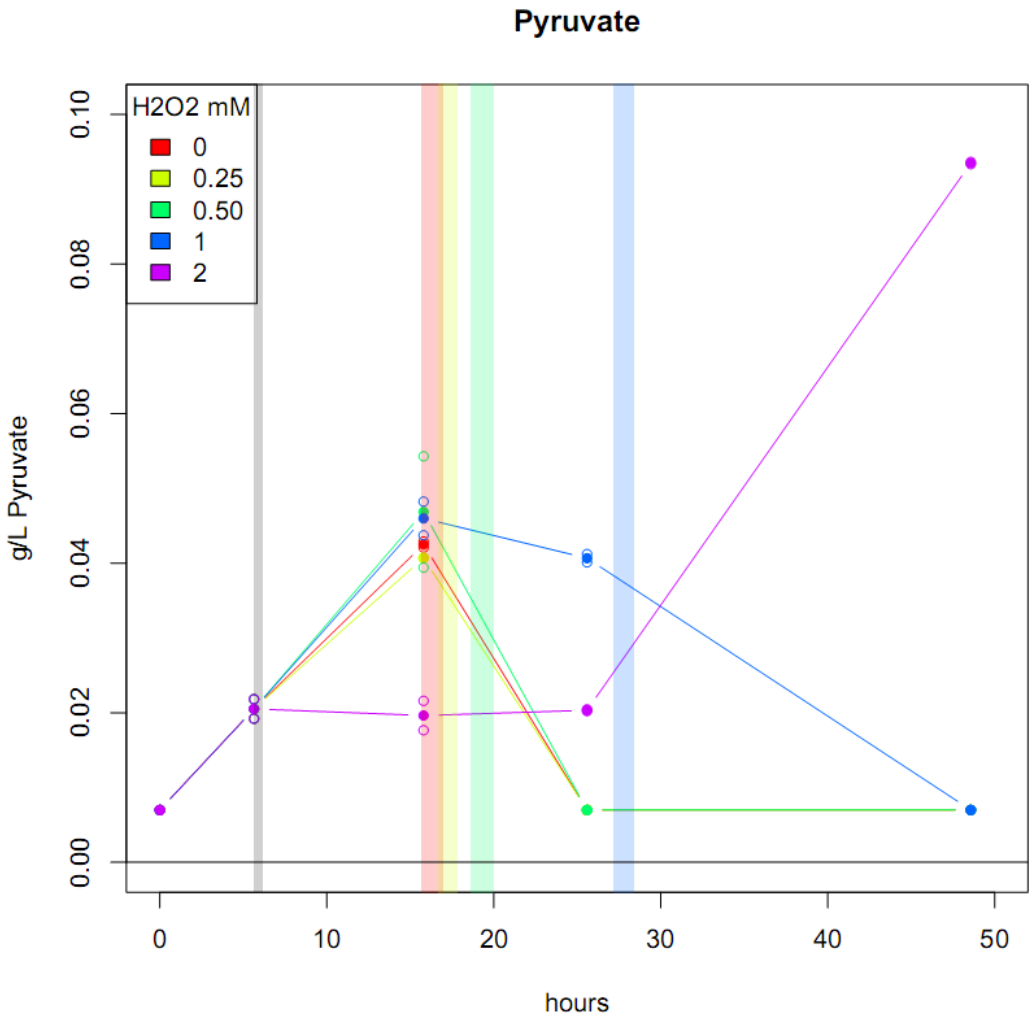

Figure 3.14: Pyruvate concentration change at different H_2O_2 concentrations by time. Coloured transparent vertical lines indicate diauxic shift time intervals

4. DISCUSSION

4.1 Growth Physiology of Strains and Gene Deletion Effects on Oxidative Stress and DNA Repair Responses

In this study, 38 protein kinase/phosphatase KO mutants and 2 wild type *Saccharomyces cerevisiae* strains were investigated according to their growth physiology. There were three types of variable used for clustering these strains: relative growth area, relative growth rate and relative diauxic phase delay times. All strains were clustered by hierarchical clustering for all three variable types (see Figure 3.5). There were 5 interesting gene clusters found by hierarchical clustering.

Since the clusters were based on the growth parameters under different concentrations of H_2O_2 stress, it could be assumed that the genes in the same cluster have similar (physiological) oxidative stress response phenotypes. Cluster IV has a complex structure which makes it difficult to interpret.

In cluster group I (*pph3*Δ, *bud32*Δ, *cka2*Δ, *ykl171w*Δ, *rad53*Δ, *dbf20*Δ), *RAD53* is a cell cycle checkpoint kinase gene and has an important function in the DNA damage response. Pph3 is a protein phosphatase and it is required for dephosphorylation of Rad53 allowing for replication fork restart to let cell cycle continue after repair [75]. In addition to this, Bud32 is involved in bud-site selection whereas Cka2 is responsible from cell growth and proliferation and Dbf20 mediates the exit from mitotic cell phase. On the other hand, *bud32*Δ is sensitive to H_2O_2 stress and the growth of *bud32*Δ is strongly affected due to increasing H_2O_2 concentration in the environment. There appears to be a similar set of processes cotrolled by the proteins of this gene cluster, because deletion of these genes created similar phenotypic profiles. A possible relationship between Bud32 and Rad53 may exist because Bud32 creates a stimulus at late G1 phase for bud site selection and hence Rad53 may also be stimulated at basal level to get ready for any DNA damage in S phase. Rad53 creates response to DNA damage and after the DNA is repaired, Pph3 deactivates Rad53 via dephosphorylation. At that time, Dbf20 and Cka2 can be triggered by Pph3 activity for continuing cell proliferation. In this possible network,

Ykl171w should be the preserving kinase to send the damaged kinases or phosphatases to proteasomal degradation.

Cluster group II (*yck3*Δ, *vps15*Δ, *pkh1*Δ) is involved in vacuolar transporting and endocytosis. It is probable that these kinases could activate each other due to sharing the same biological function. In case of activating each other, Vps15 has a central role; because *vps15*Δ is a growth deficient strain and it grows very slowly even in excess glucose media (SD media). Due to this fact, the initial absorbance of OD_{600} was set to 0.4, twice that of the other strains, for all of the microfermentation experiments to help it reach exponential phase growth at the same time as other strains in the experiment. On the other hand, diauxic phase of *vps15*Δ were so weak that they were often not detectable. This growth deficiency could be due to a lack of endocytosis caused by *vps15* deletion.

Cluster group III (*prk1*Δ, *rck1*Δ, *ssk2*Δ, *pkh2*Δ, *chk1*Δ, *dun1*Δ, *ptp2*Δ and *sps1*Δ) is a wild-type like group, because they are clustered between wild types Y7220 and BY4741. Even though these strains are KO deletions, they have the similar growth profiles to wild types. The interpretation of this could be that there are compensatory mechanisms for these deletions. In fact, there are some known compensating genes that can act due to lack of genes in cluster III. For example, *RCK1* has another homolog called *RCK2*, so if there is a deletion of *RCK1*, it would be compensated due to *RCK2*. The other example for compensatory mechanism is genes *CHK1* and *DUN1*. Rad53 and Chk1 are the effector kinases in DNA damage checkpoint and Rad53 phosphorylates Dun1 as a DNA damage response. Deletion studies showed that *CHK1* deletion has no significant effect on Dun1 phosphorylation [76], so this mechanism is compensated by Rad53 activity. Another compensatory mechanism in this cluster is related to the well-known HOG pathway (see Figure 1.19). Ptp2 dephosphorylates Hog1 in the nucleus of cell and delocalizes it from the nucleus. Moreover, the entry of Hog1 can be prevented by the activity of Ptc1 (in cluster V) when Hog1 is still in the cytosol. It is highly probable that other genes in this cluster have different compensative mechanisms.

The last group (*ptc1*Δ, *alk1*Δ, *mkk1*Δ, *hog1*Δ, *pbs2*Δ and *oca1*Δ), cluster V, is related to the HOG pathway (see section 1.3.5). In cytosol, Pbs2 phosphorylates Hog1 whereas Ptc1 dephosphorylates Hog1. Thus, a feedback system on Hog1 activation is built up. Alk1 is the regulator of both DNA damage response and cell cycle since

Mkk1 only regulates cell cycle. These two kinases, Alk1 and Mkk1, could have important roles on HOG pathway regulation or, in contrast, the branches of the HOG pathway might regulate DNA damage response and/or cell cycle as a stress inducer. More importantly, *hog1*Δ, *pbs2*Δ and *oca1*Δ are a sub-cluster, especially for the relative growth rate features. *OCA1* is required for cell cycle arrest in response to oxidative DNA damage, thus *OCA1* regulates responses of oxidative damage, DNA damage and cell cycle arrest. As *oca1*Δ has similar profile as the HOG pathway regulator MAPK (Hog1), MAPKK (Pbs2) and phosphatase (Ptc1), it may be the keystone of the regulatory network as it bridges the osmotic stress response (HOG pathway), the DNA damage response (with Alk1) and cell cycle arrest (with Mkk1).

There are four significantly slow growing strains among the 38 KO mutants: *bud32*Δ, *vps15*Δ, *ptc1*Δ and *oca1*Δ. All of these KOs are protein phosphatases except *bud32*Δ. When the cell population is faced with stress from the environment, it stimulates signalling cascades to reduce the metabolism (below discussed more) and trigger stress response pathways. As discussed, most of the stress response pathways are activated by protein kinases. Later, these protein kinases have to be shut down by protein phosphatase activity when the stress factor is gone from environment or adaption is achieved. When phosphatases are deleted, deactivation of the various kinases occurs much more slowly and cells may still behave like they are under stress conditions. Therefore cell cycle can be arrested, cells can undergo stationary phase and basically many stress responses can be still active even though there is no stress in the environment. The slow growth of protein phosphatase mutants may be due to the fact that cells cannot effectively de-activate the stress response.

4.2 Regulation of Carbon Metabolism under Oxidative Stress and Importance of Diauxic Shift

In the HPLC analysis, central extracellular key metabolites of carbon metabolism of *S. cerevisiae* wild type strain BY4741 were analyzed. The following extracellular metabolites were profiled; glucose, ethanol, glycerol, acetate and pyruvate. To our knowledge, this is the first study that shows the nutrient concentrations exactly on the time interval of *S. cerevisiae* diauxic phase.

Glucose is the main carbon source to be utilized by *S. cerevisiae*. SD media for growth was prepared to have 20 g/L glucose and the glucose concentration measured

by HPLC was ~20 g/L glucose, indicating that the growth medium contained the intended levels of carbon source [15].

The glucose was exhausted during the exponential growth phase as expected. By the diauxic phase, all the glucose was observed to be exhausted. The exhaustion of extracellular glucose in the diauxic phase has been indicated many times before [19; 20; 21]. The addition of H_2O_2 at mid-exponential growth induced a stress response and thus the glucose consumption occured over a longer time interval. The more H_2O_2 stress applied, the later the glucose was exhausted. This diauxic shift delay is an indicator that energy production metabolism is turned down more with the increasing H_2O_2 concentration in the environment. Especially at 2 mM H_2O_2 conditions, there was often an extreme time delay on glucose exhaustion to about 24 hours after treatment. After treatment with 2 mM H_2O_2, it is likely that cells undergo stress response and do not utilize glucose for 24 hours. After adaptation and/or decomposition of H_2O_2, they begin to utilize glucose as can be seen in 2 mM H_2O_2 treatment concentration growth profiles.

Pyruvate is a central metabolite that helps cells decide to undergo either TCA cycle-oxidative phosphorylation or ethanol fermentation. Except for the 2 mM H_2O_2 stress condition, cells increase their pyruvate level during exponential growth. Increasing H_2O_2 concentration affects pyruvate consumption negatively. The control, 0.25 and 0.50 mM H_2O_2 treatments all appear to display the same pyruvate consumption rate but more time points would be required to further establish this finding. Higher levels of stress do appear to decrease the pyruvate consumption rate though. This is already clear for the 1 mM H_2O_2 condition (see Figure 3.14). After treatment with 2 mM H_2O_2 stress, the level of pyruvate was stabile for 24 hours after treatment as was the case for glucose. Interestingly, the concentration of pyruvate is more than twice that of the other stress conditions in the 50 hour time point. At 26th hours, pyruvate concentration starts to increase, which is an indicator that glycolysis is taking place. On the other hand, pyruvate is not stored in the cell; it is directly consumed since it is the keystone of carbon metabolism. Therefore, it is normal to be found in low concentrations. Hence, the increased pyruvate concentration might be an indicator of more induced glycolysis reactions as it was observed only after the 2 mM H_2O_2 stress condition.

Ethanol is the marker metabolite of the fermentative metabolism in *S. cerevisiae*. The ethanol concentration in the surrounding media increased during exponential growth. This increase up to the diauxic phase indicates that cells are utilizing the carbon (glucose) for anaerobic pathway. After diauxic phase, it is obvious that ethanol is being consumed by the cells. The proof is especially seen on the data point for 0 mM and 1 mM H_2O_2 treatment (see Figure 3.11) which were sampled just before the diauxic shift. 2 mM H_2O_2 treatment, was an outlier compared to the other stress conditions as there was no significant increase of ethanol from treatment time up to 26th hour. The concentration of ethanol increases after the 26th hour for 2 mM H_2O_2 treatment.

The acetate concentration, which is an indicator of oxidative metabolism via TCA cycle, always increased during the experiment except after 2 mM H_2O_2 treatment. After this extremely acute stress, acetate concentration began to increase after 26th hour as also observed with the other metabolites in this stress condition. In addition to this, the acetate production rate was highest for non-treated cell population whereas the increasing H_2O_2 concentrations made acetate production rate lower, respectively. Basically, acetate increased before diauxic phase and after diauxic phase which means that there was always TCA cycle activity which is the strong indicator of oxidative phosphorylation.

Since glycerol production is triggered via the HOG pathway under osmotic stress conditions (see section 1.3.5), it can be interpreted that glycerol is synthesized as an oxidative stress medaitor. For each oxidative stress condition, the glycerol synthesis increases during exponential phase but remains stable after the diauxic. It is also observed that extracellular glycerol concentration was positively correlated with the H_2O_2 treatment concentration. As an exception, again, there was a very slight increase of glycerol after treatment up to 26 hours which remained constant for 2 mM H_2O_2 treatment, but after the 26th hour glycerol concentration began to increase.

As a holistic view of carbon utilization and the effect of diauxic phase regulation, it can be concluded that, cells uses both aerobic respiration (oxidative phosphorylation) and anaerobic respiration (alcoholic fermentation) during exponential growth. The increasing H_2O_2 concentration up to 1 mM appears to cause cell to reduce their metabolic activity by means of carbon utilization and the synthesis of other metabolites during exponential phase. *S. cerevisiae,* as a Crabtree positive

microorganism prefers to utilize glucose via fermentative pathway in excess glucose conditions like surrounding SD-media. During diauxic phase, there is a metabolic adjustment where cells prefer to utilize carbon via only aerobic pathway, because the concentration of ethanol decreases during post-diauxic phase. The reason why cells prefer to utilize glucose via anaerobic pathway during exponential growth is the preservative action due to the oxidative effect of aerobic pathway. After diauxic phase, there is no more glucose, so the cells have to gain energy from the other metabolites such as ethanol and acetate [21]. To cover the energy expenses of a cell after diauxic phase, aerobic respiration with ethanol, acetate and other TCA cycle molecules are used (see Figure 4.1). When all important energetic metabolites are consumed, the cells undergo stationary phase.

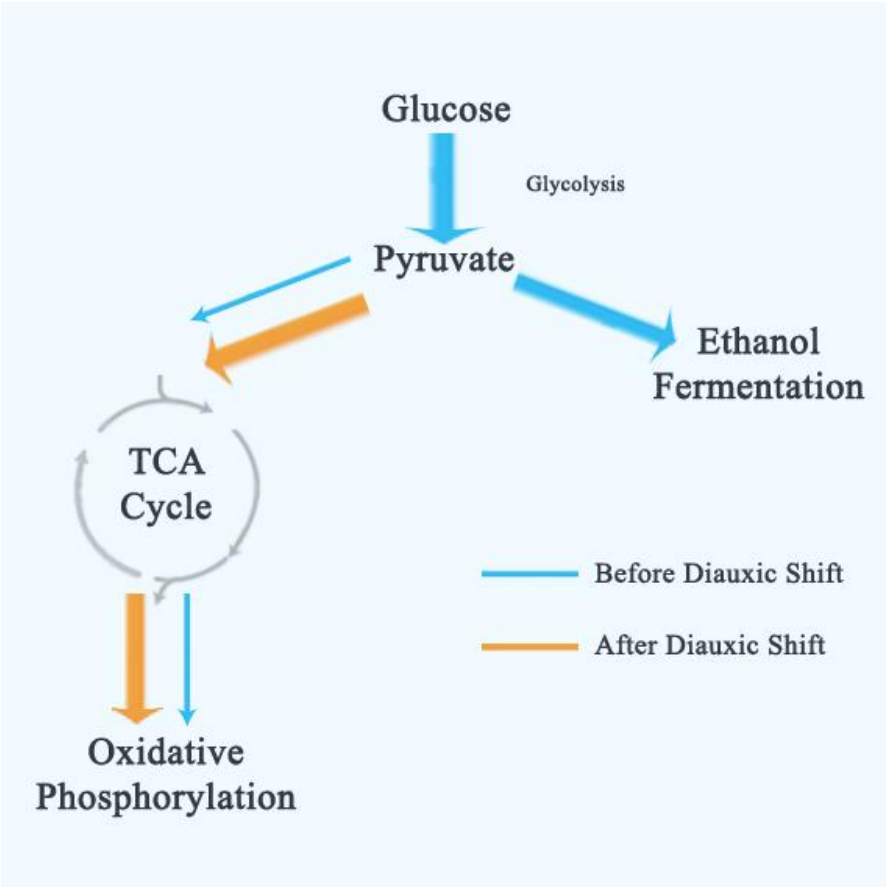

Figure 4.1: Diauxic Remodelling of Carbon Metabolism. Blue arrows: Before diauxic shift, Orange arrows: After diauxic shift, thickness of arrows (not scaled) indicates more carbon flux

Wild type *S. cerevisiae* strain BY4741 usually does not show a high growth increase in terms of LSU after treatment with 2 mM H_2O_2 and also a diauxic phase is detectable for 2 mM H_2O_2 concentrations. As seen in the growth curve of HPLC

experiment, there is a high increase in the LSU for 2 mM H_2O_2 treatment and no detection of diauxic phase. Normally, LSU is the indicator of the growth, but when the metabolite concentrations are investigated for 2 mM H_2O_2 concentrations, there is no activity on the carbon utilization metabolism. So the reason of increasing LSU for 2 mM H_2O_2 concentrations is likely for a different reason. It could be due an increase in cell volume related to an oxidative stress response. On the other hand, why would carbon metabolism remain stable for 2 mM H_2O_2 condition in the time interval between the treatment time (~5.5 hours) to 26th hour and then reactivated? It might be due to massive cell death and the induction of a second lag-phase. Even though cells prefer to utilize glucose during anaerobic metabolism and there is a high carbon flux to anaerobic metabolism during exponential growth, it does not mean there is no aerobic metabolism in exponential phase. Therefore, it is reasonable to decrease the carbon metabolism and use the remaining energy of the cell to recover from the oxidative effect of H_2O_2 at that time. After recovery from oxidative stress, the population starts to reassemble itself metabolically, but there is no growth afterwards for 2 mM H_2O_2 conditions. This could imply that the surviving cells remain in stationary phase.

4.3 Conclusion and Future Aspects

Mainly, this study is composed of two parts: effects of oxidative stress on growth physiology of *S. cerevisiae* strains and metabolic remodelling of *S. cerevisiae* strains due to oxidative stress.

There are many important findings from the growth physiology experiments as discussed above, but the most important ones can be said that the compensatory mechanism of protein kinase/phosphatase (cluster III), the central activity of *OCA1* gene (cluster V) among responses of oxidative stress, DNA damage and cell cycle arrest, and also the investigation of slow growing KO mutants (*bud32*Δ, *vps15*Δ, *ptc1*Δ and *oca1*Δ).

BioLector microfermentation platform allowed us to detect the exact time interval of diauxic phases of *S. cerevisiae* upon different H_2O_2 stress conditions. The important metabolites of carbon metabolism, which were sampled before, during and after diauxic phase of *S. cerevisiae*, were detected by HPLC. The metabolic delay of carbon utilization proved that the cells decrease the metabolic activity with

increasing H_2O_2 stress conditions in the environment. Moreover, the harsh stress concentrations like 2 mM H_2O_2 or more appear to cause the cells undergo a metabolic collapse.

Although a high increase of cellular growth rate detected for 2 mM H_2O_2 stress condition, all carbon utilization seemed to be turned down. The most probable reason is that cells got bigger just after the H_2O_2 treatment and remained in the stationary phase. To prove this hypothesis, fluorescence-activated cell sorting (FACS) analysis can be done. It is possible to detect the number of viable cells (percent viability), how many of them are in specific cell phase (G1, S, G2, and M) and the size of cells.

Growth experiments would be supported with DNA and protein level oxidative stress detection. Generation of 7,8-dihydro-8-oxoguanine (8-oxo-G) is one of the common DNA lesions generated under oxidizing conditions and can be measured by fragment length analysis using repair enzymes (FLARE) assay. This assay includes the hOGG1 enzyme which removes 8-oxo-G and DNA-containing formamidopyrimidine from the damaged DNA molecule and therefore induces the formation of a comet formed by DNA strand breaks in low-melting-agarose gel electrophoresis. On the other hand, a common indicator of protein oxidation is considered to be the carbonylation of proteins. Carbonylation is irreversible protein damage and frequently causes loss of function. Carbonyl groups of proteins can be detected by an oxidized protein detection assay.

REFERENCES

[1] **Fay, J. C., Benavides, J. A.,** 2005: Evidence for domesticated and wild populations of *Saccharomyces cerevisiae*. *PLoS Genet*, vol. 1, pp. 66-71.

[2] **Legras, J. L., Merdinoglu, D., Cornuet, J. M., Karst, F.,** 2007: Bread, beer and wine: *Saccharomyces cerevisiae* diversity reflects human history. *Mol Ecol*, vol. 16, pp. 2091-2102.

[3] **Baráth, Á., Halász, A., Németh, E., Zalán, Z.,** 2004: Selection of LAB strains for fermented red beet juice production *European Food Research and Technology*, vol. 218, pp. 184-187.

[4] **Sipiczk, M., Romano, P., Lipani, G., Miklos, I., Antunovics, Z.,** 2001: Analysis of yeasts derived from natural fermentation in a Tokaj winery. *Antonie Van Leeuwenhoek*, vol. 79, pp. 97-105.

[5] **Fan, J., Mitchell, J. R., Blanshard, J. M. V.,** 1999: A model for the oven rise of dough during baking *Journal of Food Engineering*, vol. 41, pp. 69,77.

[6] **Muller, M.,** 2003: Glycolysis, Krebs Cycle, and other Energy-Releasing Pathways. Retrieved 21.07.2010 from http://www.uic.edu/classes/bios/bios100/summer2002/lect10.htm

[7] **Adrio, J. L., Demain, A. L.,** 2003: Fungal biotechnology. *Int Microbiol*, vol. 6, pp. 191-199.

[8] **Mortimer, R. K.,** 2000: Evolution and variation of the yeast (*Saccharomyces*) genome. *Genome Res*, vol. 10, pp. 403-409.

[9] **Fukazawa, Y., Shinoda, T., Nishikawa, A., Nakase, T.,** 1980: Synonymy of *Saccharomyces cerevisiae* Hansen 1883 and *Saccharomyces uvarum* Beijerinck 1898: Significance of Cell Wall Antigens in Yeast Classification. *Int. J. Syst. Bacteriol.*, vol. 30, pp. 196-205.

[10] **Herskowitz, I.,** 1988: Life cycle of the budding yeast *Saccharomyces cerevisiae*. *Microbiology and Molecular Biology Reviews*, vol. 52, pp. 536-553.

[11] **Baldauf, S. L., Palmer, J. D.,** 1993: Animals and fungi are each other's closest relatives: congruent evidence from multiple proteins. *Proc Natl Acad Sci U S A*, vol. 90, pp. 11558-11562.

[12] **Lu, M., Campbell, J. L., Boye, E., Kleckner, N.,** 1994: SeqA: a negative modulator of replication initiation in *E. coli*. *Cell*, vol. 77, pp. 413-426.

[13] **Bitterman, K. J., Medvedik, O., Sinclair, D. A.,** 2003: Longevity regulation in *Saccharomyces cerevisiae*: linking metabolism, genome stability, and heterochromatin. *Microbiol Mol Biol Rev*, vol. 67, pp. 376-399, table of contents.

[14] **Alberts, B., Johnson, A., Lewis, J., Raff, M., Roberts, K., Walter, P.,** 2002: Molecular Biology of the Cell, Garland Science, New York, USA.

[15] **Sherman, F.,** 2002: Getting started with yeast. *Methods Enzymol*, vol. 350, pp. 3-41.

[16] **Gershon, H., Gershon, D.,** 2000: The budding yeast, *Saccharomyces cerevisiae*, as a model for aging research: a critical review. *Mechanisms of Ageing and Development*, vol. 120, pp. 1-22.

[17] **Goffeau, A., Barrell, B. G., Bussey, H., Davis, R. W., Dujon, B., Feldmann, H., Galibert, F., Hoheisel, J. D., Jacq, C., Johnston, M., Louis, E. J., Mewes, H. W., Murakami, Y., Philippsen, P., Tettelin, H., Oliver, S. G.,** 1996: Life with 6000 genes. *Science*, vol. 274, pp. 546, 563-547.

[18] **Lodish, H., Berk, A., Zipursky, L. S., Matsudaira, P., Baltimore, D., Darnel, J.,** 2000: Molecular Cell Biology, W. H. Freeman & Company, USA.

[19] **Dickinson, J. R.,** 2004: The Metabolism and Molecular Physiology of *Saccharomyces cerevisiae*. vol. 2nd Edition.

[20] **Hohmann, S., Mager, W. H.,** 2003: Yeast Stress Responses (Topics in Current Genetics), Springer.

[21] **Brauer, M. J., Saldanha, A. J., Dolinski, K., Botstein, D.,** 2005: Homeostatic adjustment and metabolic remodeling in glucose-limited yeast cultures. *Mol Biol Cell*, vol. 16, pp. 2503-2517.

[22] **Gasch, A. P., Spellman, P. T., Kao, C. M., Carmel-Harel, O., Eisen, M. B., Storz, G., Botstein, D., Brown, P. O.,** 2000: Genomic expression programs in the response of yeast cells to environmental changes. *Mol Biol Cell*, vol. 11, pp. 4241-4257.

[23] **Kensy, F., Zang, E., Faulhammer, C., Tan, R. K., Buchs, J.,** 2009: Validation of a high-throughput fermentation system based on online monitoring of biomass and fluorescence in continuously shaken microtiter plates. *Microb Cell Fact*, vol. 8, pp. 31.

[24] **Winzeler, E. A., Shoemaker, D. D., Astromoff, A., Liang, H., Anderson, K., Andre, B., Bangham, R., Benito, R., Boeke, J. D., Bussey, H., Chu, A. M., Connelly, C., Davis, K., Dietrich, F., Dow, S. W., El Bakkoury, M., Foury, F., Friend, S. H., Gentalen, E., Giaever, G., Hegemann, J. H., Jones, T., Laub, M., Liao, H., Liebundguth, N., Lockhart, D. J., Lucau-Danila, A., Lussier, M., M'Rabet, N., Menard, P., Mittmann, M., Pai, C., Rebischung, C., Revuelta, J. L., Riles, L., Roberts, C. J., Ross-MacDonald, P., Scherens, B., Snyder, M., Sookhai-Mahadeo, S., Storms, R. K., Veronneau, S., Voet, M., Volckaert, G., Ward, T. R., Wysocki, R., Yen, G. S., Yu, K., Zimmermann, K., Philippsen, P., Johnston, M., Davis, R. W.,** 1999: Functional characterization of the *S. cerevisiae* genome by gene deletion and parallel analysis. *Science*, vol. 285, pp. 901-906.

[25] **Tucker, C. L., Fields, S.,** 2004: Quantitative genome-wide analysis of yeast deletion strain sensitivities to oxidative and chemical stress. *Comp Funct Genomics*, vol. 5, pp. 216-224.

[26] **Jamieson, D. J.,** 1992: *Saccharomyces cerevisiae* has distinct adaptive responses to both hydrogen peroxide and menadione. *J Bacteriol*, vol. 174, pp. 6678-6681.

[27] **Hadwiger, J. A., Wittenberg, C., Richardson, H. E., de Barros Lopes, M., Reed, S. I.,** 1989: A family of cyclin homologs that control the G1 phase in yeast. *Proc Natl Acad Sci U S A*, vol. 86, pp. 6255-6259.

[28] **Birrell, G. W., Brown, J. A., Wu, H. I., Giaever, G., Chu, A. M., Davis, R. W., Brown, J. M.,** 2002: Transcriptional response of *Saccharomyces cerevisiae* to DNA-damaging agents does not identify the genes that protect against these agents. *Proc Natl Acad Sci U S A*, vol. 99, pp. 8778-8783.

[29] **Pearson, G., Robinson, F., Beers Gibson, T., Xu, B. E., Karandikar, M., Berman, K., Cobb, M. H.,** 2001: Mitogen-activated protein (MAP) kinase pathways: regulation and physiological functions. *Endocr Rev*, vol. 22, pp. 153-183.

[30] **Cheetham, J., Smith, D. A., da Silva Dantas, A., Doris, K. S., Patterson, M. J., Bruce, C. R., Quinn, J.,** 2007: A single MAPKKK regulates the Hog1 MAPK pathway in the pathogenic fungus *Candida albicans*. *Mol Biol Cell*, vol. 18, pp. 4603-4614.

[31] **Hohmann, S., Krantz, M., Nordlander, B.,** 2007: Yeast osmoregulation. *Methods Enzymol*, vol. 428, pp. 29-45.

[32] **Ames, B. N., Shigenaga, M. K., Hagen, T. M.,** 1993: Oxidants, antioxidants, and the degenerative diseases of aging. *Proc Natl Acad Sci U S A*, vol. 90, pp. 7915-7922.

[33] **Halliwell, B.,** 1997: Antioxidants and human disease: a general introduction. *Nutr Rev*, vol. 55, pp. S44-49; discussion S49-52.

[34] **Temple, M. D., Perrone, G. G., Dawes, I. W.,** 2005: Complex cellular responses to reactive oxygen species. *Trends Cell Biol*, vol. 15, pp. 319-326.

[35] **Perrone, G. G., Tan, S. X., Dawes, I. W.,** 2008: Reactive oxygen species and yeast apoptosis. *Biochim Biophys Acta*, vol. 1783, pp. 1354-1368.

[36] **Jamieson, D. J.,** 1998: Oxidative stress responses of the yeast *Saccharomyces cerevisiae*. *Yeast*, vol. 14, pp. 1511-1527.

[37] **Muller, E. G.,** 1996: A glutathione reductase mutant of yeast accumulates high levels of oxidized glutathione and requires thioredoxin for growth. *Mol Biol Cell*, vol. 7, pp. 1805-1813.

[38] **Rodriguez-Manzaneque, M. T., Ros, J., Cabiscol, E., Sorribas, A., Herrero, E.,** 1999: Grx5 glutaredoxin plays a central role in protection against protein oxidative damage in *Saccharomyces cerevisiae*. *Mol Cell Biol*, vol. 19, pp. 8180-8190.

[39] **Hanson, G. T., Aggeler, R., Oglesbee, D., Cannon, M., Capaldi, R. A., Tsien, R. Y., Remington, S. J.,** 2004: Investigating mitochondrial redox potential with redox-sensitive green fluorescent protein indicators. *J Biol Chem*, vol. 279, pp. 13044-13053.

[40] **Meyer, A. J., Brach, T., Marty, L., Kreye, S., Rouhier, N., Jacquot, J. P., Hell, R.,** 2007: Redox-sensitive GFP in Arabidopsis thaliana is a quantitative biosensor for the redox potential of the cellular glutathione redox buffer. *Plant J*, vol. 52, pp. 973-986.

[41] **Tamai, K. T., Gralla, E. B., Ellerby, L. M., Valentine, J. S., Thiele, D. J.,** 1993: Yeast and mammalian metallothioneins functionally substitute for yeast copper-zinc superoxide dismutase. *Proc Natl Acad Sci U S A*, vol. 90, pp. 8013-8017.

[42] **Chae, H. Z., Chung, S. J., Rhee, S. G.,** 1994: Thioredoxin-dependent peroxide reductase from yeast. *J Biol Chem*, vol. 269, pp. 27670-27678.

[43] **Pedrajas, J. R., Kosmidou, E., Miranda-Vizuete, A., Gustafsson, J. A., Wright, A. P., Spyrou, G.,** 1999: Identification and functional characterization of a novel mitochondrial thioredoxin system in *Saccharomyces cerevisiae*. *J Biol Chem*, vol. 274, pp. 6366-6373.

[44] **Herrero, E., Ros, J., Belli, G., Cabiscol, E.,** 2008: Redox control and oxidative stress in yeast cells. *Biochim Biophys Acta*, vol. 1780, pp. 1217-1235.

[45] **Thorpe, G. W., Fong, C. S., Alic, N., Higgins, V. J., Dawes, I. W.,** 2004: Cells have distinct mechanisms to maintain protection against different reactive oxygen species: oxidative-stress-response genes. *Proc Natl Acad Sci U S A*, vol. 101, pp. 6564-6569.

[46] **Jackson, A. L., Loeb, L. A.,** 2001: The contribution of endogenous sources of DNA damage to the multiple mutations in cancer. *Mutat Res*, vol. 477, pp. 7-21.

[47] **Ikner, A., Shiozaki, K.,** 2005: Yeast signaling pathways in the oxidative stress response. *Mutat Res*, vol. 569, pp. 13-27.

[48] **Singh, K. K.,** 2000: The *Saccharomyces cerevisiae* Sln1p-Ssk1p two-component system mediates response to oxidative stress and in an oxidant-specific fashion. *Free Radic Biol Med*, vol. 29, pp. 1043-1050.

[49] **Curran, B. P., Khalawan, S. A., Chatterjee, M. T.,** 2000: Dioctyl phthalate increases the percentage of unsaturated fatty acids with a concomitant decrease in cellular heat shock sensitivity in the yeast *Saccharomyces cerevisiae*. *Microbiology*, vol. 146 (Pt 10), pp. 2679-2684.

[50] **Arguelles, J. C.,** 2000: Physiological roles of trehalose in bacteria and yeasts: a comparative analysis. *Arch Microbiol*, vol. 174, pp. 217-224.

[51] **Zaragoza, O., Gonzalez-Parraga, P., Pedreno, Y., Alvarez-Peral, F. J., Arguelles, J. C.,** 2003: Trehalose accumulation induced during the oxidative stress response is independent of TPS1 mRNA levels in *Candida albicans*. *Int Microbiol*, vol. 6, pp. 121-125.

[52] **Singer, M. A., Lindquist, S.,** 1998: Thermotolerance in *Saccharomyces cerevisiae*: the Yin and Yang of trehalose. *Trends Biotechnol*, vol. 16, pp. 460-468.

[53] **SGD, *S*. G. D.,** 2010: *Saccharomyces cerevisiae* S288c Pathway: trehalose biosynthesis. Retrieved 25.10.2010 from http://pathway.yeastgenome.org/YEAST/new-image?type=PATHWAY&object=TRESYN-PWY&detail-level=2

[54] **Boy-Marcotte, E., Lagniel, G., Perrot, M., Bussereau, F., Boudsocq, A., Jacquet, M., Labarre, J.,** 1999: The heat shock response in yeast: differential regulations and contributions of the Msn2p/Msn4p and Hsf1p regulons. *Mol Microbiol*, vol. 33, pp. 274-283.

[55] **Tanghe, A., Van Dijck, P., Colavizza, D., Thevelein, J. M.,** 2004: Aquaporin-mediated improvement of freeze tolerance of *Saccharomyces cerevisiae* is restricted to rapid freezing conditions. *Appl Environ Microbiol*, vol. 70, pp. 3377-3382.

[56] **Panadero, J., Pallotti, C., Rodriguez-Vargas, S., Randez-Gil, F., Prieto, J. A.,** 2006: A downshift in temperature activates the high osmolarity glycerol (HOG) pathway, which determines freeze tolerance in *Saccharomyces cerevisiae*. *J Biol Chem*, vol. 281, pp. 4638-4645.

[57] **Hirasawa, T., Yoshikawa, K., Nakakura, Y., Nagahisa, K., Furusawa, C., Katakura, Y., Shimizu, H., Shioya, S.,** 2007: Identification of target genes conferring ethanol stress tolerance to *Saccharomyces cerevisiae* based on DNA microarray data analysis. *J Biotechnol*, vol. 131, pp. 34-44.

[58] **Howlett, N. G., Avery, S. V.,** 1997: Induction of lipid peroxidation during heavy metal stress in *Saccharomyces cerevisiae* and influence of plasma membrane fatty acid unsaturation. *Appl Environ Microbiol*, vol. 63, pp. 2971-2976.

[59] **Shanmuganathan, A., Avery, S. V., Willetts, S. A., Houghton, J. E.,** 2004: Copper-induced oxidative stress in *Saccharomyces cerevisiae* targets enzymes of the glycolytic pathway. *FEBS Lett*, vol. 556, pp. 253-259.

[60] **Stadler, J. A., Schweyen, R. J.,** 2002: The yeast iron regulon is induced upon cobalt stress and crucial for cobalt tolerance. *J Biol Chem*, vol. 277, pp. 39649-39654.

[61] **Harrison, J. C., Haber, J. E.,** 2006: Surviving the breakup: the DNA damage checkpoint. *Annu Rev Genet*, vol. 40, pp. 209-235.

[62] **Kolodner, R. D., Putnam, C. D., Myung, K.,** 2002: Maintenance of genome stability in *Saccharomyces cerevisiae*. *Science*, vol. 297, pp. 552-557.

[63] **Elledge, S. J.,** 1996: Cell cycle checkpoints: preventing an identity crisis. *Science*, vol. 274, pp. 1664-1672.

[64] **Desany, B. A., Alcasabas, A. A., Bachant, J. B., Elledge, S. J.,** 1998: Recovery from DNA replicational stress is the essential function of the S-phase checkpoint pathway. *Genes Dev*, vol. 12, pp. 2956-2970.

[65] **Cooke, M. S., Evans, M. D., Dizdaroglu, M., Lunec, J.,** 2003: Oxidative DNA damage: mechanisms, mutation, and disease. *FASEB J*, vol. 17, pp. 1195-1214.

[66] **Friedberg, E. C., Walker, G. C., Siede, W., Wood, R. D., Schultz, R. A., Ellenburger, T.,** 2006: DNA Repair and Mutagenesis, 2nd Edition 2nd Edition ed., ASM Press.

[67] **van Loon, B., Markkanen, E., Hubscher, U.,** 2010: Oxygen as a friend and enemy: How to combat the mutational potential of 8-oxo-guanine. *DNA Repair (Amst)*, vol. 9, pp. 604-616.

[68] **Doudican, N. A., Song, B., Shadel, G. S., Doetsch, P. W.,** 2005: Oxidative DNA damage causes mitochondrial genomic instability in *Saccharomyces cerevisiae*. *Mol Cell Biol*, vol. 25, pp. 5196-5204.

[69] **Bruner, S. D., Norman, D. P., Verdine, G. L.,** 2000: Structural basis for recognition and repair of the endogenous mutagen 8-oxoguanine in DNA. *Nature*, vol. 403, pp. 859-866.

[70] **Cherry, J. M., Ball, C., Weng, S., Juvik, G., Schmidt, R., Adler, C., Dunn, B., Dwight, S., Riles, L., Mortimer, R. K., Botstein, D.,** 1997: Genetic and physical maps of *Saccharomyces cerevisiae*. *Nature*, vol. 387, pp. 67-73.

[71] **SGD-project,** 2010: Saccharomyces Genome Database. Retrieved 07.02.2010 from http://www.yeastgenome.org/

[72] **Jansen, G., Wu, C., Schade, B., Thomas, D. Y., Whiteway, M.,** 2005: Drag&Drop cloning in yeast. *Gene*, vol. 344, pp. 43-51.

[73] **Kelley, R., Ideker, T.,** 2009: Genome-wide fitness and expression profiling implicate Mga2 in adaptation to hydrogen peroxide. *PLoS Genet*, vol. 5, pp. e1000488.

[74] **Eisen, M. B., Spellman, P. T., Brown, P. O., Botstein, D.,** 1998: Cluster analysis and display of genome-wide expression patterns. *Proc Natl Acad Sci U S A*, vol. 95, pp. 14863-14868.

[75] **O'Neill, B. M., Szyjka, S. J., Lis, E. T., Bailey, A. O., Yates, J. R., 3rd, Aparicio, O. M., Romesberg, F. E.,** 2007: Pph3-Psy2 is a phosphatase complex required for Rad53 dephosphorylation and replication fork restart during recovery from DNA damage. *Proc Natl Acad Sci U S A*, vol. 104, pp. 9290-9295.

[76] **Chen, S. H., Smolka, M. B., Zhou, H.,** 2007: Mechanism of Dun1 activation by Rad53 phosphorylation in *Saccharomyces cerevisiae*. *J Biol Chem*, vol. 282, pp. 986-995.

[77] **Tong, A., Boone, C.,** 2005: Synthetic Genetic Array (SGA) Analysis in *Saccharomyces cerevisiae Methods in Molecular Biology*, vol. 313.

APPENDICES

APPENDIX A: Background genotype of the wild types

APPENDIX B: Genotype of the mutant strains. All of the mutants are constructed by Synthetic Genetic Array (SGA) strategy [77].

APPENDIX C: Information about knock-out genes: names, functions and descriptions

APPENDIX D: The Whole Growth Curves and LSU to OD Conversions of 38 KO Mutants and Wild Types

APPENDIX A: Background genotype of the wild types

Y7092

MATα, can1::STE2pr-Sp_his5 lyp1Δ his3Δ leu2Δ ura3Δ met15Δ

Y7220

MATα, can1::STE2pr-Sp_his5 ura3::NatR lyp1Δ cyh2 his3Δ leu2Δ met15Δ0

BY4741

*MAT*a, *his3Δ1 leu2Δ0 met15Δ0 ura3Δ0*

W303

*MAT*a/*MAT*α {*leu2-3,112 trp1-1 can1-100 ura3-1 ade2-1 his3-11,15*} [*phi*$^{+}$]

APPENDIX B: Genotype of the mutant strains. All of the mutants are constructed by Synthetic Genetic Array (SGA) strategy [77].

ORF	Deleted Gene	Relevant Genotype	WT Background	Additional (Auxotrophic) Markers	
				Lysine	Methionine
YGL021W	ALK1	*alk1Δ::KanR, MAT*a	Y7092	+	-
YBL009W	ALK2	*alk2Δ::KanR, MAT*a	Y7220	+	+
YNL020C	ARK1	*ark1Δ::KanR, MAT*a	Y7092	+	+
YGR262C	BUD32	*bud32Δ::KanR, MAT*a	Y7220	+	-
YBR274W	CHK1	*chk1Δ::KanR, MAT*a	Y7220	+	-
YOR061W	CKA2	*cka2Δ::KanR, MAT*a	Y7220	+	-
YPR111W	DBF20	*dbf20Δ::KanR, MAT*a	Y7220	+	+
YDL101C	DUN1	*dun1Δ::KanR, MAT*a	BY4741	+	-
YJL165C	HAL5	*hal5Δ::KanR, MAT*a	Y7220	+	+
YLR113W	HOG1	*hog1Δ::KanR, MAT*a	BY4741	+	-
YDR122W	KIN1	*kin1Δ::KanR, MAT*a	Y7220	+	-
YBR136W	MEC1	*sml1Δ::HIS3, mec1Δ::TRP1, bar1::LEU2, MAT*a	W303	+	-
YOR351C	MEK1	*mek1Δ::KanR, MAT*a	BY4741	+	-
YOR231W	MKK1	*mkk1Δ::KanR, MAT*a	Y7092	+	-
YNL099C	OCA1	*oca1Δ::KanR, MAT*a	Y7220	+	+
YJL128C	PBS2	*pbs2Δ::KanR, MAT*a	BY4741	+	-
YDR490C	PKH1	*pkhΔ1::KanR, MAT*a	Y7220	+	-
YOL100W	PKH2	*pkh2Δ::KanR, MAT*a	Y7092	+	-
YIL042C	PKP1	*pkp1Δ::KanR, MAT*a	Y7220	+	+
YDR075W	PPH3	*pph3Δ::KanR, MAT*a	Y7220	+	-
YIL095W	PRK1	*prk1Δ::KanR, MAT*a	Y7220	+	-
YDL006W	PTC1	*ptc1Δ::KanR, MAT*a	BY4741	+	-
YBL056W	PTC3	*ptc3Δ::KanR, MAT*a	BY4741	+	-
YOR208W	PTP2	*ptp2Δ::KanR, MAT*a	Y7092	+	+
YPL153C	RAD53	*sml1Δ::HIS3, rad53-1, MAT*a	W303	+	-
YGL158W	RCK1	*rck1Δ::KanR, MAT*a	Y7220	+	-
YLR248W	RCK2	*rck2Δ::KanR, MAT*a	BY4741	+	+
YNL032W	SIW14	*siw14Δ::KanR, MAT*a	Y7092	+	-
YDR523C	SPS1	*sps1Δ::KanR, MAT*a	Y7220	+	-
YNR031C	SSK2	*ssk2Δ::KanR, MAT*a	Y7220	+	-
YCR073C	SSK22	*ssk22Δ::KanR, MAT*a	BY4741	+	-
YBL088C	TEL1	*tel1Δ::KanR, MAT*a	BY4741	+	-
YDR247W	VHS1	*vhs1Δ::KanR, MAT*a	BY4741	+	-
YBR097W	VPS15	*vps15Δ::KanR, MAT*a	BY4741	+	-
YHR135C	YCK1	*yck1Δ::KanR, MAT*a	Y7092	+	-
YER123W	YCK3	*yck3Δ::KanR, MAT*a	Y7092	+	-
YOL128C	YGK3	*ygk3Δ::KanR, MAT*a	Y7220	+	-
YKL171W	YKL171W	*ykl171wΔ::KanR, MAT*a	Y7092	+	-

ORF: Open Reading Frame, **WT:** Wild Type

APPENDIX C: Information about knock-out genes: names, functions and descriptions

Gene	Function	Description
ALK1	Protein Kinase	Protein kinase; accumulation and phosphorylation are periodic during the cell cycle; phosphorylated in response to DNA damage; contains characteristic motifs for degradation via the APC pathway; similar to Alk2p and to mammalian haspins
ALK2	Protein Kinase	Protein kinase; accumulation and phosphorylation are periodic during the cell cycle; phosphorylated in response to DNA damage; contains characteristic motifs for degradation via the APC pathway; similar to Alk1p and to mammalian haspins
ARK1	Protein Kinase	Serine/threonine protein kinase involved in regulation of the cortical actin cytoskeleton; involved in control of endocytosis
BUD32	Protein Kinase	Protein kinase proposed to be involved in bud-site selection, telomere uncapping and elongation, and transcription; component of the EKC/KEOPS protein complex with Kae1p, Cgi121p, Pcc1p, and Gon7p
CHK1	Protein Kinase	Serine/threonine kinase and DNA damage checkpoint effector, mediates cell cycle arrest via phosphorylation of Pds1p; phosphorylated by checkpoint signal transducer Mec1p; homolog of S. pombe and mammalian Chk1 checkpoint kinase
CKA2	Protein Kinase	Alpha' catalytic subunit of casein kinase 2, a Ser/Thr protein kinase with roles in cell growth and proliferation; the holoenzyme also contains CKA1, CKB1 and CKB2, the many substrates include transcription factors and all RNA polymerases
DBF20	Protein Kinase	Ser/Thr kinase involved in late nuclear division, one of the mitotic exit network (MEN) proteins; necessary for the execution of cytokinesis
DUN1	Protein Kinase	Cell-cycle checkpoint serine-threonine kinase required for DNA damage-induced transcription of certain target genes, phosphorylation of Rad55p and Sml1p, and transient G2/M arrest after DNA damage; also regulates postreplicative DNA repair
HAL5	Protein Kinase (Putative)	Putative protein kinase; overexpression increases sodium and lithium tolerance, whereas gene disruption increases cation and low pH sensitivity and impairs potassium uptake, suggesting a role in regulation of Trk1p and/or Trk2p transporters
HOG1	Protein Kinase	Mitogen-activated protein kinase involved in osmoregulation via three independent osmosensors; mediates the recruitment and activation of RNA Pol II at Hot1p-dependent promoters; localization regulated by Ptp2p and Ptp3p
KIN1	Protein Kinase	Serine/threonine protein kinase involved in regulation of exocytosis; localizes to the cytoplasmic face of the plasma membrane; closely related to Kin2p
MEC1	Protein Kinase	Genome integrity checkpoint protein and PI kinase superfamily member; signal transducer required for cell cycle arrest and transcriptional responses prompted by damaged or unreplicated DNA; monitors and participates in meiotic recombination
MEK1	Protein Kinase	Meiosis-specific serine/threonine protein kinase, functions in meiotic checkpoint, promotes recombination between homologous chromosomes by suppressing double strand break repair between sister chromatids
MKK1	Protein Kinase	Mitogen-activated kinase kinase involved in protein kinase C signaling pathway that controls cell integrity; upon activation by Bck1p phosphorylates downstream target, Slt2p; functionally redundant with Mkk2p
OCA1	Protein Phosphatase (Putative)	Putative protein tyrosine phosphatase, required for cell cycle arrest in response to oxidative damage of DNA
PBS2	Protein Kinase	MAP kinase kinase that plays a pivotal role in the osmosensing signal-transduction pathway, activated under severe osmotic stress; plays a role in regulating Ty1 transposition

PKH1	Protein Kinase	Serine/threonine protein kinase involved in sphingolipid-mediated signaling pathway that controls endocytosis; activates Ypk1p and Ykr2p, components of signaling cascade required for maintenance of cell wall integrity; redundant with Pkh2p
PKH2	Protein Kinase	Serine/threonine protein kinase involved in sphingolipid-mediated signaling pathway that controls endocytosis; activates Ypk1p and Ykr2p, components of signaling cascade required for maintenance of cell wall integrity; redundant with Pkh1p
PKP1	Protein Kinase	Mitochondrial protein kinase involved in negative regulation of pyruvate dehydrogenase complex activity by phosphorylating the ser-133 residue of the Pda1p subunit; acts in concert with kinase Pkp2p and phosphatases Ptc5p and Ptc6p
PPH3	Protein Phosphatase	Catalytic subunit of an evolutionarily conserved protein phosphatase complex containing Psy2p and the regulatory subunit Psy4p; required for cisplatin resistance; involved in activation of Gln3p
PRK1	Protein Kinase	Protein serine/threonine kinase; regulates the organization and function of the actin cytoskeleton through the phosphorylation of the Pan1p-Sla1p-End3p protein complex
PTC1	Protein Phosphatase	Type 2C protein phosphatase (PP2C); inactivates the osmosensing MAPK cascade by dephosphorylating Hog1p; mutation delays mitochondrial inheritance; deletion reveals defects in precursor tRNA splicing, sporulation and cell separation
PTC3	Protein Phosphatase	Type 2C protein phosphatase; dephosphorylates Hog1p (see also Ptc2p) to limit maximal kinase activity induced by osmotic stress; dephosphorylates T169 phosphorylated Cdc28p (see also Ptc2p); role in DNA checkpoint inactivation
PTP2	Protein Phosphatase	Phosphotyrosine-specific protein phosphatase involved in the inactivation of mitogen-activated protein kinase (MAPK) during osmolarity sensing; dephosporylates Hog1p MAPK and regulates its localization; localized to the nucleus
RAD53	Protein Kinase	Protein kinase, required for cell-cycle arrest in response to DNA damage; activated by trans autophosphorylation when interacting with hyperphosphorylated Rad9p; also interacts with ARS1 and plays a role in initiation of DNA replication
RCK1	Protein Kinase	Protein kinase involved in the response to oxidative stress; identified as suppressor of S. pombe cell cycle checkpoint mutations
RCK2	Protein Kinase	Protein kinase involved in the response to oxidative and osmotic stress; identified as suppressor of S. pombe cell cycle checkpoint mutations
SIW14	Protein Phosphatase	Tyrosine phosphatase that plays a role in actin filament organization and endocytosis; localized to the cytoplasm
SPS1	Protein Kinase (Putative)	Putative protein serine/threonine kinase expressed at the end of meiosis and localized to the prospore membrane, required for correct localization of enzymes involved in spore wall synthesis
SSK2	Protein Kinase	MAP kinase kinase kinase of the HOG1 mitogen-activated signaling pathway; interacts with Ssk1p, leading to autophosphorylation and activation of Ssk2p which phosphorylates Pbs2p; also mediates actin cytoskeleton recovery from osmotic stress
SSK22	Protein Kinase	MAP kinase kinase kinase of the HOG1 mitogen-activated signaling pathway; functionally redundant with, and homologous to, Ssk2p; interacts with and is activated by Ssk1p; phosphorylates Pbs2p
TEL1	Protein Kinase	Protein kinase primarily involved in telomere length regulation; contributes to cell cycle checkpoint control in response to DNA damage; functionally redundant with Mec1p; homolog of human ataxia telangiectasia (ATM) gene
VHS1	Protein Kinase	Cytoplasmic serine/threonine protein kinase; identified as a high-copy suppressor of the synthetic lethality of a sis2 sit4 double mutant, suggesting a role in G1/S phase progression; homolog of Sks1p
VPS15	Protein Kinase	Myristoylated serine/threonine protein kinase involved in vacuolar protein sorting; functions as a membrane-associated complex with Vps34p; active form recruits Vps34p to the Golgi membrane; interacts with the GDP-bound form of Gpa1p

YCK1	Protein Kinase	Palmitoylated plasma membrane-bound casein kinase I isoform; shares redundant functions with Yck2p in morphogenesis, proper septin assembly, endocytic trafficking; provides an essential function overlapping with that of Yck2p
YCK3	Protein Kinase	Palmitoylated, vacuolar membrane-localized casein kinase I isoform; negatively regulates vacuole fusion during hypertonic stress via phosphorylation of Vps41p; shares essential functions with Hrr25p; regulates vesicle fusion in AP-3 pathway
YGK3	Protein Kinase	Protein kinase related to mammalian glycogen synthase kinases of the GSK-3 family; GSK-3 homologs (Mck1p, Rim11p, Mrk1p, Ygk3p) are involved in control of Msn2p-dependent transcription of stress responsive genes and in protein degradation
YKL171W	Protein Kinase	Protein kinase; implicated in proteasome function; interacts with TORC1, Ure2 and Gdh2; overexpression leads to hypersensitivity to rapamycin and nuclear accumulation of Gln3; epitope-tagged protein localizes to the cytoplasm

APPENDIX D: The Whole Growth Curves and LSU to OD Conversions of 38 KO Mutants and Wild Types

All experiments listed below are in order of date. Each plate run has its particular synonym composed of protocol name, date, stress factor and user (e.g. Ferm48_20100304_H2O2_Ali). Vertical black lines show the treatment times with H_2O_2. In all growth plots, x-axis is the $\log_2$ (LSU) and y-axis is the time (hours). Linear fits of LSU and OD are shown at the very end of each plate run. y-axis: LSU; x-axis: OD; Rsq: R^2; all equations are in form of $y = mx + n$, where m: slope and n: offset

Ferm48_20100304_H2O2_Ali

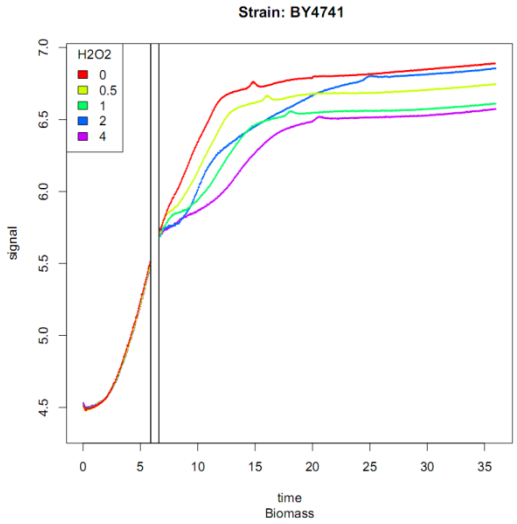

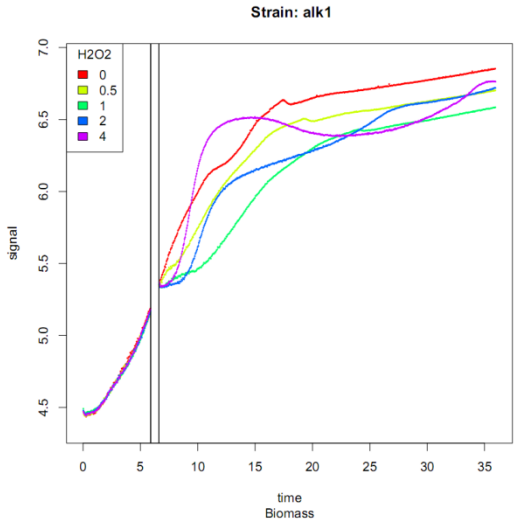

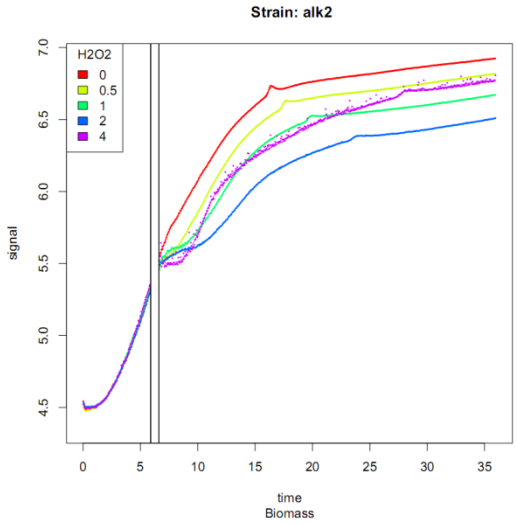

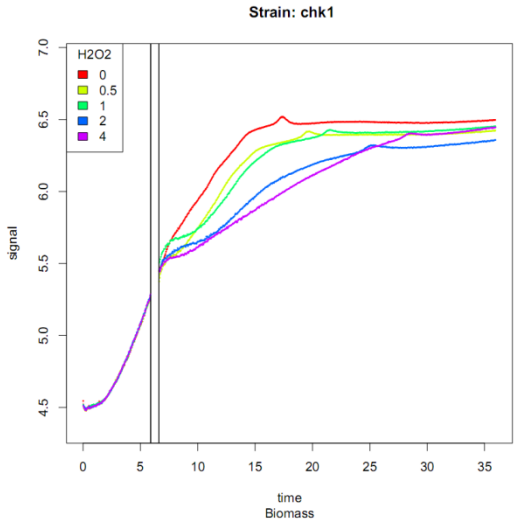

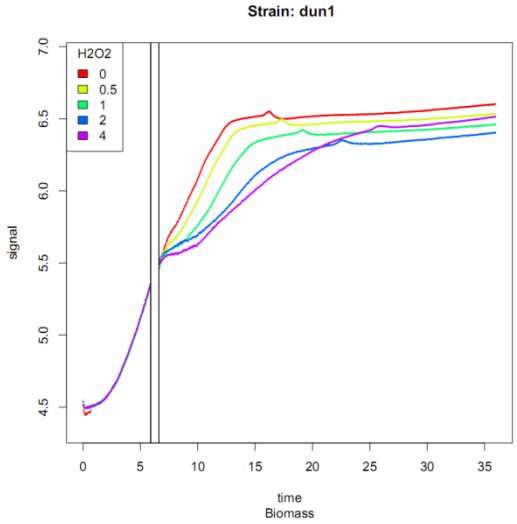

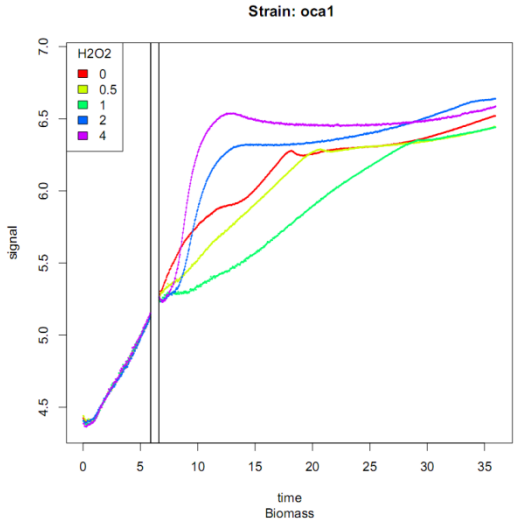

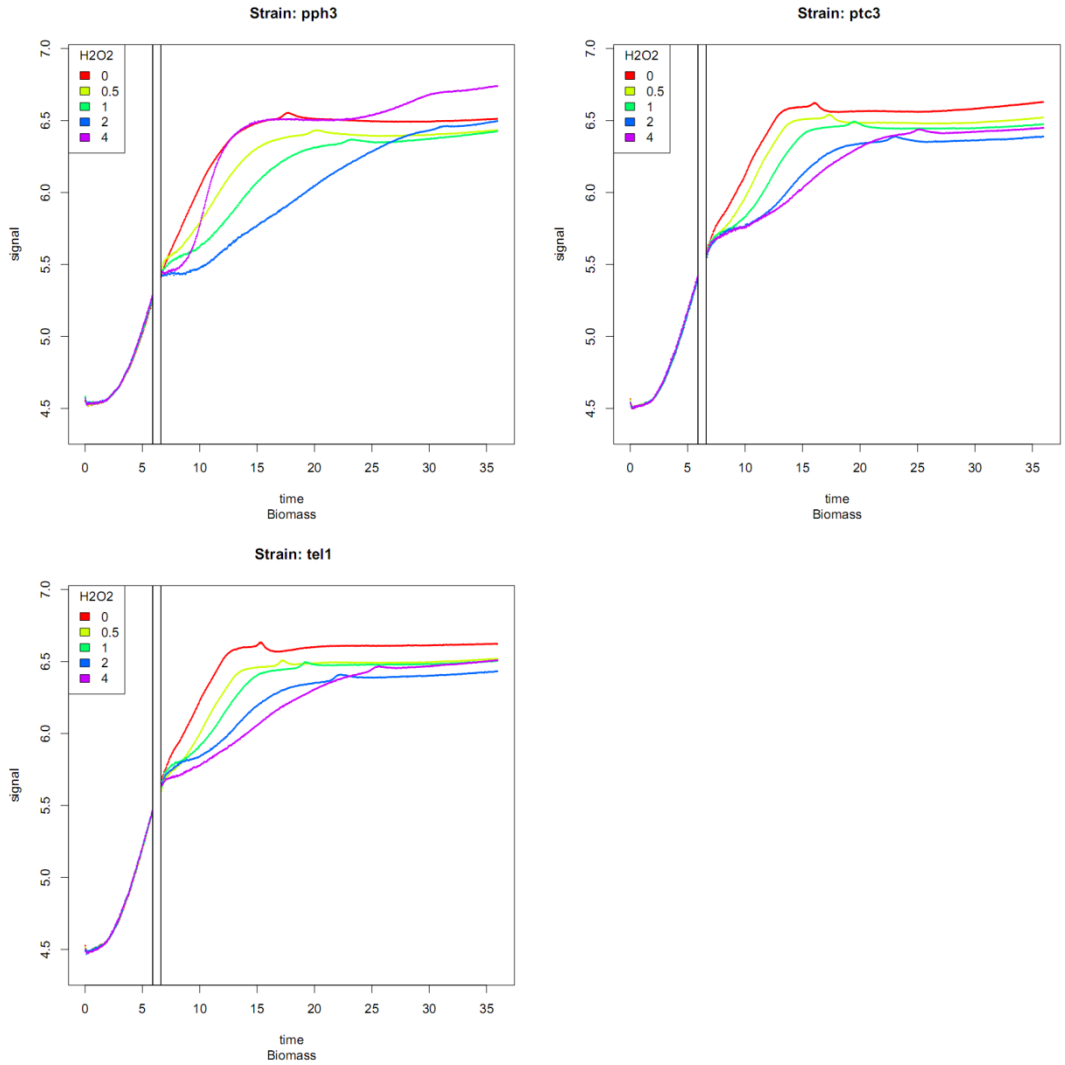
Strain: pph3
Strain: ptc3
Strain: tel1
H2O2
0
0.5
1
2
4
signal
time
Biomass

Ferm48_20100401_H2O2_Ali

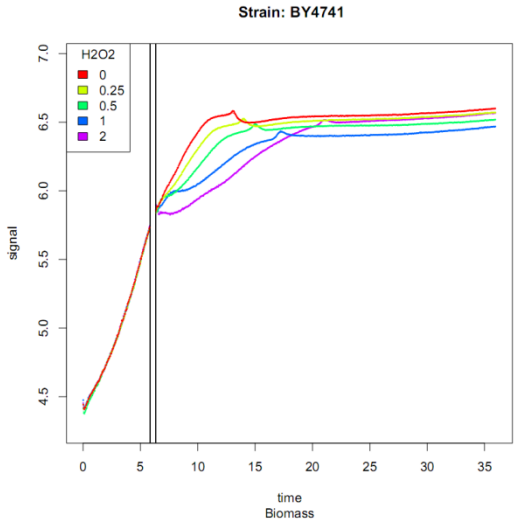

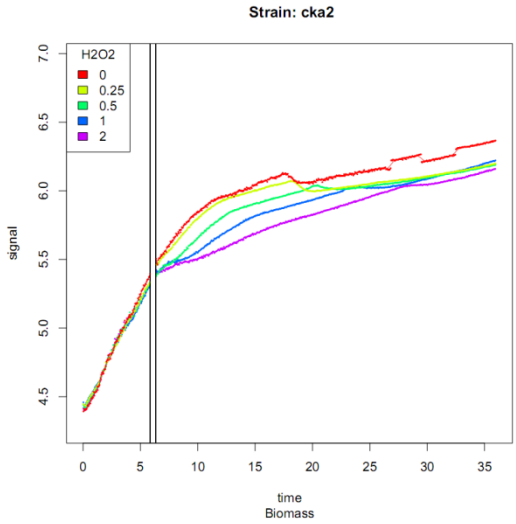

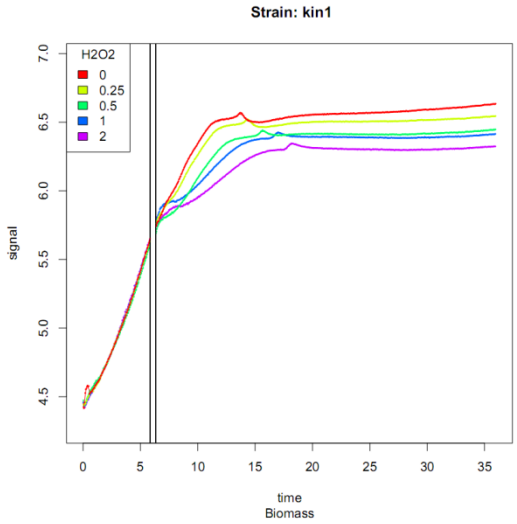

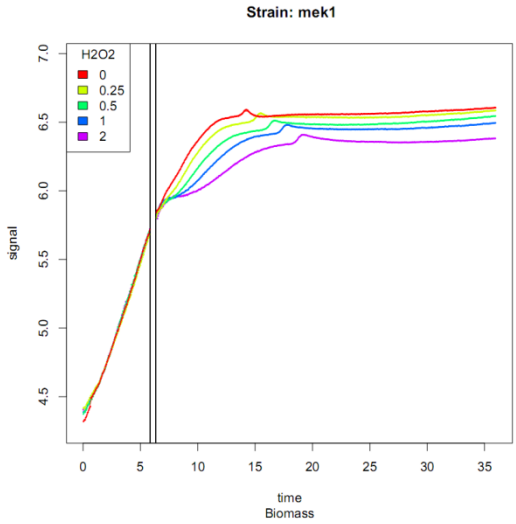

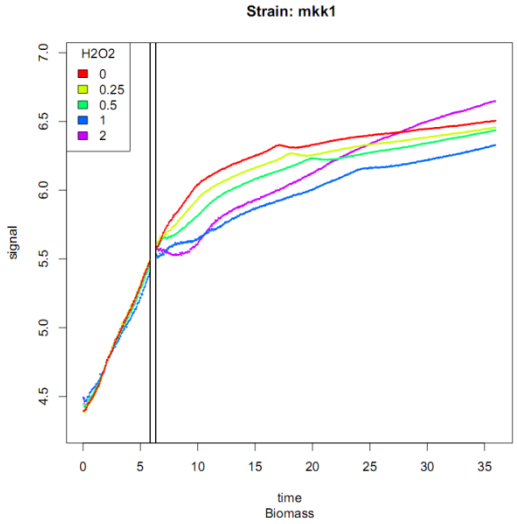

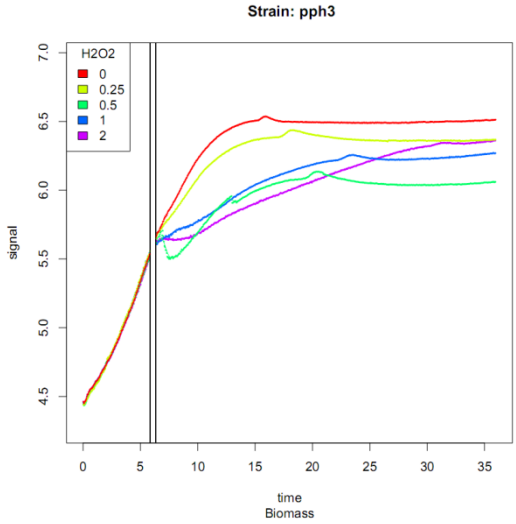

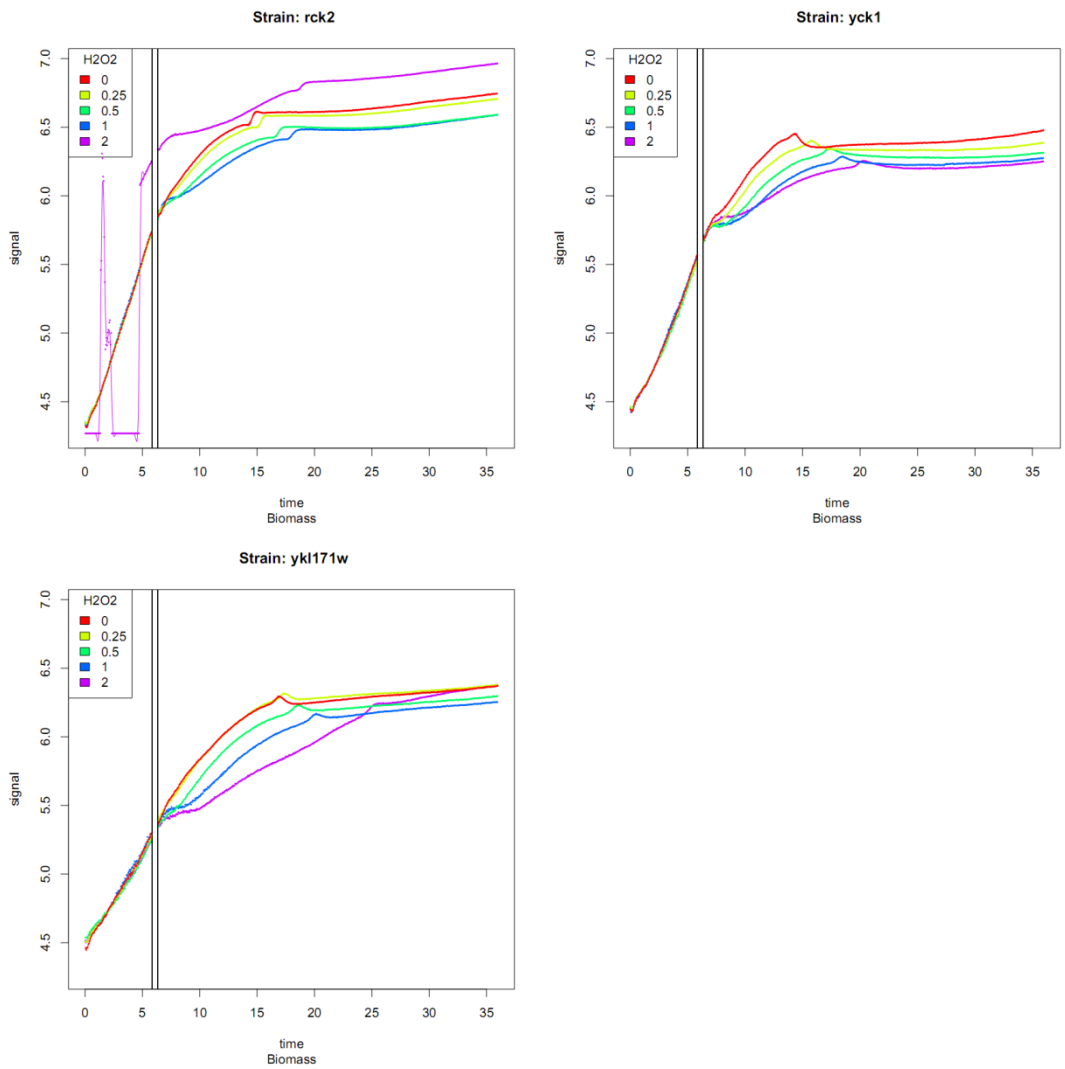
Strain: rck2
Strain: yck1
Strain: ykl171w
H2O2
0
0.25
0.5
1
2
signal
time
Biomass

Ferm48_20100407_H2O2_Ali

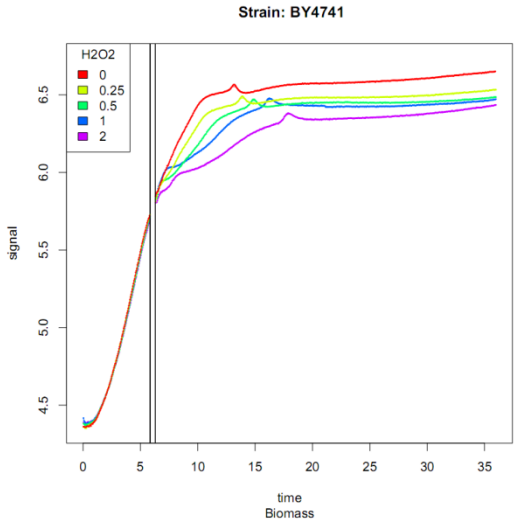

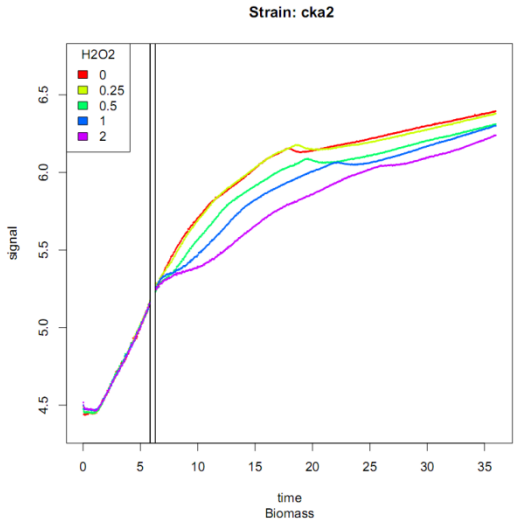

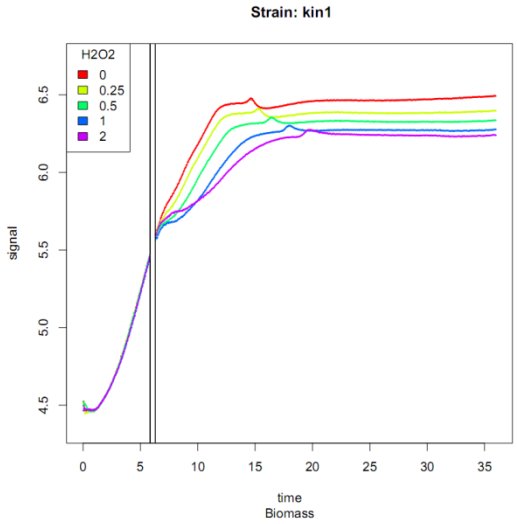

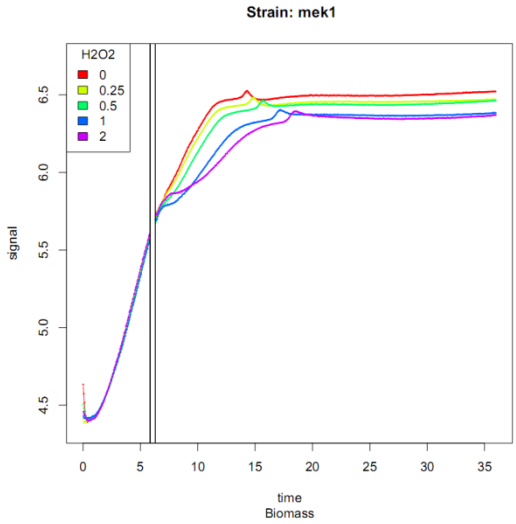

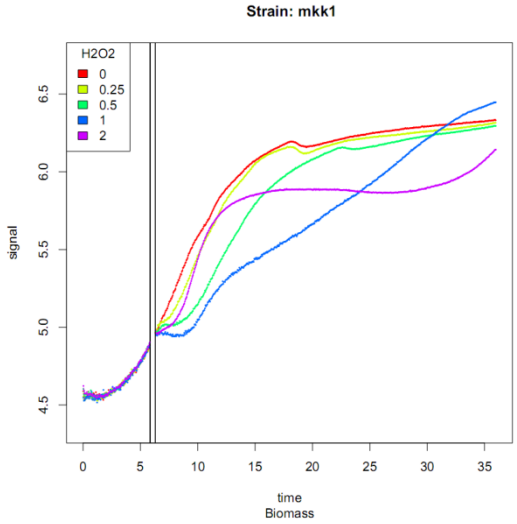

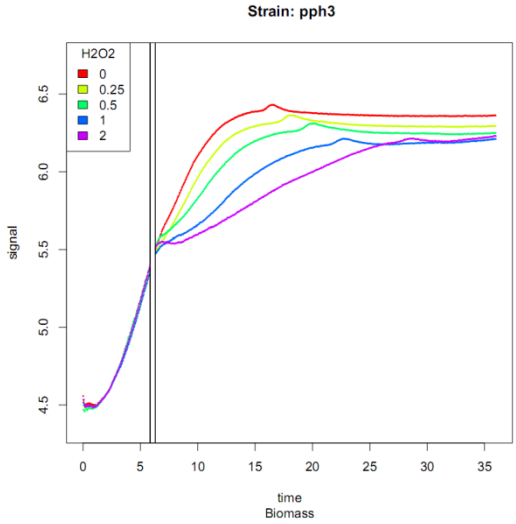

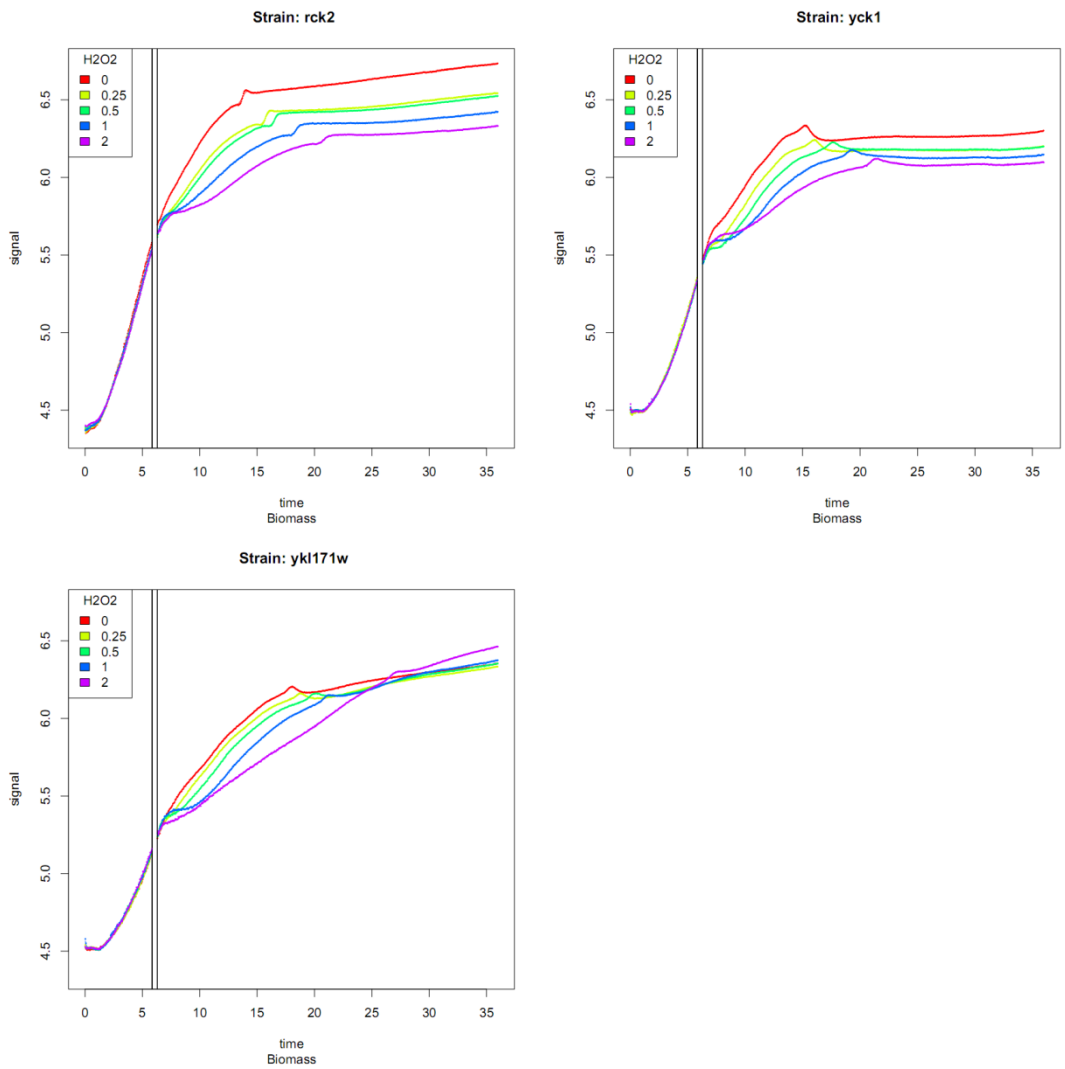
Strain: rck2
Strain: yck1
Strain: ykl171w
H2O2
0
0.25
0.5
1
2
signal
time
Biomass

Ferm48_20100412_H2O2_Ali

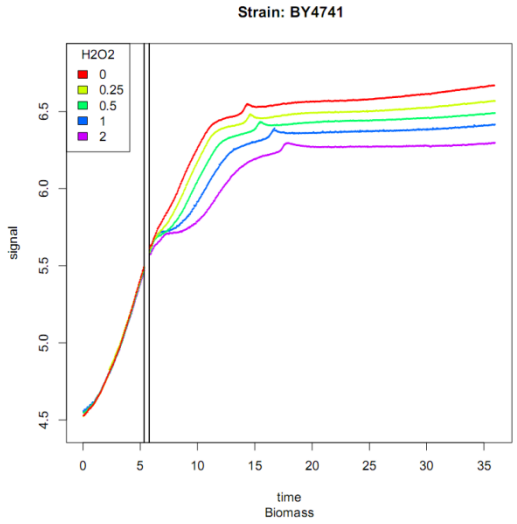

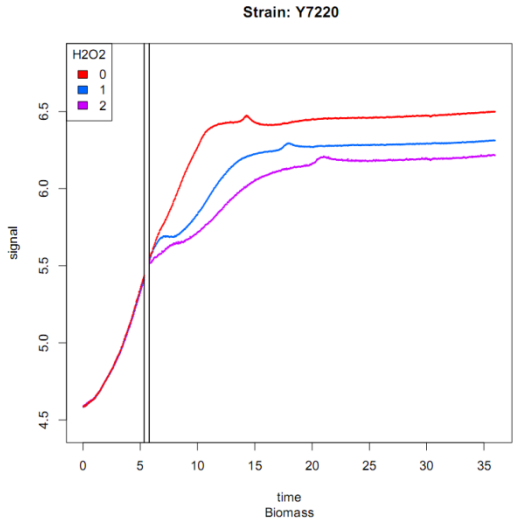

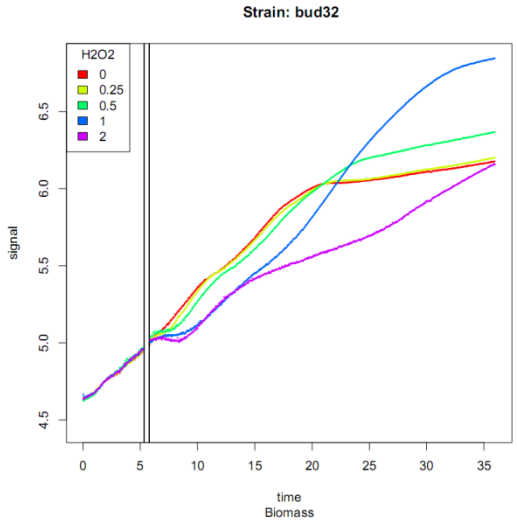

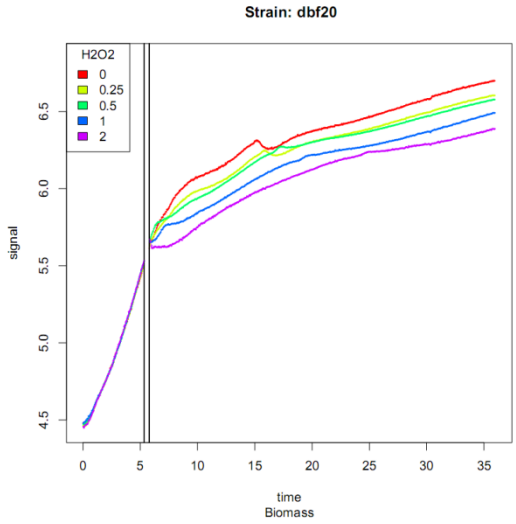

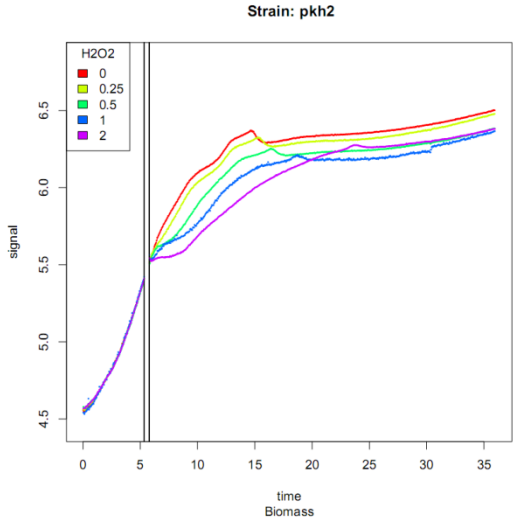

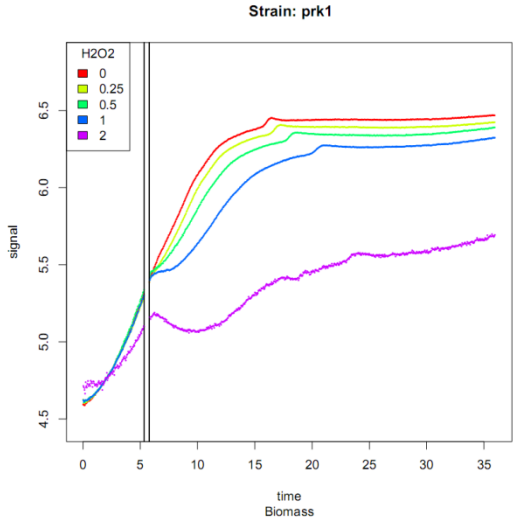

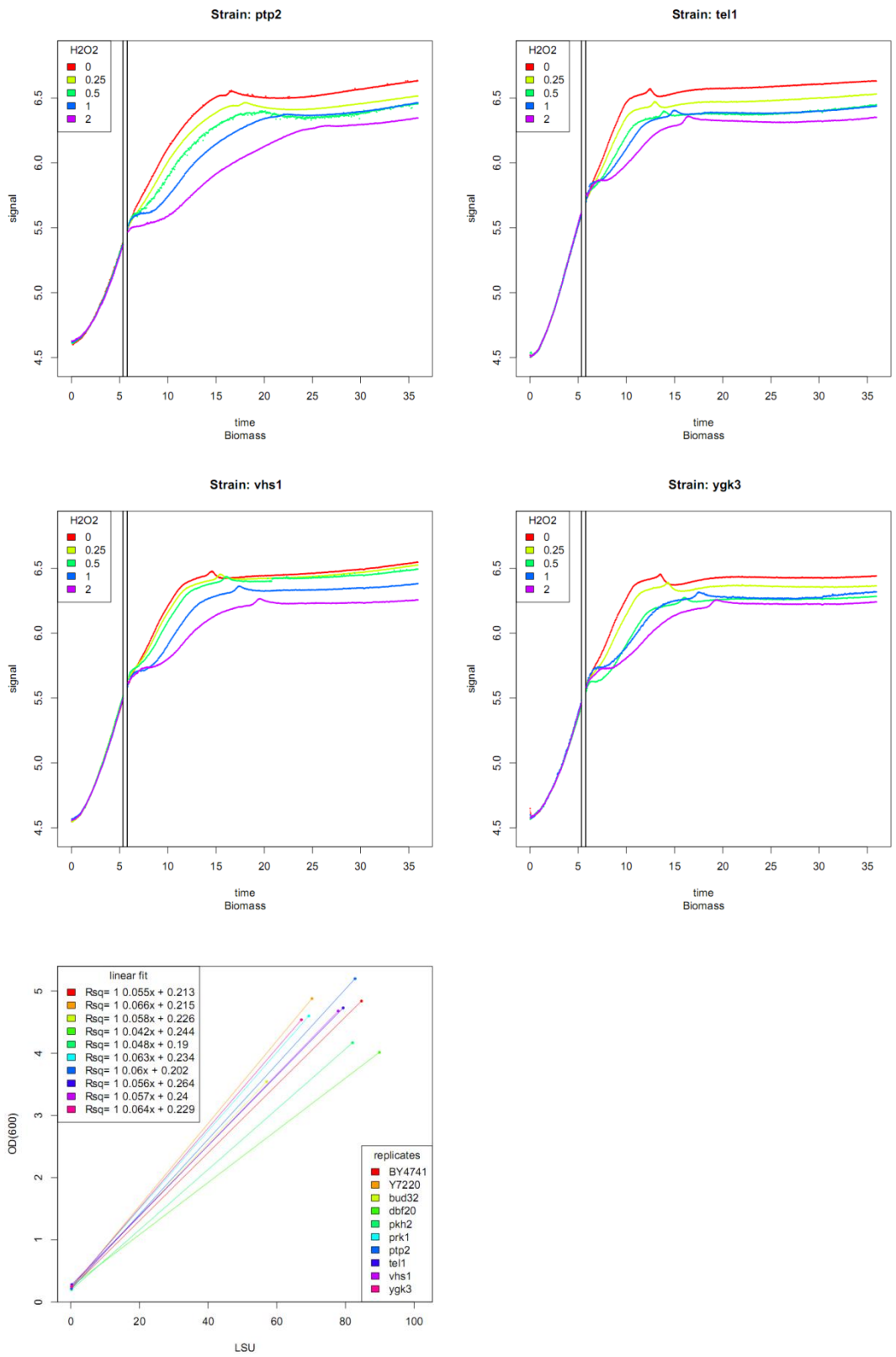
Strain: ptp2
Strain: tel1
Strain: vhs1
Strain: ygk3
H2O2
0
0.25
0.5
1
2
signal
time
Biomass
linear fit
Rsq= 1 0.055x + 0.213
Rsq= 1 0.066x + 0.215
Rsq= 1 0.058x + 0.226
Rsq= 1 0.042x + 0.244
Rsq= 1 0.048x + 0.19
Rsq= 1 0.063x + 0.234
Rsq= 1 0.06x + 0.202
Rsq= 1 0.056x + 0.264
Rsq= 1 0.057x + 0.24
Rsq= 1 0.064x + 0.229
replicates
BY4741
Y7220
bud32
dbf20
pkh2
prk1
ptp2
tel1
vhs1
ygk3
OD(600)
LSU

Ferm48_20100414_H2O2_Ali

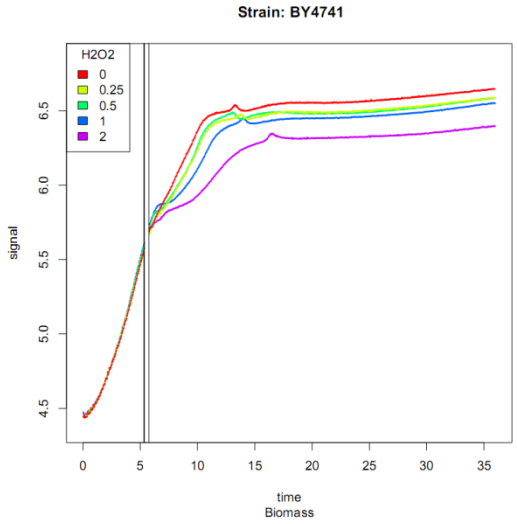

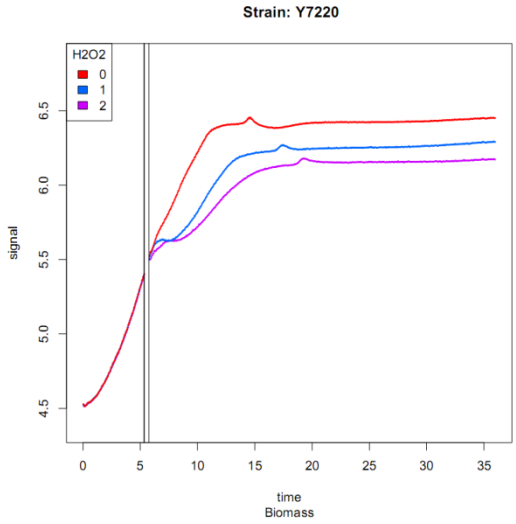

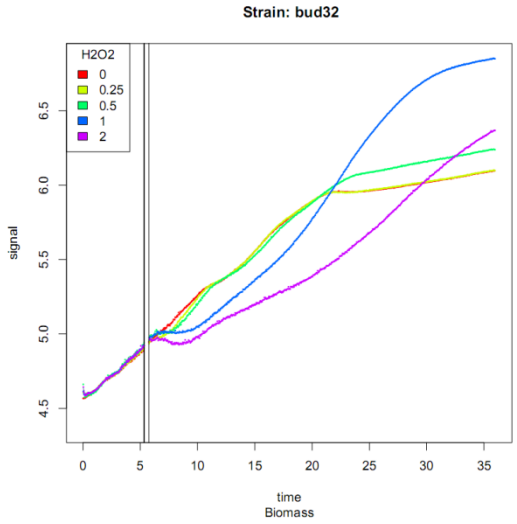

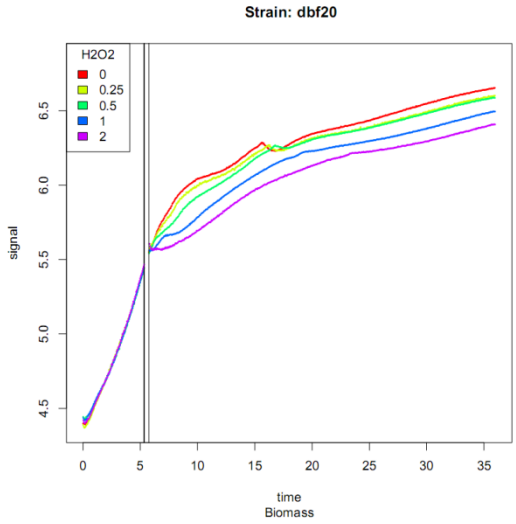

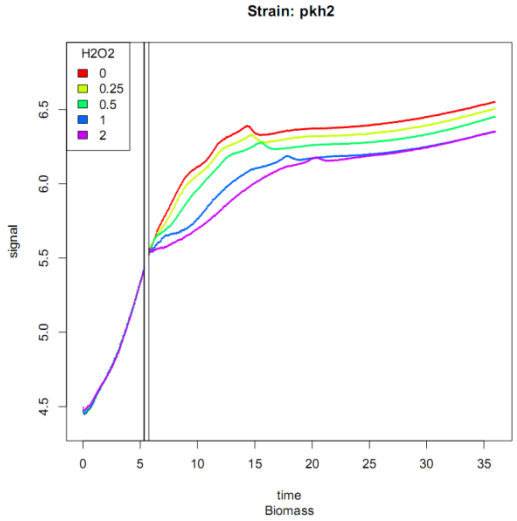

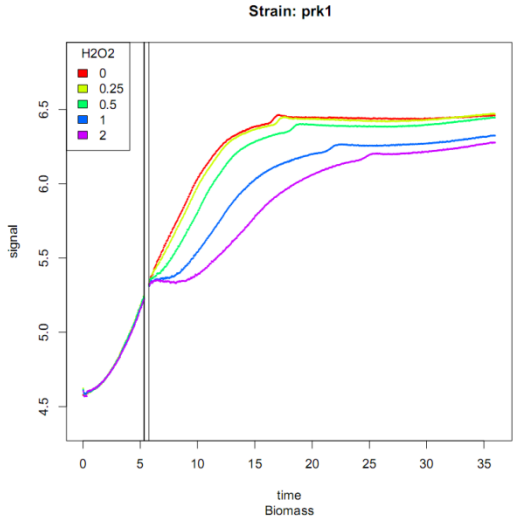

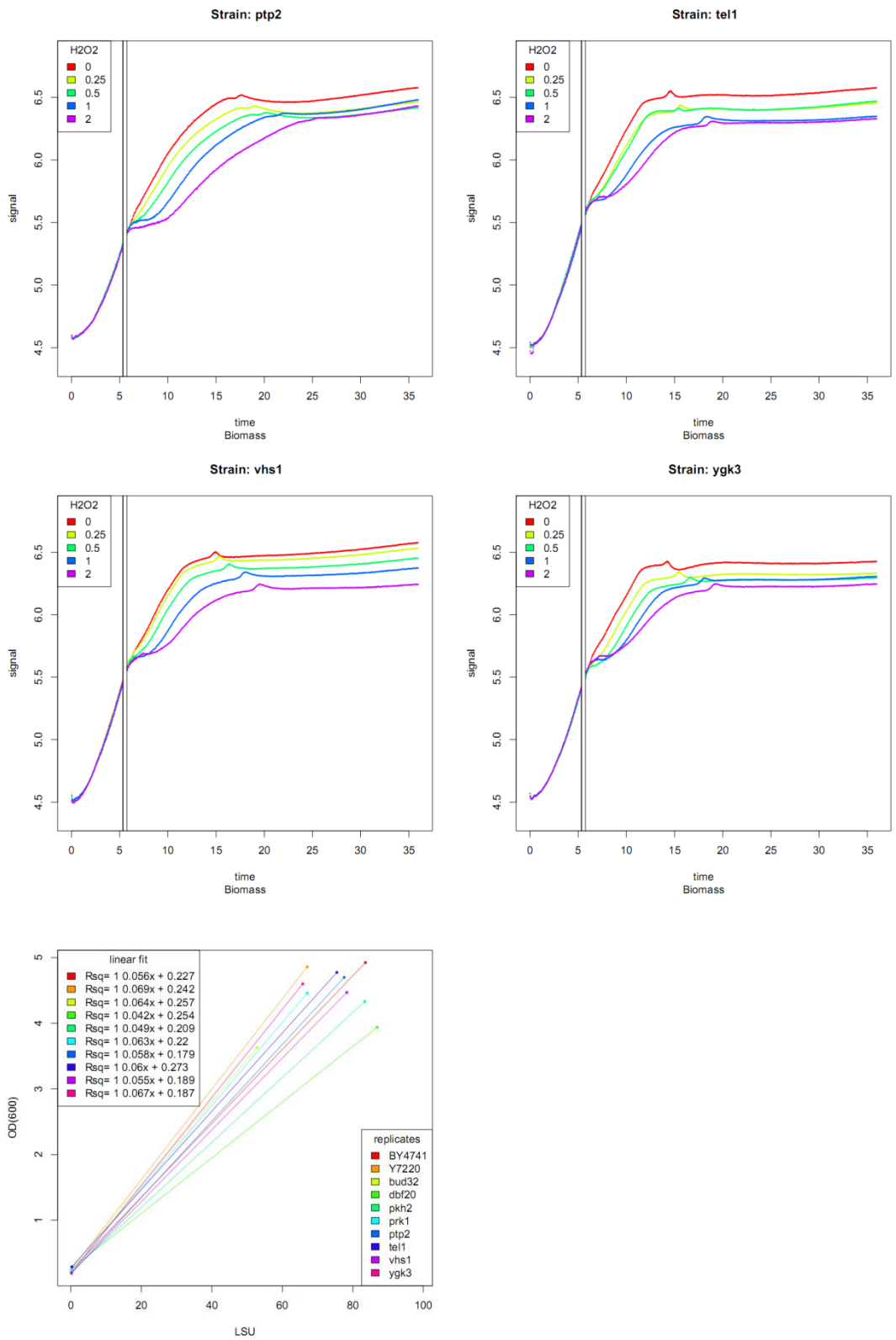
Strain: ptp2
Strain: tel1
Strain: vhs1
Strain: ygk3
H2O2
0
0.25
0.5
1
2
signal
time
Biomass
linear fit
Rsq= 1 0.056x + 0.227
Rsq= 1 0.069x + 0.242
Rsq= 1 0.064x + 0.257
Rsq= 1 0.042x + 0.254
Rsq= 1 0.049x + 0.209
Rsq= 1 0.063x + 0.22
Rsq= 1 0.058x + 0.179
Rsq= 1 0.06x + 0.273
Rsq= 1 0.055x + 0.189
Rsq= 1 0.067x + 0.187
replicates
BY4741
Y7220
bud32
dbf20
pkh2
prk1
ptp2
tel1
vhs1
ygk3
OD(600)
LSU

Ferm48_20100418_H2O2_Ali

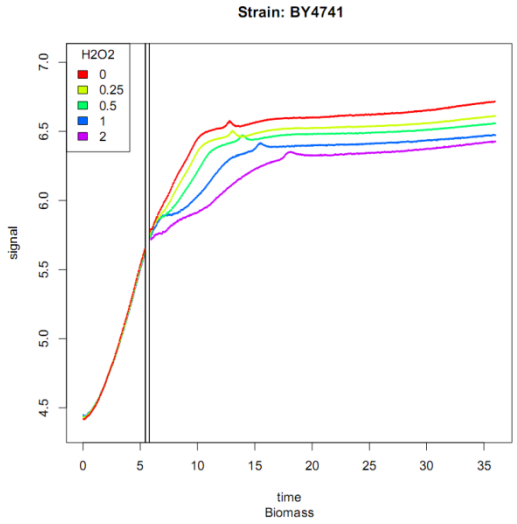

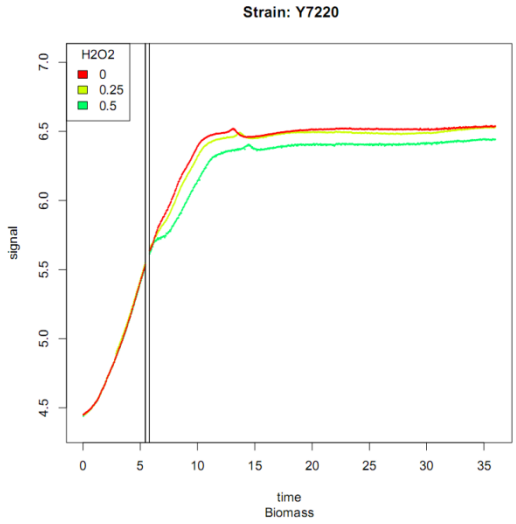

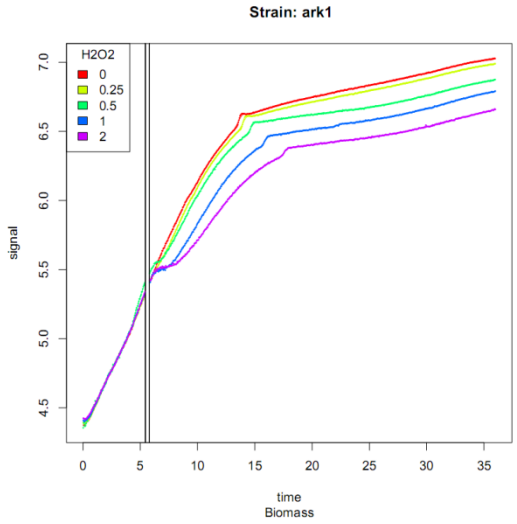

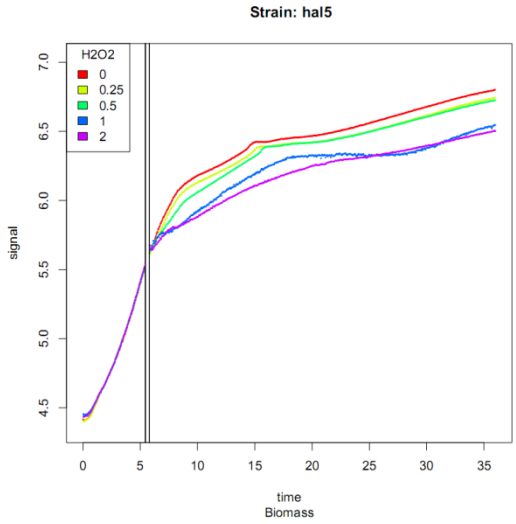

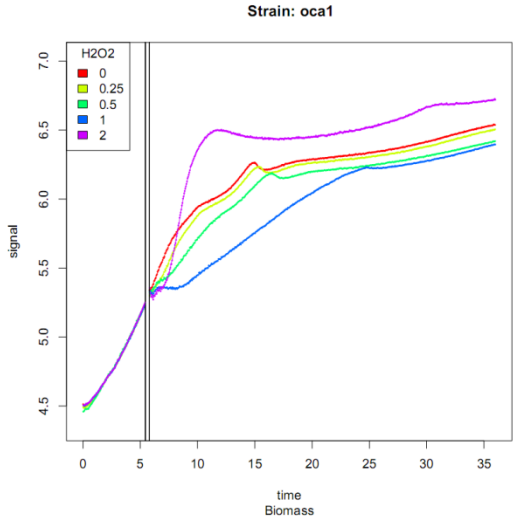

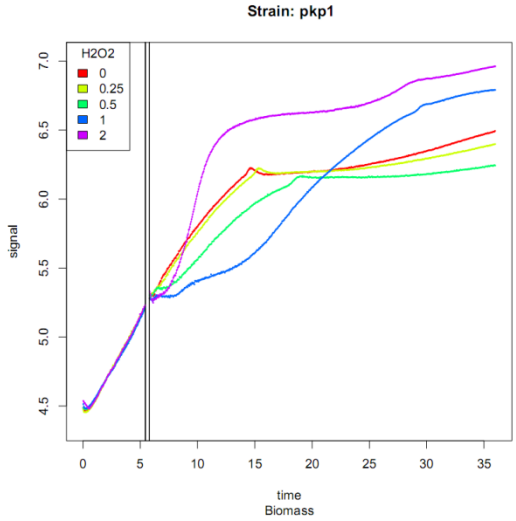

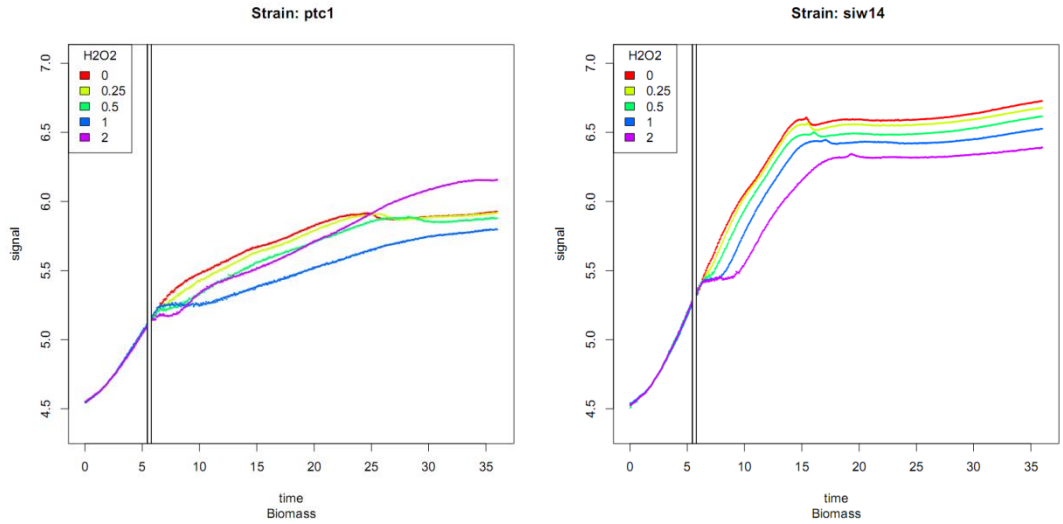
Strain: ptc1
Strain: siw14
H2O2
0
0.25
0.5
1
2
signal
time
Biomass

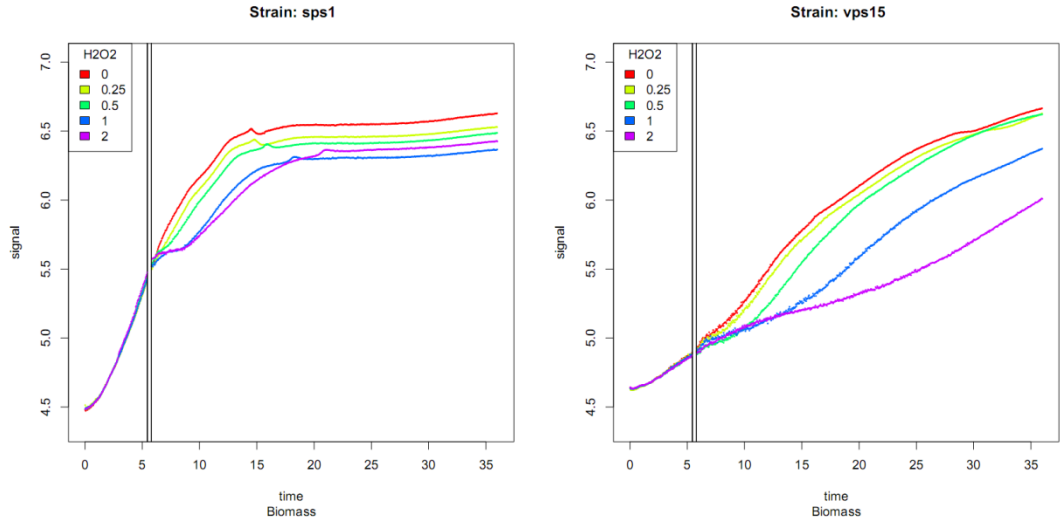
Strain: sps1
Strain: vps15
H2O2
0
0.25
0.5
1
2
signal
time
Biomass

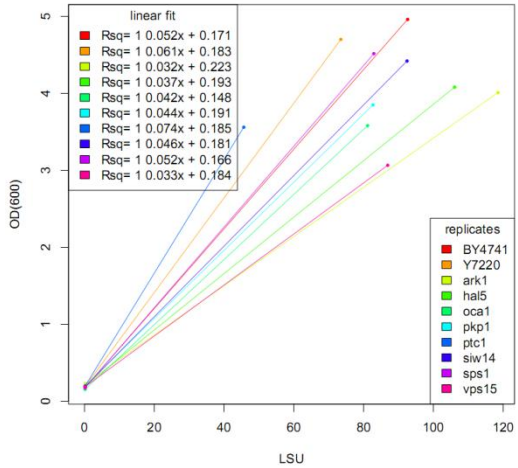
linear fit
Rsq= 1 0.052x + 0.171
Rsq= 1 0.061x + 0.183
Rsq= 1 0.032x + 0.223
Rsq= 1 0.037x + 0.193
Rsq= 1 0.042x + 0.148
Rsq= 1 0.044x + 0.191
Rsq= 1 0.074x + 0.185
Rsq= 1 0.046x + 0.181
Rsq= 1 0.052x + 0.166
Rsq= 1 0.033x + 0.184
replicates
BY4741
Y7220
ark1
hal5
oca1
pkp1
ptc1
siw14
sps1
vps15
OD(600)
LSU

Ferm48_20100528_H2O2_Ali

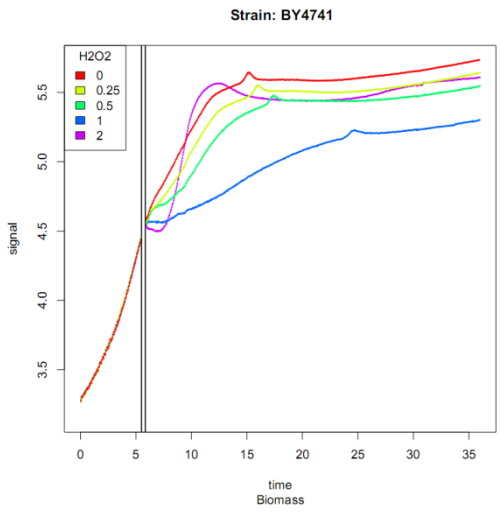

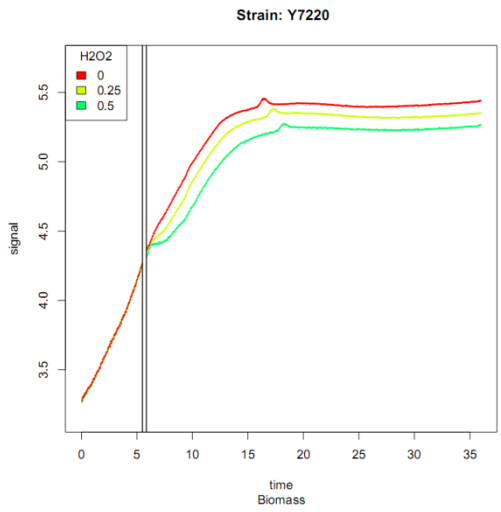

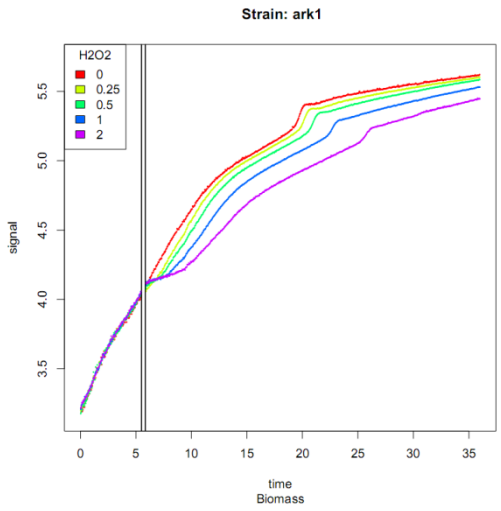

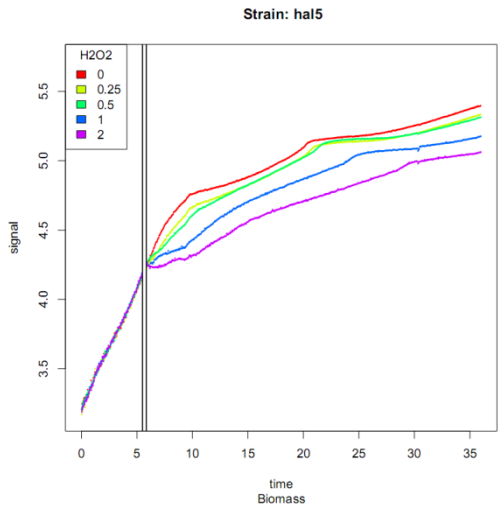

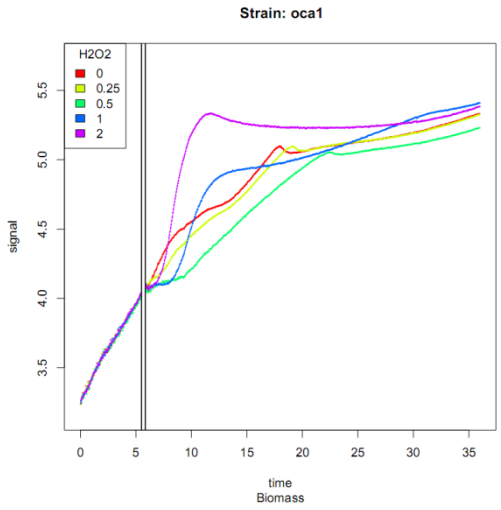

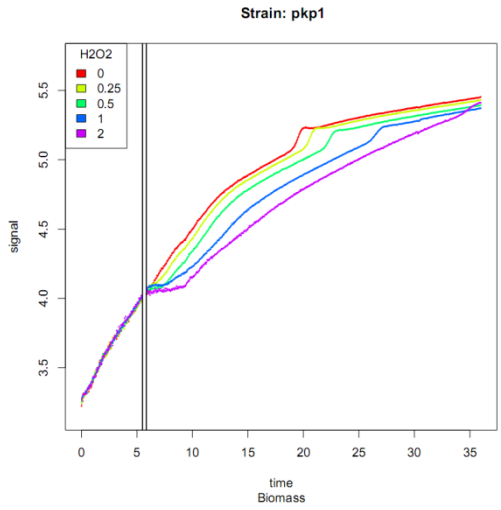

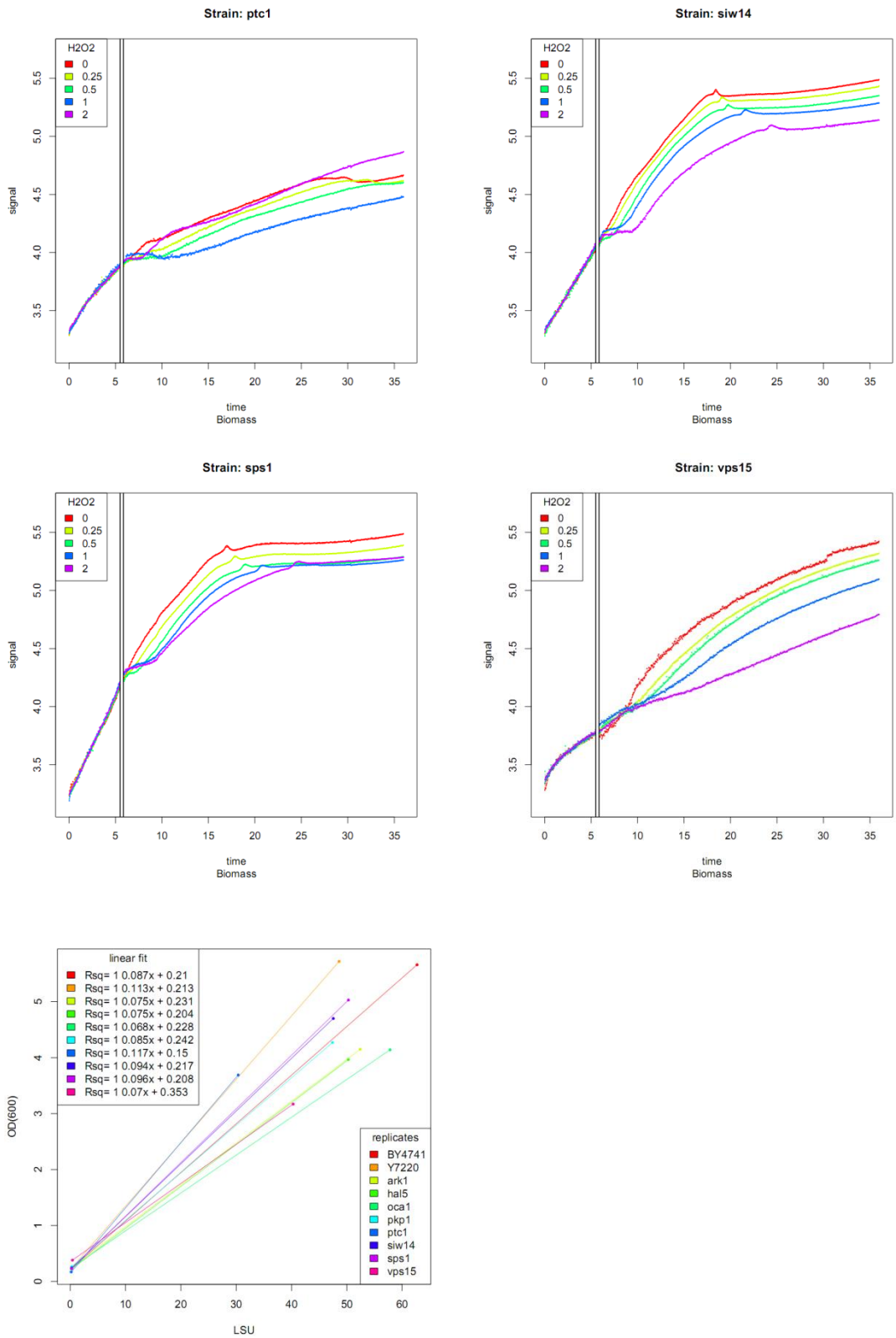
Strain: ptc1
Strain: siw14
Strain: sps1
Strain: vps15
H2O2
0
0.25
0.5
1
2
signal
time
Biomass
linear fit
Rsq= 1 0.087x + 0.21
Rsq= 1 0.113x + 0.213
Rsq= 1 0.075x + 0.231
Rsq= 1 0.075x + 0.204
Rsq= 1 0.068x + 0.228
Rsq= 1 0.085x + 0.242
Rsq= 1 0.117x + 0.15
Rsq= 1 0.094x + 0.217
Rsq= 1 0.096x + 0.208
Rsq= 1 0.07x + 0.353
replicates
BY4741
Y7220
ark1
hal5
oca1
pkp1
ptc1
siw14
sps1
vps15
OD(600)
LSU

Ferm48_20100604_H2O2_Ali

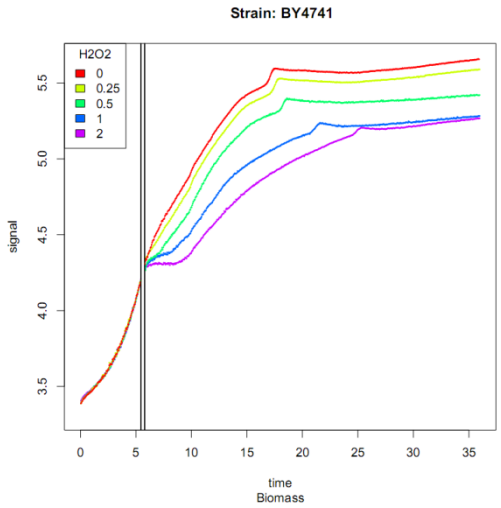

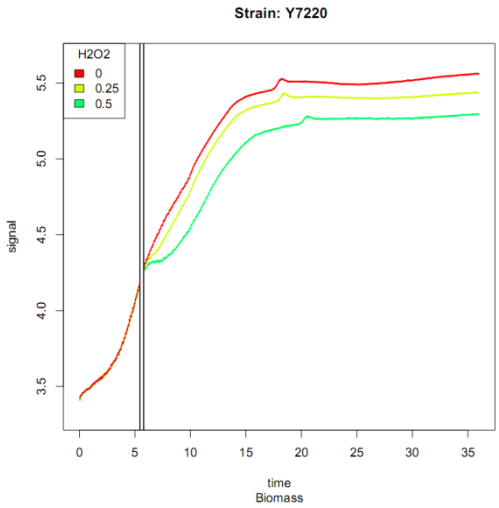

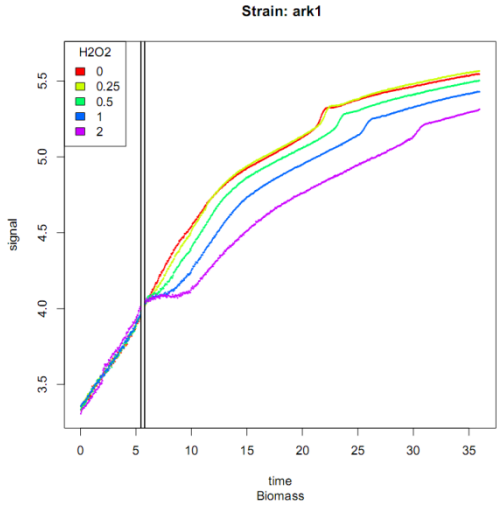

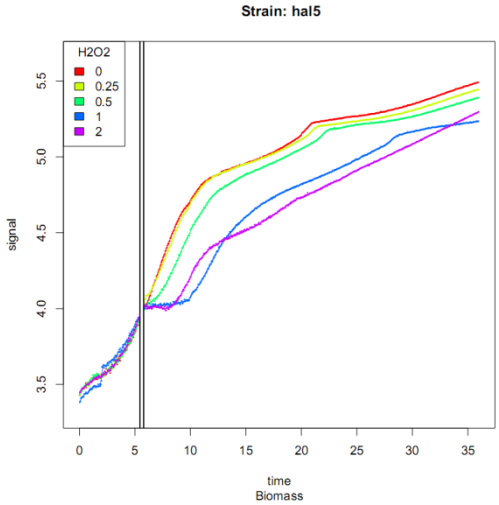

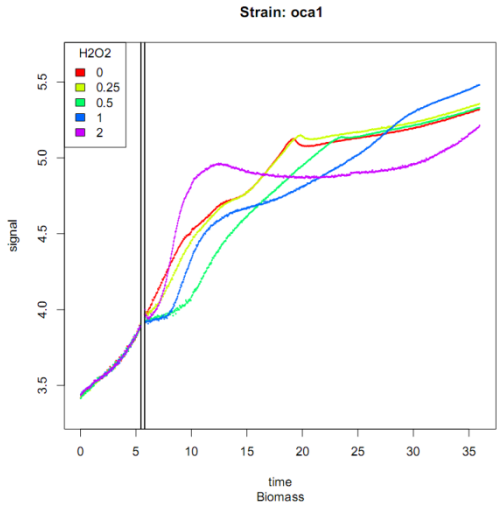

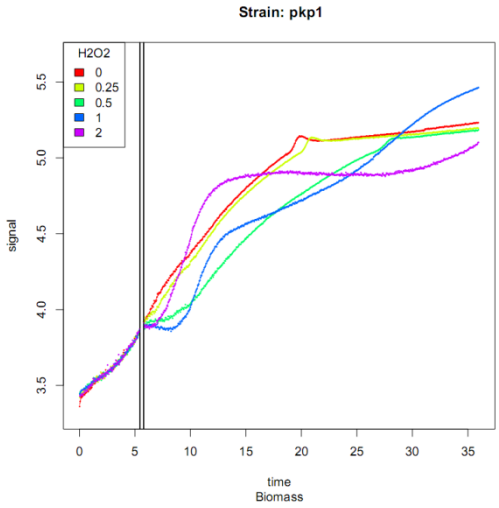

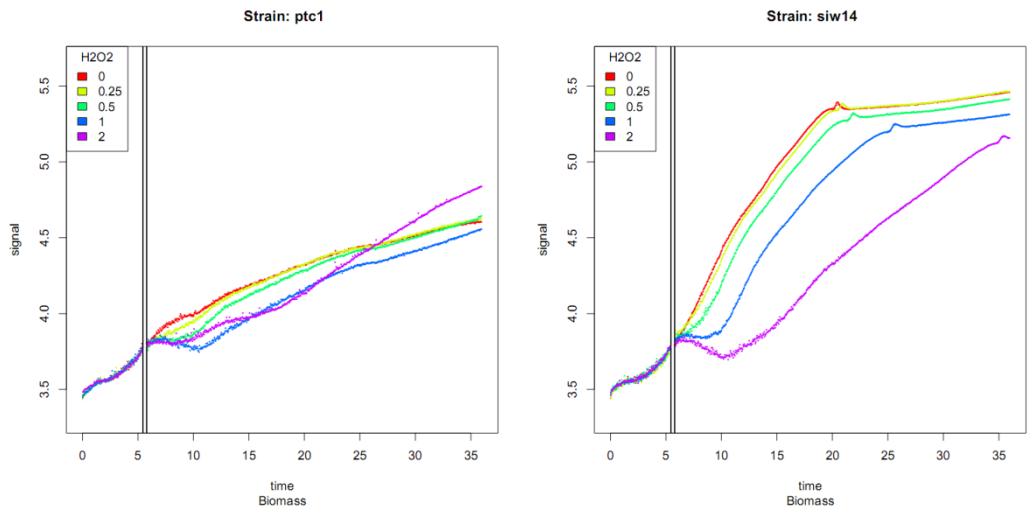
Strain: ptc1
H2O2
0
0.25
0.5
1
2
signal
time
Biomass

Strain: siw14
H2O2
0
0.25
0.5
1
2
signal
time
Biomass

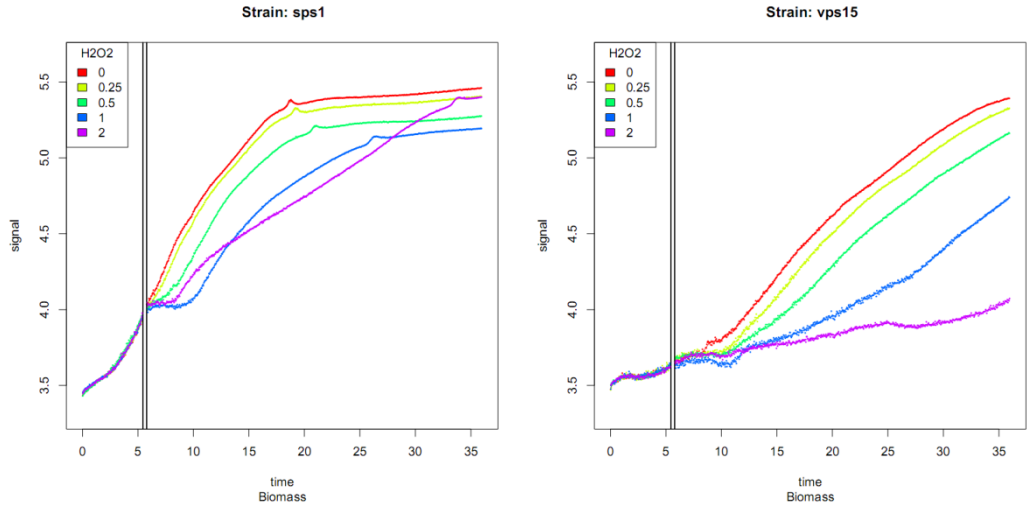
Strain: sps1
H2O2
0
0.25
0.5
1
2
signal
time
Biomass
Strain: vps15
H2O2
0
0.25
0.5
1
2
signal
time
Biomass

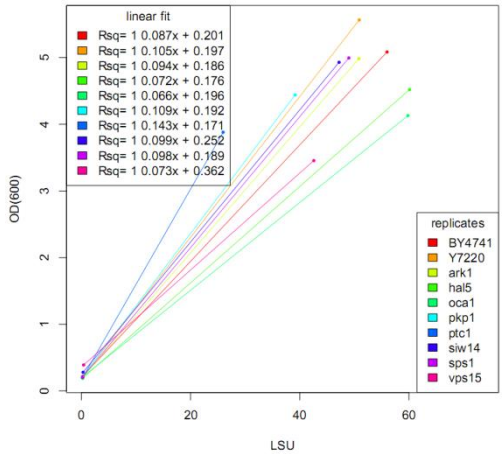
linear fit
Rsq= 1 0.087x + 0.201
Rsq= 1 0.105x + 0.197
Rsq= 1 0.094x + 0.186
Rsq= 1 0.072x + 0.176
Rsq= 1 0.066x + 0.196
Rsq= 1 0.109x + 0.192
Rsq= 1 0.143x + 0.171
Rsq= 1 0.099x + 0.252
Rsq= 1 0.098x + 0.189
Rsq= 1 0.073x + 0.362
replicates
BY4741
Y7220
ark1
hal5
oca1
pkp1
ptc1
siw14
sps1
vps15
OD(600)
LSU

Ferm48_20100608_H2O2_Ali

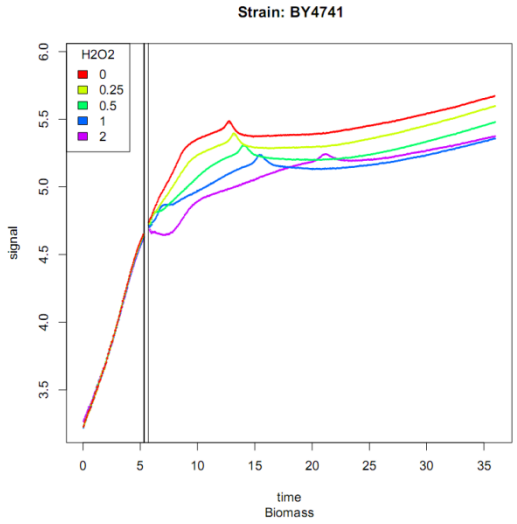

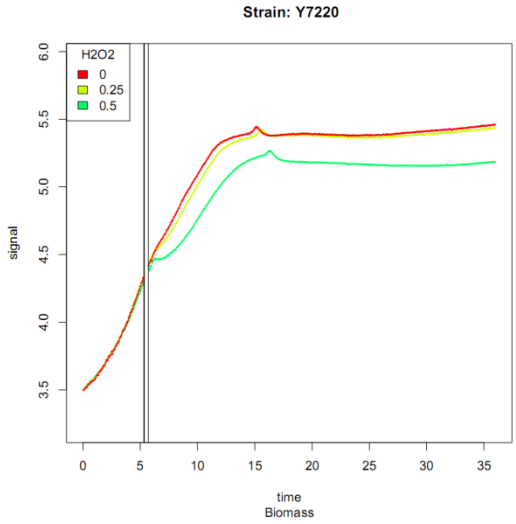

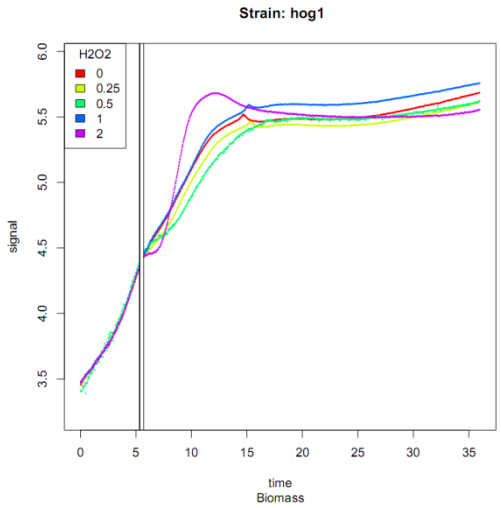

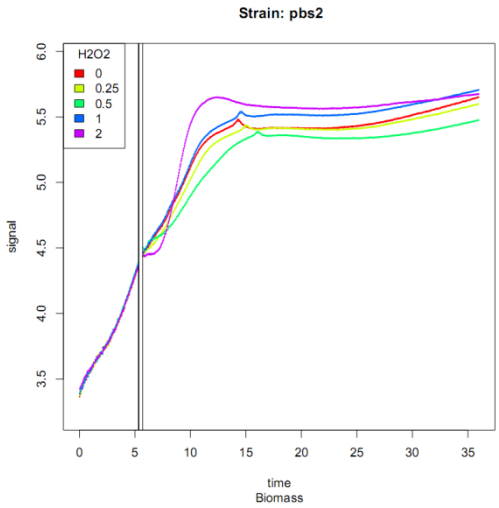

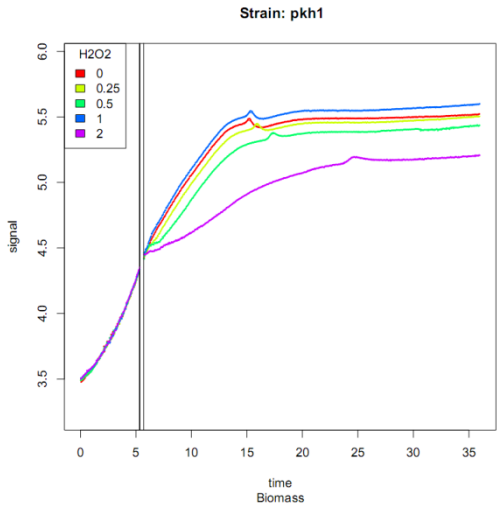

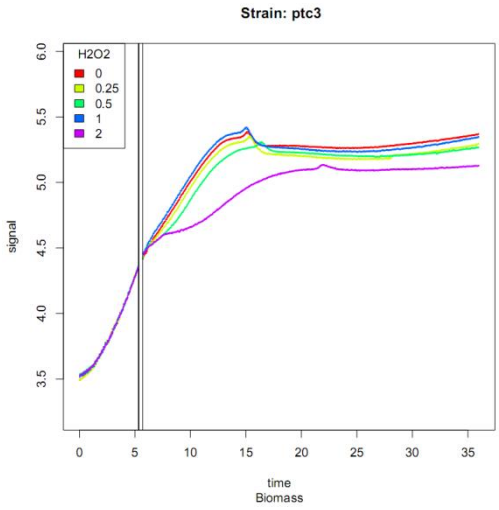

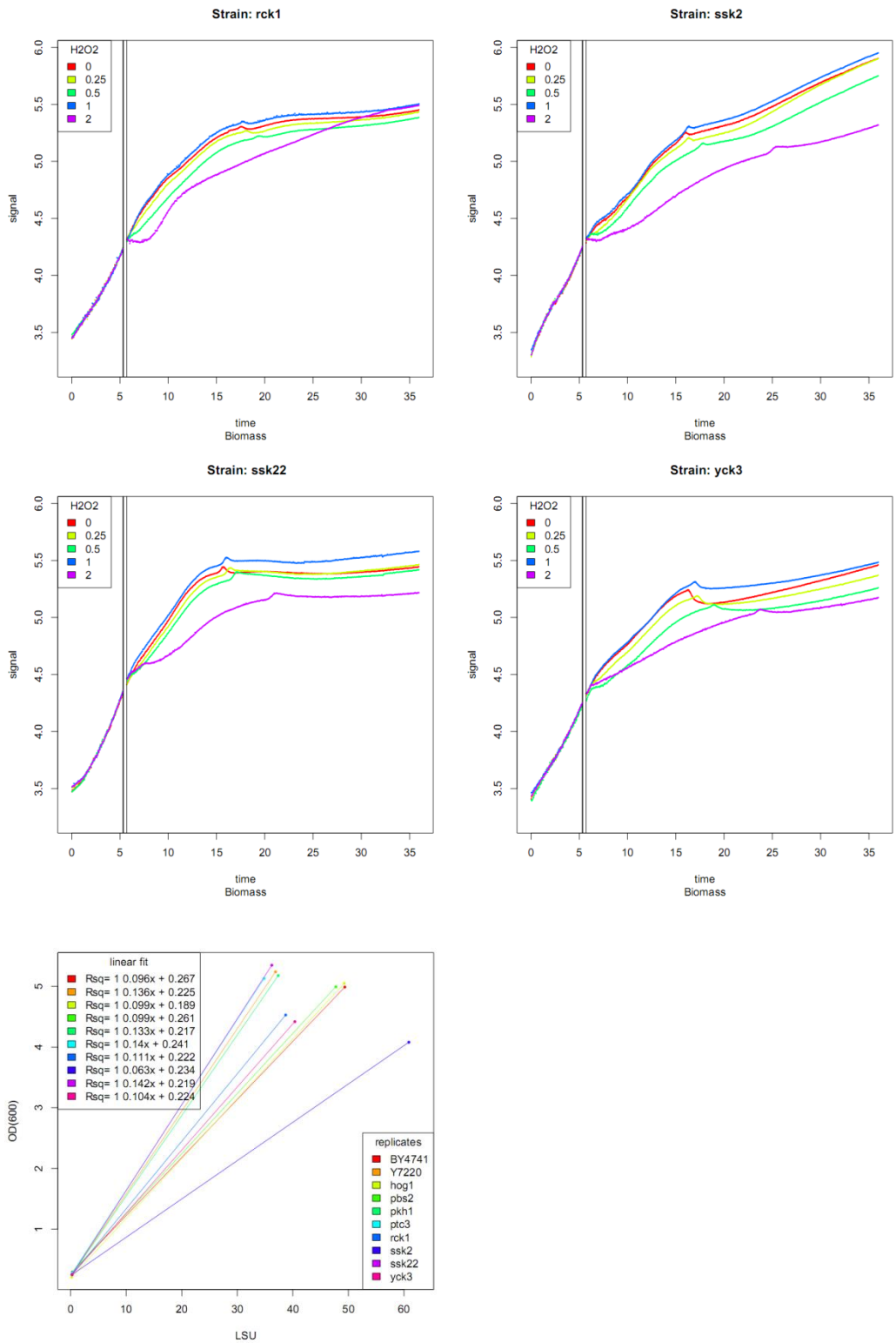
Strain: rck1
Strain: ssk2
Strain: ssk22
Strain: yck3
H2O2
0
0.25
0.5
1
2
signal
time
Biomass
linear fit
Rsq= 1 0.096x + 0.267
Rsq= 1 0.136x + 0.225
Rsq= 1 0.099x + 0.189
Rsq= 1 0.099x + 0.261
Rsq= 1 0.133x + 0.217
Rsq= 1 0.14x + 0.241
Rsq= 1 0.111x + 0.222
Rsq= 1 0.063x + 0.234
Rsq= 1 0.142x + 0.219
Rsq= 1 0.104x + 0.224
replicates
BY4741
Y7220
hog1
pbs2
pkh1
ptc3
rck1
ssk2
ssk22
yck3
OD(600)
LSU

Ferm48_20100610_H2O2_Ali

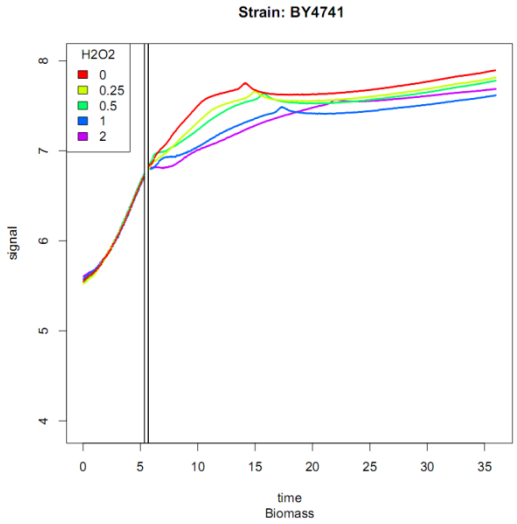

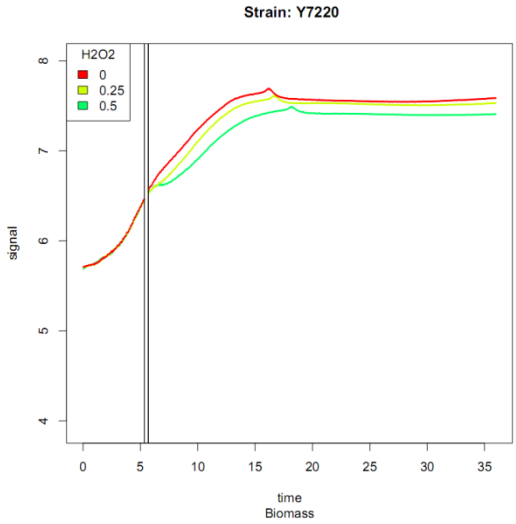

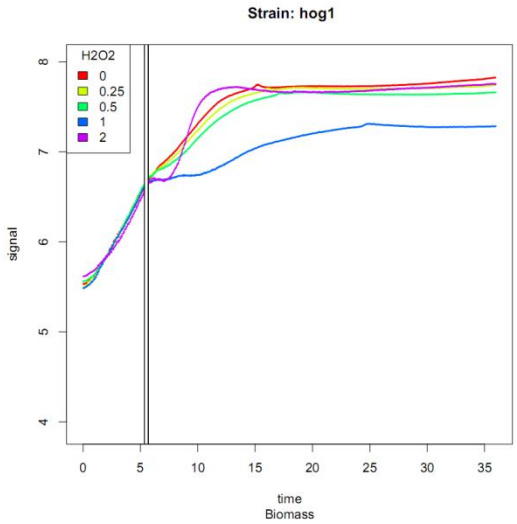

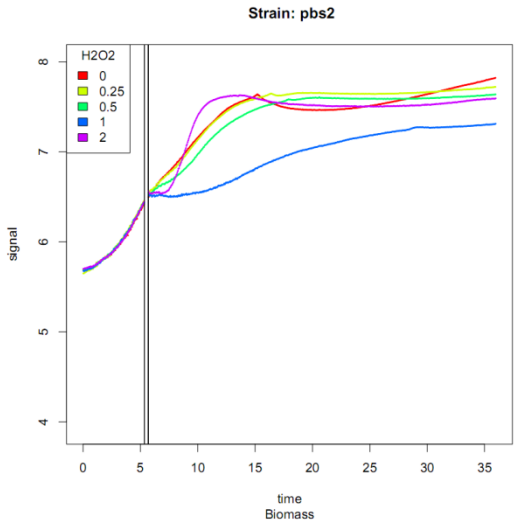

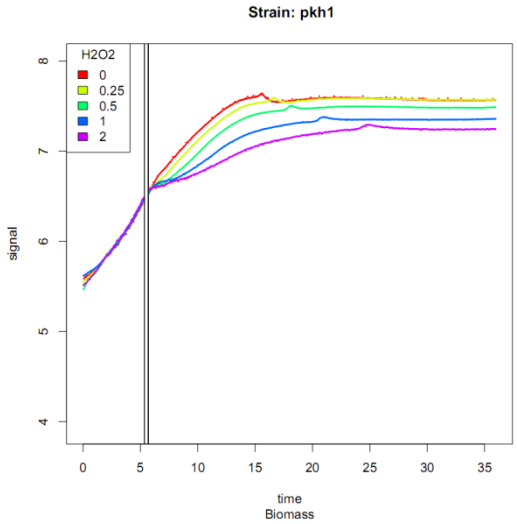

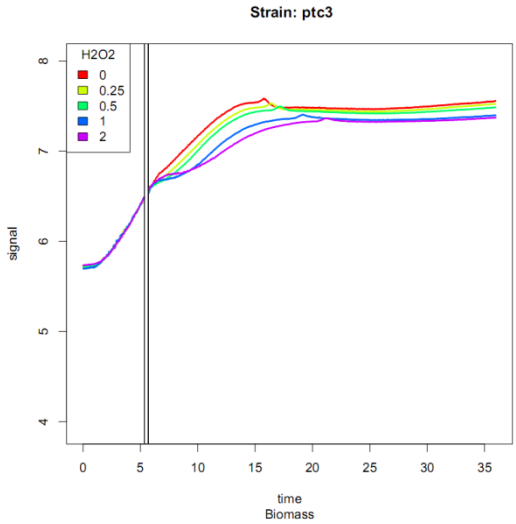

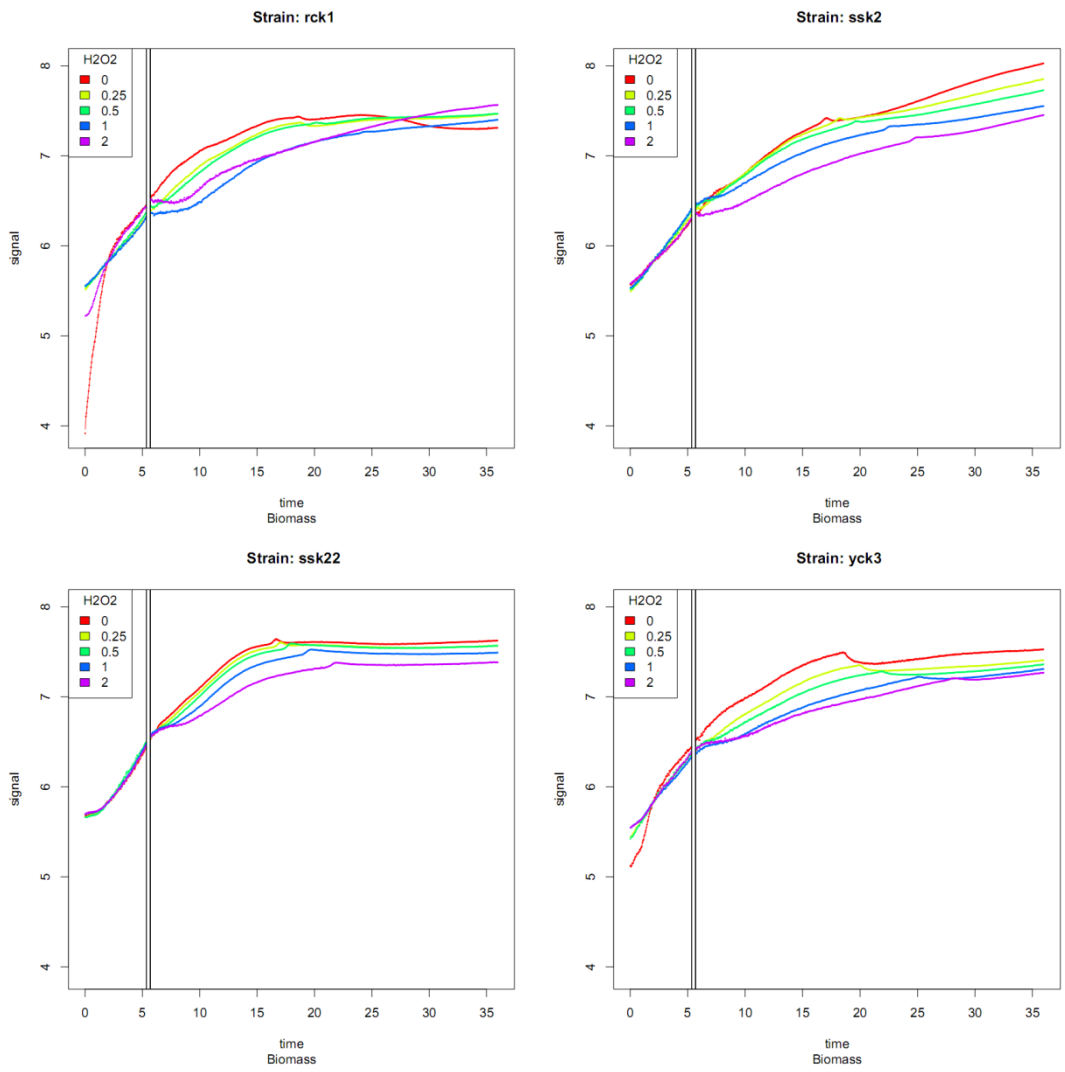
Strain: rck1
Strain: ssk2
Strain: ssk22
Strain: yck3
H2O2
0
0.25
0.5
1
2
signal
time
Biomass

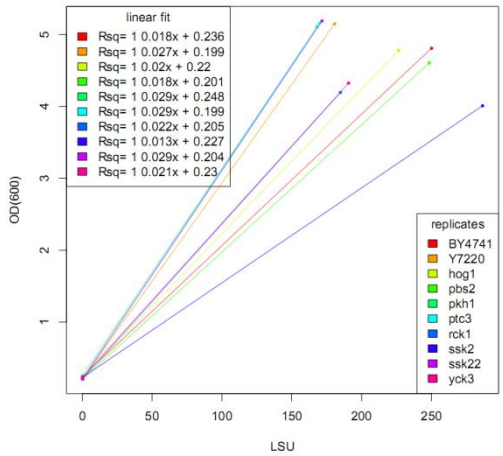
linear fit
Rsq= 1 0.018x + 0.236
Rsq= 1 0.027x + 0.199
Rsq= 1 0.02x + 0.22
Rsq= 1 0.018x + 0.201
Rsq= 1 0.029x + 0.248
Rsq= 1 0.029x + 0.199
Rsq= 1 0.022x + 0.205
Rsq= 1 0.013x + 0.227
Rsq= 1 0.029x + 0.204
Rsq= 1 0.021x + 0.23
replicates
BY4741
Y7220
hog1
pbs2
pkh1
ptc3
rck1
ssk2
ssk22
yck3
OD(600)
LSU

Ferm48_20100614_H2O2_Ali

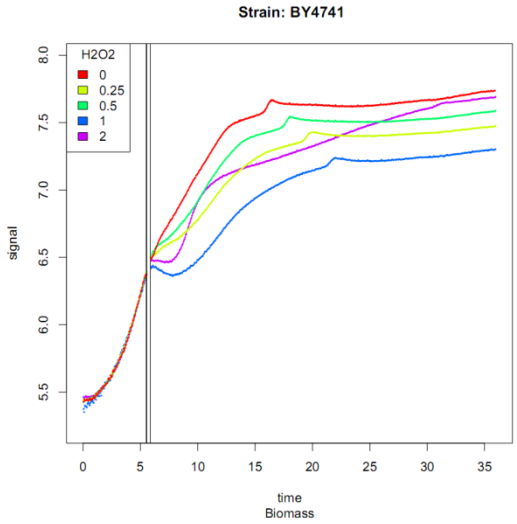

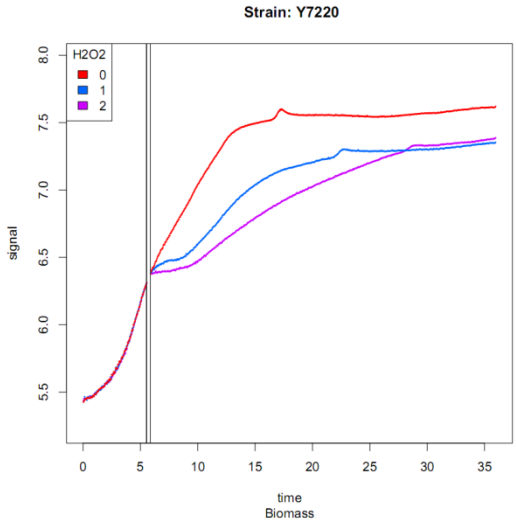

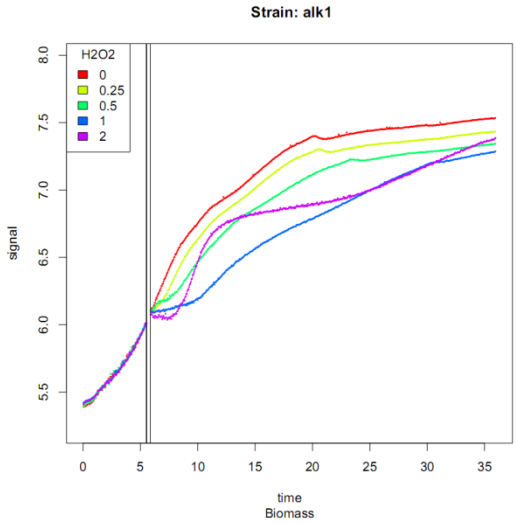

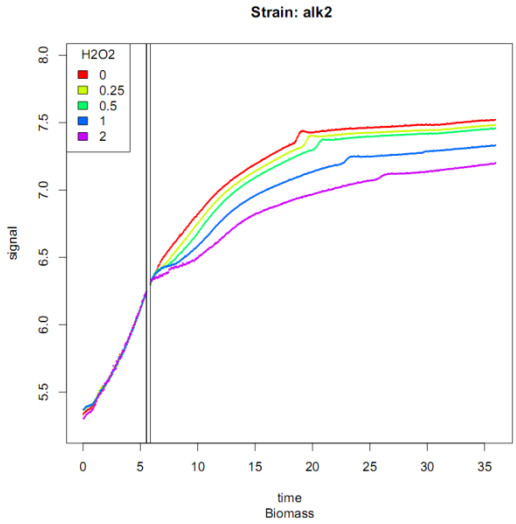

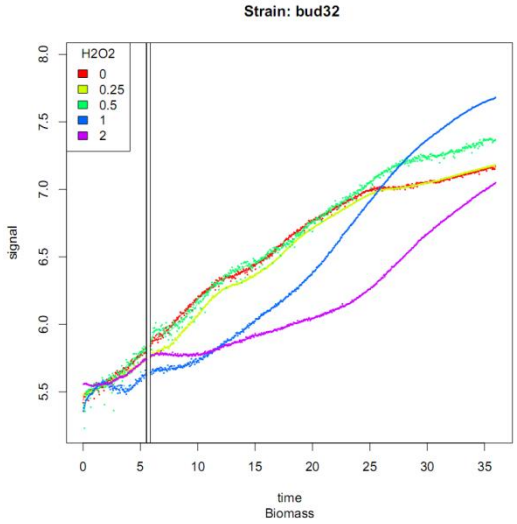

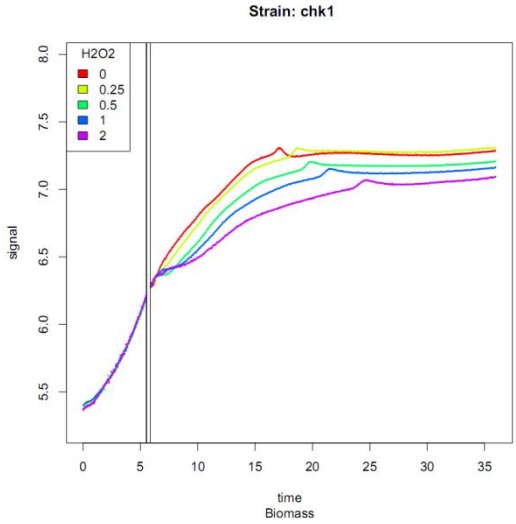

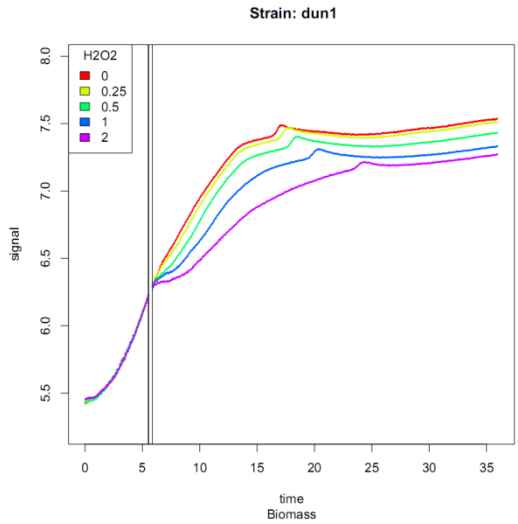
Strain: dun1
H2O2
0
0.25
0.5
1
2
signal
time
Biomass

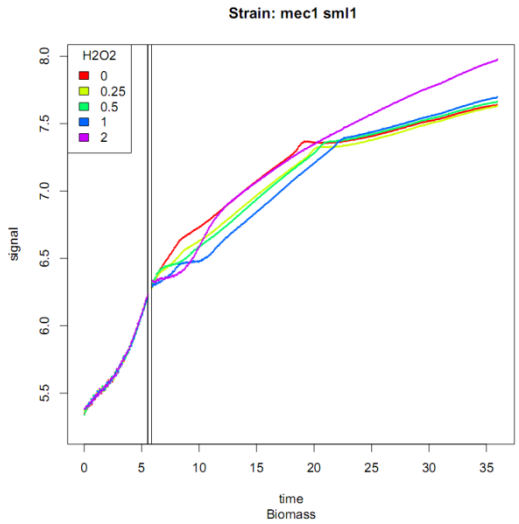
Strain: mec1 sml1
H2O2
0
0.25
0.5
1
2
signal
time
Biomass

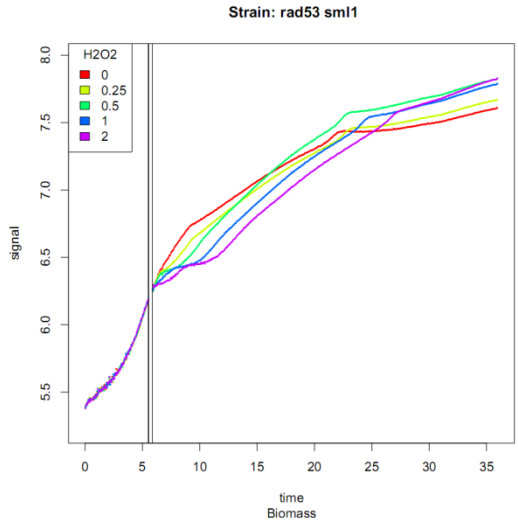
Strain: rad53 sml1
H2O2
0
0.25
0.5
1
2
signal
time
Biomass

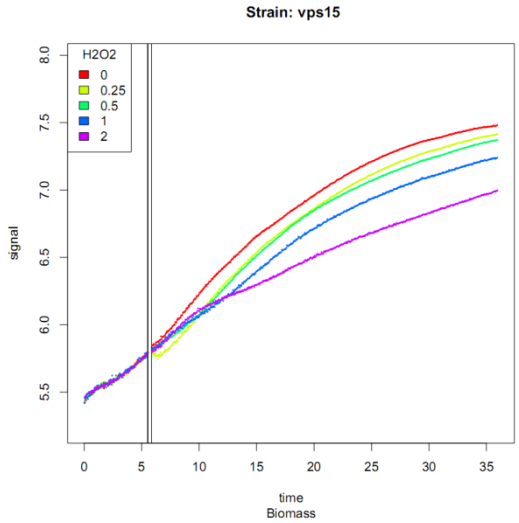
Strain: vps15
H2O2
0
0.25
0.5
1
2
signal
time
Biomass

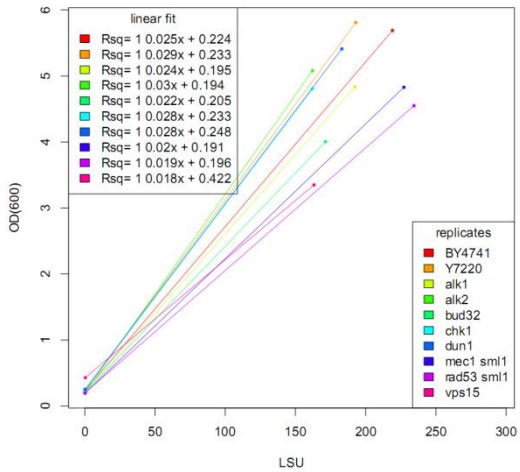
linear fit
Rsq= 1 0.025x + 0.224
Rsq= 1 0.029x + 0.233
Rsq= 1 0.024x + 0.195
Rsq= 1 0.03x + 0.194
Rsq= 1 0.022x + 0.205
Rsq= 1 0.028x + 0.233
Rsq= 1 0.028x + 0.248
Rsq= 1 0.02x + 0.191
Rsq= 1 0.019x + 0.196
Rsq= 1 0.018x + 0.422
replicates
BY4741
Y7220
alk1
alk2
bud32
chk1
dun1
mec1 sml1
rad53 sml1
vps15
OD(600)
LSU

Ferm48_20100617_H2O2_Ali

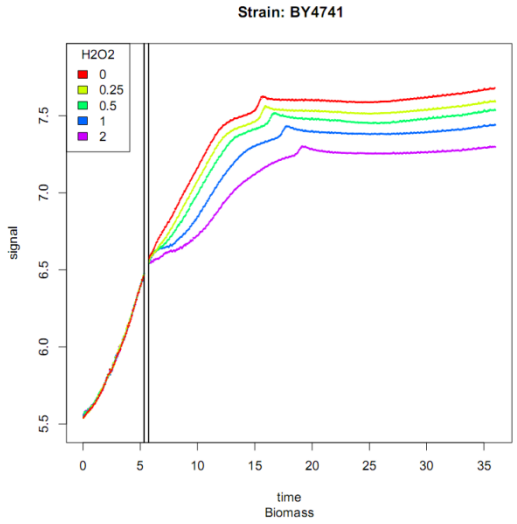

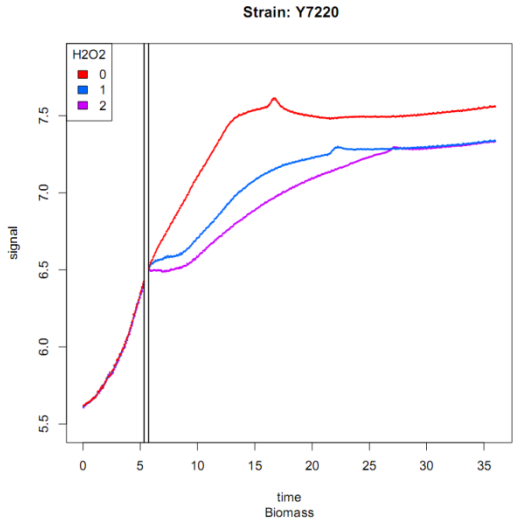

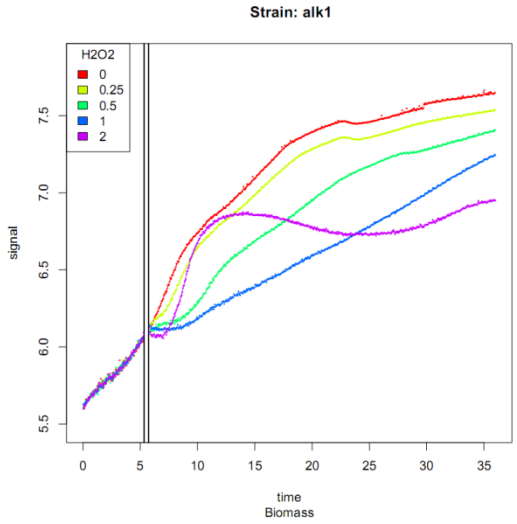

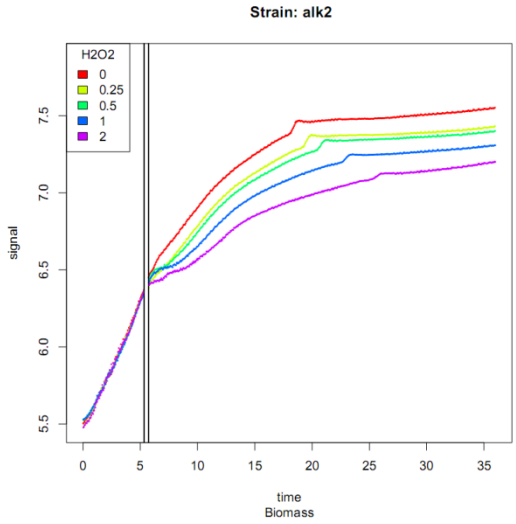

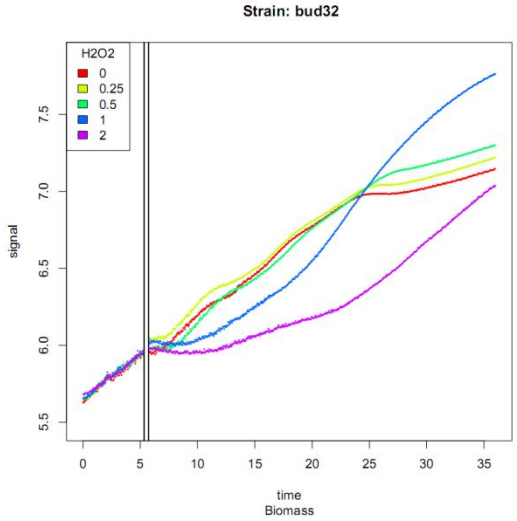

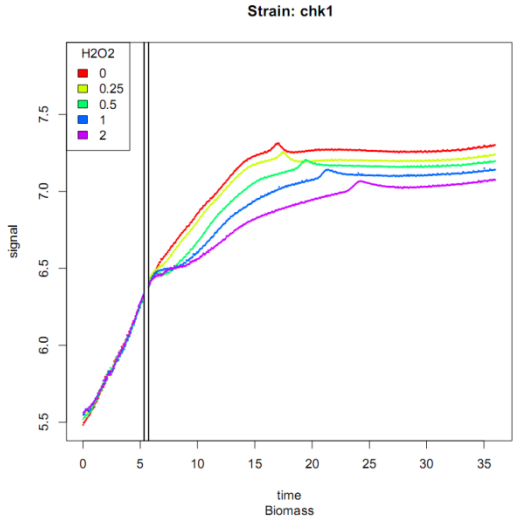

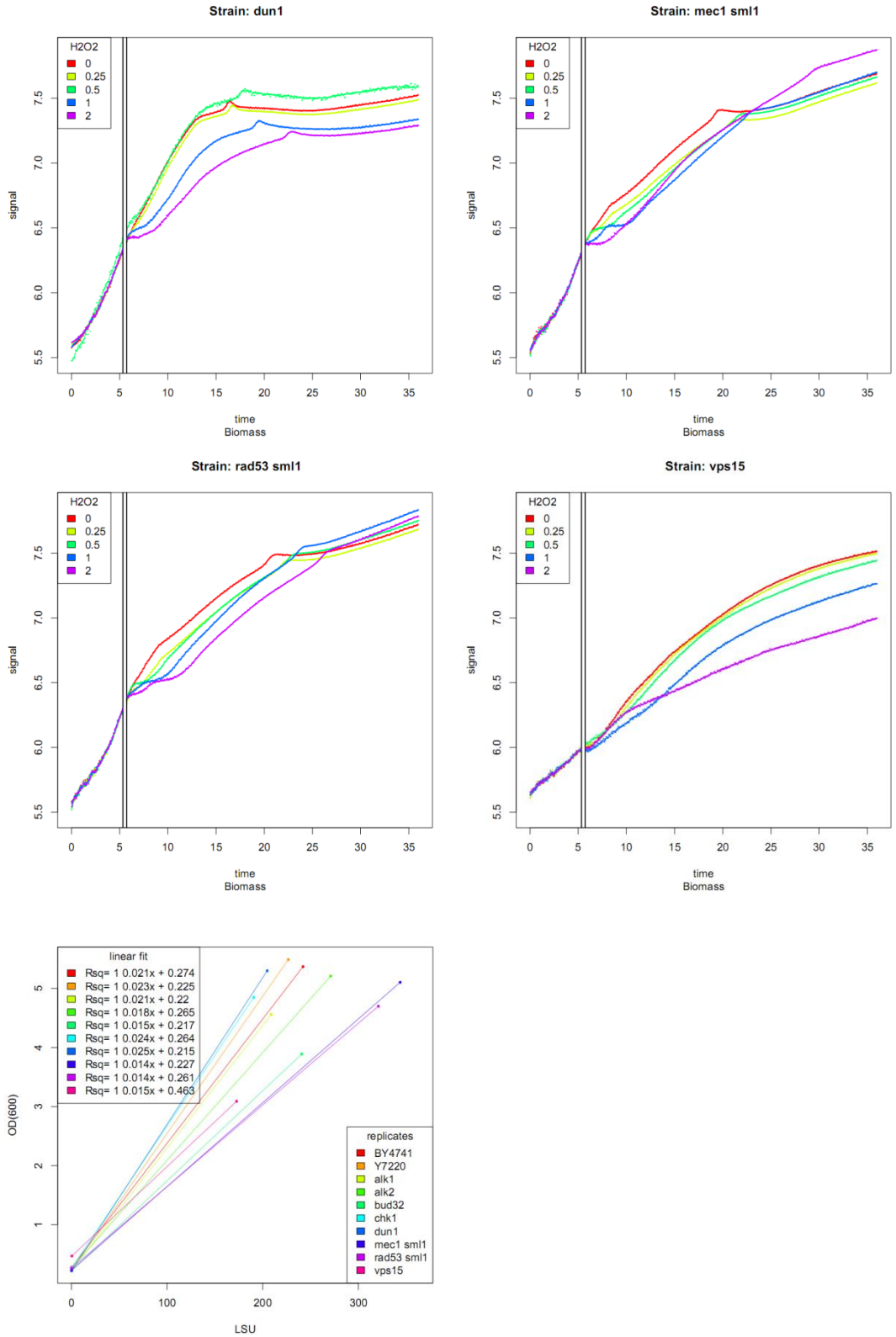
Strain: dun1
Strain: mec1 sml1
Strain: rad53 sml1
Strain: vps15
H2O2
0
0.25
0.5
1
2
signal
time
Biomass
linear fit
Rsq= 1 0.021x + 0.274
Rsq= 1 0.023x + 0.225
Rsq= 1 0.021x + 0.22
Rsq= 1 0.018x + 0.265
Rsq= 1 0.015x + 0.217
Rsq= 1 0.024x + 0.264
Rsq= 1 0.025x + 0.215
Rsq= 1 0.014x + 0.227
Rsq= 1 0.014x + 0.261
Rsq= 1 0.015x + 0.463
replicates
BY4741
Y7220
alk1
alk2
bud32
chk1
dun1
mec1 sml1
rad53 sml1
vps15
OD(600)
LSU

Ferm48_20100628_H2O2_Ali

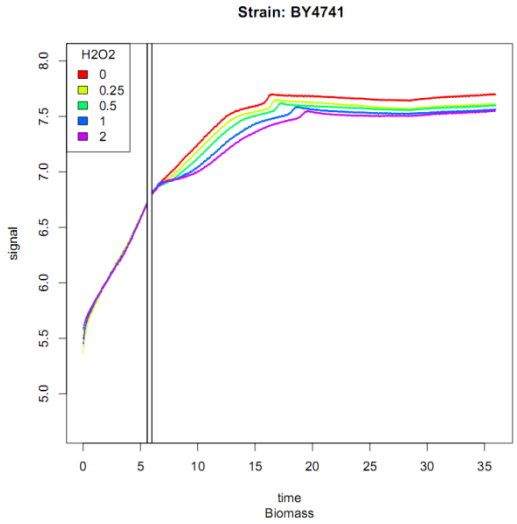

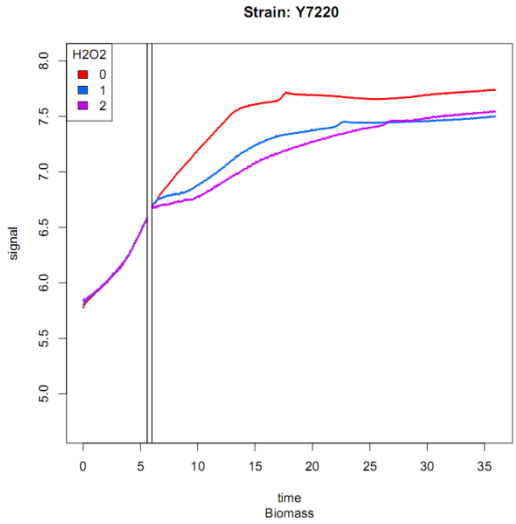

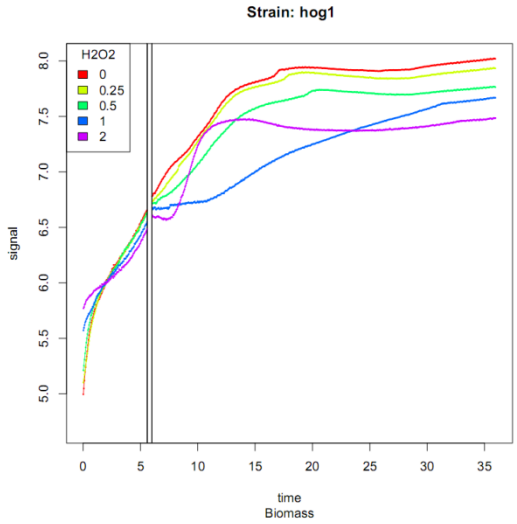

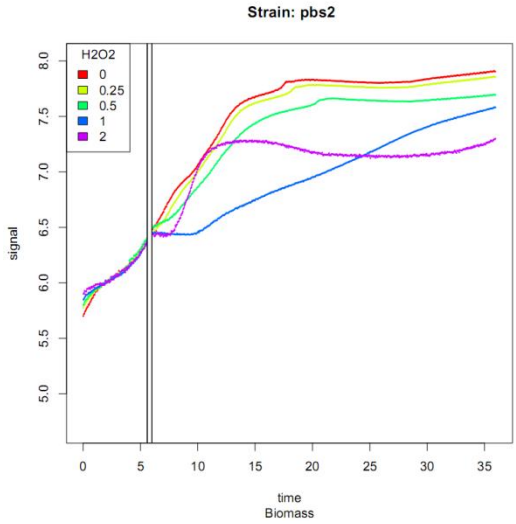

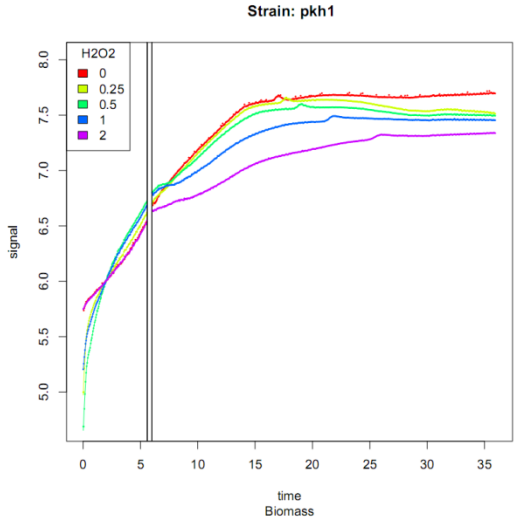

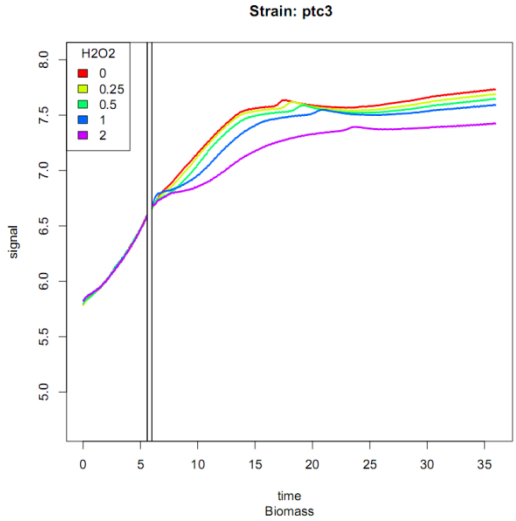

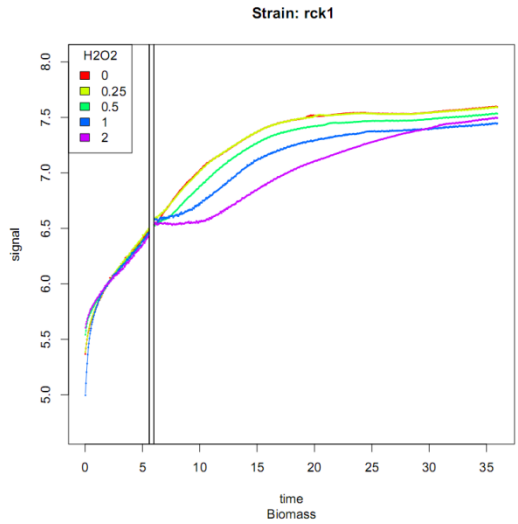
Strain: rck1
H2O2
0
0.25
0.5
1
2
signal
time
Biomass

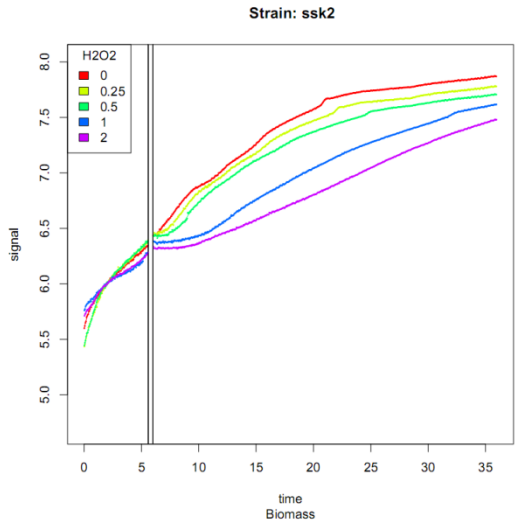
Strain: ssk2
H2O2
0
0.25
0.5
1
2
signal
time
Biomass

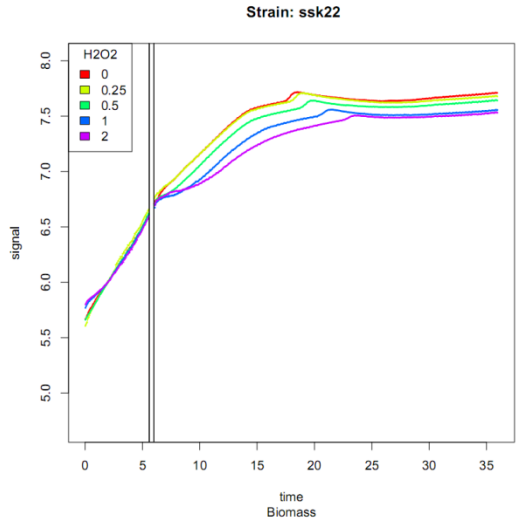
Strain: ssk22
H2O2
0
0.25
0.5
1
2
signal
time
Biomass

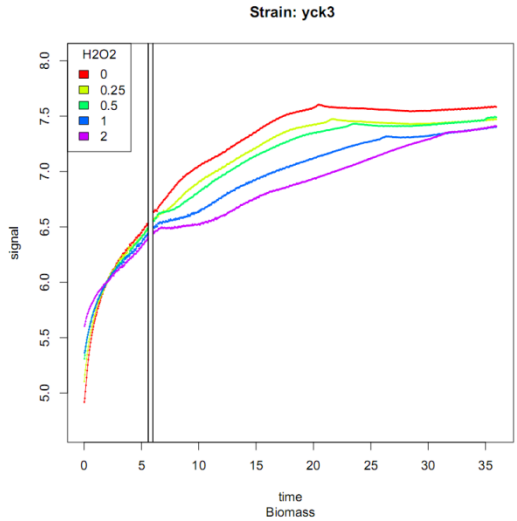
Strain: yck3
H2O2
0
0.25
0.5
1
2
signal
time
Biomass

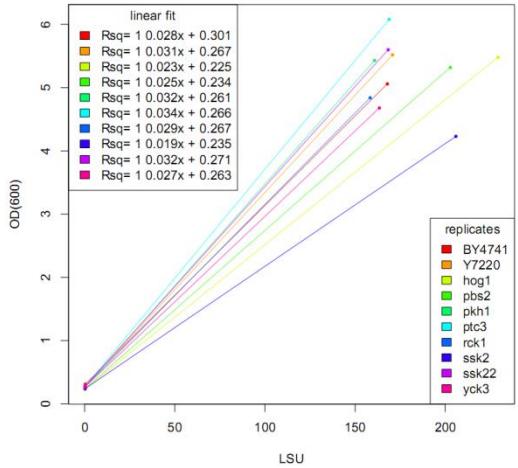
linear fit
Rsq= 1 0.028x + 0.301
Rsq= 1 0.031x + 0.267
Rsq= 1 0.023x + 0.225
Rsq= 1 0.025x + 0.234
Rsq= 1 0.032x + 0.261
Rsq= 1 0.034x + 0.266
Rsq= 1 0.029x + 0.267
Rsq= 1 0.019x + 0.235
Rsq= 1 0.032x + 0.271
Rsq= 1 0.027x + 0.263
replicates
BY4741
Y7220
hog1
pbs2
pkh1
ptc3
rck1
ssk2
ssk22
yck3
OD(600)
LSU

CURRICULUM VITAE

Candidate's full name: ALİ ALTINTAŞ

Place and date of birth: Uşak, 20.01.1985

Permanent Address: Köme Mah. Irak Sok. No: 28, 64100 Uşak

Universities and Colleges attended:

M.Sc. (2008-Present), Istanbul Technical University (ITU), Molecular Biology-Genetics & Biotechnology

M.Sc. (2009-2010), Technical Universtiy of Denmark (DTU), Erasmus Exchange Student in Department of Systems Biology

B.Sc. (2004-2008), Istanbul Technical University (ITU), Molecular Biology & Genetics

Publications:

- **Altintas, A.**, Growth Physiology And Metabolic Remodelling of Saccharomyces cerevisiae under Oxidative Stress Conditions, August 2010, M.Sc. Project, DTU Center for Biological Sequence of Analysis (CBS), Denmark
- **Altıntaş, A.**, Growth Physiology and Transcriptomic Analysis of a Cobalt-Resistant Yeast Mutant Obtained via Evolutionary Engineering, May 2008, B.Sc. Thesis, ITU Faculty of Science and Letters, Istanbul
- Vata, C., K., Yilmaz, B., **Altintas, A.**, Sachs, M., Akcetin, Z., Cakar, Z., P., (2008), Combinatorial Data-Mining Using Pdq_Med And Treeview: A Gene-Disease Story, HIBIT 2008: Proceedings of International Symposium on Health Informatics and Bioinformatics (http://hibit08.sezermanlab.com)
- **Altintas, A.**, Alkim, C., Yilmaz, B., Aloglu, T., Turanli, B., Cakar, Z.P. 2007. B vitaminleri varliginin ve kultur kosullarinin yaban tip ile mutant mayalarin buyume fizyolojisi ve stres direncine etkileri (Stress resistance and growth physiology of wild type and mutant yeast cells in the presence of vitamin B). Molekuler Biyoloji ve Genetik Ogrenci Kongresi [Molecular Biology and Genetic Scholar Congress], Proceeding, No: 22, Istanbul Technical University, 8-11 September 2007, Istanbul, Turkey